



Fundusze Europejskie
Wiedza Edukacja Rozwój

Unia Europejska
Europejski Fundusz Społeczny



„BioTechNan – Program Interdyscyplinarnych Środowiskowych Studiów Doktoranckich KNOW z obszaru Biotechnologii i Nanotechnologii”

Instytut Immunologii i Terapii Doświadczalnej im. Ludwika Hirszfelda
Polskiej Akademii Nauk



Sandra Daria Stannitz

Charakterystyka biologiczna mezenchymalnych komórek macierzystych (MSC) pozyskanych ze szpiku kostnego owiec oraz ocena efektywności zastosowania bioimplantu wzbogaconego w MSC w rekonstrukcji dużych ubytków tkanki kostnej w eksperymentalnym modelu owcy

Rozprawa doktorska w dyscyplinie nauk biologicznych

Promotorzy:

prof. dr hab. Aleksandra Klimczak
prof. dr hab. Zdzisław Kiełbowicz

Samodzielne Laboratorium Biologii Komórek Macierzystych i Nowotworowych

Wrocław 2022



Politechnika Wroclawska



Uniwersytet
Wrocławski



UNIWERSYTET
PRZYRODNICZY
WE WROCŁAWIU



**European
Funds**
Knowledge Education Development

European Union
European Social Fund



Hirsfeld Institute of Immunology and Experimental Therapy
Polish Academy of Sciences



Sandra Daria Stammnitz

**Biological characterization of mesenchymal stem cells (MSCs)
isolated from ovine bone marrow and evaluation of the effectiveness
of using MSC-enriched bioimplant in reconstruction of large bone
defects in an experimental sheep model**

Doctoral Thesis in the scientific discipline biological sciences

Supervisors:

Professor Aleksandra Klimczak
Professor Zdzisław Kielbowicz

Laboratory of Biology of Stem and Neoplastic Cells

Wrocław 2022



Wrocław University
of Science and Technology



Uniwersytet
Wrocławski



WROCLAW UNIVERSITY
OF ENVIRONMENTAL
AND LIFE SCIENCES

Badania w ramach niniejszej dysertacji doktorskiej przeprowadzono przy wsparciu finansowym dwóch podmiotów w ramach Interdyscyplinarnych Środowiskowych Studiów Doktoranckich BioTechNan:

1. Instytut Immunologii i Terapii Doświadczalnej im. L. Hirszfelda PAN, Samodzielne Laboratorium Biologii Komórek Macierzystych i Nowotworowych, promotor: prof. dr hab. Aleksandra Klimczak, dyscyplina: nauki biologiczne,

2. Uniwersytet Przyrodniczy we Wrocławiu, Katedra i Klinika Chirurgii Wydziału Medycyny Weterynaryjnej, promotor: prof. dr hab. Zdzisław Kiełbowicz, dyscyplina: weterynaria.

Składam serdeczne podziękowania

*Prof. Aleksandrze Klimczak,
za nieocenioną pomoc, poświęcony czas,
cierpliwość oraz cenne rady i wskazówki.*

*Prof. Zdzisławowi Kielbowiczowi,
za wsparcie merytoryczne
w dziedzinie medycyny weterynaryjnej.*

*Koleżankom z Laboratorium,
za życzliwość oraz dzielenie się
swoim doświadczeniem i wiedzą.*

*Rodzicom i Mężowi,
bez których ta praca by nie powstała,
za troskę i wiarę w moje możliwości.*

*Rozprawę doktorską dedykuję babci, dzięki której
znajduję się na tym etapie mojej naukowej podróży.*

Table of contents

Streszczenie.....	6
Summary.....	9
List of publications.....	12
Co-authors' declarations	13
Publications	32
Biological Characteristics and Osteogenic Differentiation of Ovine Bone Marrow Derived Mesenchymal Stem Cells Stimulated with FGF-2 and BMP-2	33
Osteogenic Potential of Sheep Mesenchymal Stem Cells Preconditioned with BMP-2 and FGF-2 and Seeded on an nHAP-Coated PCL/HAP/ β -TCP Scaffold	58
Mesenchymal Stem Cells, Bioactive Factors, and Scaffolds in Bone Repair: From Research Perspectives to Clinical Practice	86
Conclusions.....	112

Streszczenie

Na całym świecie systematycznie rośnie liczba ludzi cierpiących z powodu urazów kości spowodowanych wypadkami komunikacyjnymi, złamaniami osteoporotycznymi, chorobami układu kostnego, czy resekcjami guzów. Pomimo zdolności tkanki kostnej do samoregeneracji, około 10-20% złamań zrasta się nieprawidłowo lub wcale, co może prowadzić do powstania ubytków o krytycznych rozmiarach, większych niż 1-2 cm długości i 50% obwodu kości. Obecnie pozostają one najtrudniejszym problemem w chirurgii ortopedycznej, a także ogromnym obciążeniem ekonomicznym dla systemu opieki zdrowotnej, mimo nowoczesnych metod leczenia o wysokich standardach technologicznych.

Współczesne metody terapeutyczne dużych ubytków kostnych opierają się na przeszczepieniach kości, w tym autoprzeszczepach, alloprzeszczepach oraz przeszczepach syntetycznych. Jednakże, w przypadku krytycznych ubytków kości, autologiczne przeszczepy kostne nie mają zastosowania z uwagi na ograniczoną możliwość pobrania tkanki kostnej, natomiast łatwo dostępne alloprzeszczepy mogą wywołać odpowiedź immunologiczną. Z kolei przeszczepy syntetyczne są dostępne nieograniczenie, ale proces osteointegracji implantu jest spowolniony, a sam materiał nie posiada właściwości osteogennych. W związku z tym poszukiwane są nowe, alternatywne metody leczenia, wśród których obiecującym podejściem jest zastosowanie konstruktyw inżynierii tkankowej, składających się z bioimplantu z komórkami o właściwościach osteogennych oraz czynników biologicznie aktywnych.

Koniec ubiegłego stulecia przyniósł dynamiczny rozwój badań dotyczących biologii mezenchymalnych komórek macierzystych (MSC) oraz ich potencjalnego zastosowania w medycynie regeneracyjnej. MSC budzą zainteresowanie z uwagi na ich zdolność do wieloliniowego różnicowania, w tym osteogenne. Jednakże, regeneracja dużych ubytków kostnych z wykorzystaniem jedynie terapii komórkowych często kończy się niepowodzeniem, ponieważ brakuje matrycy, na której komórki mogą tworzyć struktury 3D, jak to ma miejsce w przypadku ich naturalnego środowiska w tkance. Problem ten może zostać rozwiązany poprzez stworzenie konstruktu inżynierii tkankowej, składającego się z biokompatybilnego rusztowania oraz MSC o zwiększonym potencjale osteogennym.

Celami rozprawy doktorskiej były: 1) charakterystyka biologiczna mezenchymalnych komórek macierzystych pochodzących ze szpiku kostnego owiec (BM-MSC); 2) ocena efektu stymulacji osteogennej komórek BM-MSC z użyciem cytokin FGF-2 i BMP-2; 3) charakterystyka właściwości osteogennych konstruktu rusztowanie-BM-MSC stymulowanych FGF-2 i BMP-2 *in vitro*; 4) ocena biokompatybilności i potencjału

osteogennego konstrukt rusztowanie-BM-MSC po heterotopowej implantacji do tkanek w okolicy żuchwy owcy.

Rozprawę doktorską stanowi cykl prac powiązanych tematycznie w postaci trzech publikacji naukowych. Wyniki badań zostały przedstawione w dwóch oryginalnych publikacjach, natomiast w publikacji przeglądowej podsumowano aktualny stan wiedzy o zastosowaniu MSC, rusztowań komórkowych oraz czynników biologicznie aktywnych w regeneracji tkanki kostnej.

Pierwsza publikacja (IJMS, 2020, 21(24):9726) obejmuje badania właściwości biologicznych owczych BM-MSC, które dotychczas były niedostatecznie scharakteryzowane. Ponadto, oceniono wpływ FGF-2 i BMP-2 na potencjał osteogeny BM-MSC *in vitro*. Badania podstawowe obejmowały ocenę fenotypu, morfologii, proliferacji, zdolności do różnicowania w kierunku komórek tkanki kostnej, chrzęstnej i tłuszczowej oraz profilu wydzielniczego owczych BM-MSC w warunkach kontrolnych oraz po stymulacji FGF-2 lub FGF-2 w kombinacji z BMP-2. W celu zbadania wpływu cytokin na zdolność BM-MSC do różnicowania w kierunku komórek tkanki kostnej, oceniono obecność białek związanych z osteogenezą: kolagenu I oraz osteokalcyny za pomocą barwienia immunofluorescencyjnego, a także przeanalizowano poziom ekspresji mRNA genów kodujących białka wczesnych etapów różnicowania osteogenego: *BMP-2*, *Runx2*, *osterix*, *kolagen typu I* oraz późnych markerów osteogenezy: *osteokalcyny* i *osteopontyny*. Wykazano, że komórki MSC wyizolowane ze szpiku kostnego owiec, prekondycjonowane FGF-2 i BMP-2, zachowały swoje pierwotne właściwości komórek MSC, co potwierdzono obecnością markerów powierzchniowych CD73, CD90 i CD105 oraz brakiem ekspresji markerów komórek hematopoetycznych CD34, CD45 i antygeny głównego układu zgodności tkankowej klasy II (DR). Stymulowanie cytokinami skutkowało wydajniejszym tempem proliferacji, w porównaniu z komórkami nietraktowanymi. Zaobserwowano synergistyczne działanie pro-osteogenne FGF-2 i BMP-2 na BM-MSC, potwierdzone barwieniem depozytów wapniowych za pomocą czerwieni alizarinowej oraz zwiększoną intensywnością fluorescencji białek osteogennych: kolagenu I i osteokalcyny. Ponadto, stymulacja komórek BM-MSC cytokinami FGF-2 i BMP-2 indukowała wzrost poziomu ekspresji mRNA genów wszystkich analizowanych markerów osteogennych. Wykazano również, że owcze BM-MSC produkowały czynniki bioaktywne, w tym zaangażowane w osteogenezę (np. dekorynę), a stymulacja komórek FGF-2 i BMP-2 modulowała ich profil wydzielniczy.

W drugiej publikacji (Cells, 2022, 11(21):3446) opracowano konstrukt inżynierii tkankowej, składający się z rusztowania PCL/HAP/ β -TCP pokrytego warstwą n-HAP

(wyprodukowanego na Wydziale Inżynierii Materiałowej Politechniki Warszawskiej) i owczych BM-MSC, traktowanych/ lub nie FGF-2 i BMP-2. Badano wpływ FGF-2 i BMP-2 na potencjał osteogeny komórek hodowanych na rusztowaniu *in vitro* i *in vivo* w eksperymentalnym modelu owcy. Badania *in vitro* wykazały, że prekondycjonowanie komórek FGF-2 i BMP-2 zwiększało ich zdolność do osadzania się i proliferacji na rusztowaniu kompozytowym. Za pomocą barwienia czerwienią alizarinową, oceny aktywności ALP oraz poziomu ekspresji markerów osteogennych, wykazano, że BM-MSC hodowane na rusztowaniu i traktowane obiema cytokinami mają zdecydowanie większą zdolność do różnicowania w kierunku komórek tkanki kostnej niż w przypadku braku suplementacji medium hodowlanego. Pilotażowe badania *in vivo* (procedury chirurgiczne zostały wykonane na Wydziale Medycyny Weterynaryjnej Uniwersytetu Przyrodniczego we Wrocławiu) pokazały, że wytworzony konstrukt inżynierii tkankowej był biokompatybilny z tkankami owcy i indukował regenerację kości, co potwierdzono obecnością białek osteogennych kolagenu I i osteokalcyny w obrębie wszczepionego bioimplantu oraz brakiem podwyższonego poziomu cytokin prozapalnych w surowicach owiec po operacjach chirurgicznych.

Trzecia publikacja (Cells 2021, 10(8):1925) opisuje kompleksowy proces tworzenia konstruktów biologicznie czynnych w inżynierii tkanki kostnej. Praca podsumowuje najnowsze osiągnięcia w zastosowaniu MSC, różnego rodzaju rusztowań komórkowych (ceramicznych, polimerowych, czy kompozytowych) oraz cytokin wspomagających osteogenezę w regeneracji kości. Ponadto, przedstawiono przykłady przedklinicznych badań *in vivo* na zwierzętach oraz badania kliniczne z ostatniej dekady.

Badania przeprowadzone w ramach niniejszej dysertacji doktorskiej wykazały, że stymulacja owczych BM-MSC cytokinami FGF-2 i BMP-2 zwiększała ich potencjał osteogeny w hodowli standardowej 2D, jak również 3D z wykorzystaniem rusztowania kompozytowego. Badany biomateriał wspierał adhezję i proliferację BM-MSC, a ponadto był biokompatybilny, co potwierdzono badaniami *in vivo*. Pilotażowe badania nad implantacją konstruktów rusztowanie-BM-MSC do tkanek owcy wskazały na korzystny efekt indukcji osteogennej w obszarze wszczepionego bioimplantu. Podsumowując, przeprowadzone badania interdyscyplinarne wykazały, że zastosowany konstrukt inżynierii tkankowej posiada właściwości proosteogenne i może przynieść oczekiwane efekty terapeutyczne w naprawie dużych ubytków kostnych.

Summary

The number of people suffering from bone injuries caused by traffic accidents, osteoporotic fractures, skeletal diseases, or tumor resections, is steadily increasing worldwide. Despite the fact that bone tissue has the ability to self-renew, about 10-20% of fractures heal abnormally or not at all. These abnormalities can lead to critical-sized bone defects, more than 1-2 cm long, covering more than half of the bone's diameter. At present, they remain the most difficult problem in orthopedic surgery, as well as a huge economic burden on the health care system, despite modern treatments with high technological standards.

Modern therapies for large bone defects are based on bone grafts, including autologous, allogenic and synthetic grafts. However, for critical-sized bone defects, autologous bone grafts are inapplicable due to limited bone supply, while readily available allografts can induce an immune response. Synthetic grafts, on the other hand, are freely available, but the process of osteointegration of the implant is slowed down, and the material itself lacks osteogenic properties. Consequently, new alternative treatments are being sought, among which a promising approach is the use of tissue engineering constructs, consisting of a bioimplant with osteogenic cells and biologically active agents.

The end of the last century brought a rapid development of research on the biology of mesenchymal stem cells (MSCs) and their potential application in regenerative medicine. MSCs have attracted an attention because of their ability to undergo multilineage differentiation, including osteogenic differentiation. However, regeneration of large bone defects using only cell therapies often fails because there is lack of matrix on which the cells can form 3D structures, similarly as in their natural tissue environment. This problem can be solved by creating a tissue engineering construct consisting of a biocompatible cell scaffold and MSCs with enhanced osteogenic potential.

The objectives of the doctoral dissertation were: 1) biological characterization of ovine bone marrow-derived mesenchymal stem cells (BM-MSCs); 2) evaluation of the effect of osteogenic stimulation of BM-MSCs with the cytokines FGF-2 and BMP-2; 3) characterization of the osteogenic properties of the scaffold-BM-MSCs construct stimulated with FGF-2 and BMP-2 *in vitro*; 4) evaluation of the biocompatibility and osteogenic potential of the scaffold-BM-MSCs construct after heterotopic implantation into tissues in the ovine mandibular region.

The dissertation is a series of thematically related works in the form of three scientific publications. The results of the research are presented in two original articles, while the review

publication summarizes the current state of knowledge on the use of MSCs, scaffolds and biologically active factors in bone tissue regeneration.

The first publication (IJMS, 2020, 21(24):9726) includes studies of the biological properties of sheep BM-MSCs, which have been insufficiently characterized to date. In addition, the effect of FGF-2 and BMP-2 on the osteogenic potential of BM-MSCs *in vitro* was investigated. Baseline studies included evaluation of the phenotype, morphology, proliferation, ability to differentiate into bone, cartilage and adipose tissue cells, and secretory profile of ovine BM-MSCs under control culture conditions and after stimulation with FGF-2 or FGF-2 in combination with BMP-2. To investigate the effect of cytokines on the ability of BM-MSCs to differentiate into bone tissue cells, the presence of osteogenesis-related proteins collagen type I and osteocalcin was assessed by immunofluorescence staining, and the mRNA expression levels of genes encoding proteins of the early stages of osteogenic differentiation were analyzed: *BMP-2*, *Runx2*, *osterix*, *type I collagen*, and late markers of osteogenesis: *osteocalcin* and *osteopontin*. MSCs isolated from sheep bone marrow, preconditioned with FGF-2 and BMP-2, were shown to maintain their primary MSCs properties, as evidenced by the presence of surface markers CD73, CD90 and CD105 and the absence of expression of hematopoietic cell markers CD34, CD45 and major histocompatibility complex class II (DR) antigen. Stimulation with cytokines resulted in a more efficient proliferation rate, compared to untreated cells. Synergistic pro-osteogenic effects of FGF-2 and BMP-2 on BM-MSCs were observed, confirmed by alizarin red staining of calcium deposits and increased fluorescence intensity of osteogenic proteins: collagen I and osteocalcin. In addition, stimulation of BM-MSCs with cytokines FGF-2 and BMP-2 induced an increase in mRNA expression levels of genes of all analyzed osteogenic markers. It was also shown that sheep BM-MSCs produced biologically active factors, including those involved in osteogenesis (e.g., decorin), and stimulation of the cells with FGF-2 and BMP-2 modulated their secretory profile.

In the second publication (Cells, 2022, 11(21):3446), a tissue engineering construct consisting of a PCL/HAP/ β -TCP scaffold coated with a n-HAP layer (fabricated at the Department of Materials Science and Engineering, Warsaw University of Technology) and sheep BM-MSCs treated with/ or without FGF-2 and BMP-2 was developed. The effects of FGF-2 and BMP-2 on the osteogenic potential of cells cultured on the scaffold were studied *in vitro* and *in vivo* in an experimental sheep model. *In vitro* studies showed that preconditioning the cells with FGF-2 and BMP-2 increased their ability to deposit and proliferate on the scaffold. Using alizarin red staining, assessment of ALP activity and expression levels

of osteogenic markers, BM-MSCs cultured on the scaffold and treated with both cytokines were shown to have a significantly higher capacity to differentiate into bone tissue cells than in the absence of culture medium supplementation. The pilot *in vivo* studies (surgical procedures were performed at the Faculty of Veterinary Medicine, Wrocław University of Life Sciences) have shown that the fabricated tissue engineering construct was biocompatible with sheep tissues and induced bone regeneration, as confirmed by the presence of the osteogenic proteins collagen type I and osteocalcin within the implanted bioimplant and the absence of elevated levels of pro-inflammatory cytokines in sheep serum after surgical operations.

The third publication (Cells 2021, 10(8):1925) describes the complex process of creating biologically active constructs for bone tissue engineering. The paper summarizes the latest developments in the use of MSCs, various types of scaffolds (ceramic, polymeric, or composite), and cytokines to promote osteogenesis in bone regeneration. In addition, examples of preclinical *in vivo* animal studies and clinical trials from the last decade are presented.

Studies conducted within this doctoral dissertation showed that stimulation of ovine BM-MSCs with FGF-2 and BMP-2 cytokines increased their osteogenic potential in 2D standard culture, as well as in 3D culture using a composite scaffold. The tested biomaterial promoted BM-MSCs adhesion and proliferation, and was biocompatible, as confirmed by *in vivo* studies. Pilot studies on implantation of the scaffold-BM-MSCs construct into sheep tissues indicated a beneficial effect of osteogenic induction in the area of the implanted bioimplant. In conclusion, the interdisciplinary research showed that the applied tissue engineering construct possesses pro-osteogenic properties and can bring the expected therapeutic effects in the repair of large bone defects.

List of publications

- 1) **Sandra Gromolak** (currently **Stamnitz**), Agnieszka Krawczenko, Agnieszka Antończyk, Krzysztof Buczak, Zdzisław Kielbowicz, Aleksandra Klimczak. Biological Characteristics and Osteogenic Differentiation of Ovine Bone Marrow Derived Mesenchymal Stem Cells Stimulated with FGF-2 and BMP-2. *International Journal of Molecular Sciences*. 2020, 21(24):9726.
Impact Factor = 5.924.
- 2) **Sandra Stamnitz**, Agnieszka Krawczenko, Urszula Szałaj, Żaneta Górecka, Agnieszka Antończyk, Zdzisław Kielbowicz, Wojciech Świążkowski, Witold Łojkowski, Aleksandra Klimczak. Osteogenic Potential of Sheep Mesenchymal Stem Cells Preconditioned with BMP-2 and FGF-2 and Seeded on an nHAP-Coated PCL/HAP/ β -TCP Scaffold. *Cells*. 2022, 11(21):3446.
Impact Factor = 7.666.
- 3) **Sandra Stamnitz**, Aleksandra Klimczak. Mesenchymal Stem Cells, Bioactive Factors, and Scaffolds in Bone Repair: From Research Perspectives to Clinical Practice. *Cells*. 2021, 10(8):1925.
Impact Factor = 7.666.

Co-authors' declarations

07.11.2022 r.

Sandra Starnitz

Laboratory of Biology of Stem and Neoplastic Cells,
Hirsfeld Institute of Immunology and Experimental Therapy, Polish Academy of Sciences,
R. Weigla 12, 53-114 Wrocław, Poland

Declaration

I hereby declare that my contribution to the following manuscript:

Sandra Gromolak (currently Starnitz), Agnieszka Krawczenko, Agnieszka Antończyk, Krzysztof Buczak, Zdzisław Kielbowicz, Aleksandra Klimczak. Biological Characteristics and Osteogenic Differentiation of Ovine Bone Marrow Derived Mesenchymal Stem Cells Stimulated with FGF-2 and BMP-2. International Journal of Molecular Sciences. 2020, 21(24):9726

is correctly characterized in the table below.

Contributor	Contribution [%]	Description of main tasks
Sandra Starnitz	60%	conceptualization; methodology: cell isolation and culture, MTT assay, flow cytometry analysis, immunofluorescence staining, RT-PCR, real-time PCR, cell differentiation, cytokine array, statistical analysis; data curation and visualization; formal analysis; writing—original draft preparation
Agnieszka Krawczenko	10%	methodology: cell isolation, real-time PCR, cytokine array; formal analysis
Agnieszka Antończyk	5%	methodology: anesthesia, sheep bone marrow aspiration
Krzysztof Buczak	5%	methodology: sheep bone marrow aspiration
Zdzisław Kielbowicz	5%	supervision; funding acquisition
Aleksandra Klimczak	15%	conceptualization; formal analysis; data curation; writing—review and editing; supervision; funding acquisition

.....Starnitz.....

07.11.2022 r.

Agnieszka Krawczenko

Laboratory of Biology of Stem and Neoplastic Cells,
Hirsfeld Institute of Immunology and Experimental Therapy, Polish Academy of Sciences,
R. Weigla 12, 53-114 Wrocław, Poland

Declaration

I hereby declare that my contribution to the following manuscript:

Sandra Gromolak (currently Stammitz), Agnieszka Krawczenko, Agnieszka Antończyk, Krzysztof Buczak, Zdzisław Kielbowicz, Aleksandra Klimczak. Biological Characteristics and Osteogenic Differentiation of Ovine Bone Marrow Derived Mesenchymal Stem Cells Stimulated with FGF-2 and BMP-2. International Journal of Molecular Sciences. 2020, 21(24):9726

is correctly characterized in the table below.

Contributor	Contribution [%]	Description of main tasks
Sandra Stammitz	60%	conceptualization; methodology: cell isolation and culture, MTT assay, flow cytometry analysis, immunofluorescence staining, RT-PCR, real-time PCR, cell differentiation, cytokine array, statistical analysis; data curation and visualization; formal analysis; writing—original draft preparation
Agnieszka Krawczenko	10%	methodology: cell isolation, real-time PCR, cytokine array; formal analysis
Agnieszka Antończyk	5%	methodology: anesthesia, sheep bone marrow aspiration
Krzysztof Buczak	5%	methodology: sheep bone marrow aspiration
Zdzisław Kielbowicz	5%	supervision; funding acquisition
Aleksandra Klimczak	15%	conceptualization; formal analysis; data curation; writing—review and editing; supervision; funding acquisition

.....A. Krawczenko.....

07.11.2022 r.

Agnieszka Antończyk

Department of Surgery, Faculty of Veterinary Medicine,
Wrocław University of Environmental and Life Sciences,
pl. Grunwaldzki 51, 50-366 Wrocław, Poland

Declaration

I hereby declare that my contribution to the following manuscript:

Sandra Gromolak (currently Stammnitz), Agnieszka Krawczenko, Agnieszka Antończyk, Krzysztof Buczak, Zdzisław Kielbowicz, Aleksandra Klimczak. Biological Characteristics and Osteogenic Differentiation of Ovine Bone Marrow Derived Mesenchymal Stem Cells Stimulated with FGF-2 and BMP-2. International Journal of Molecular Sciences. 2020, 21(24):9726

is correctly characterized in the table below.

Contributor	Contribution [%]	Description of main tasks
Sandra Stammnitz	60%	conceptualization; methodology: cell isolation and culture, MTT assay, flow cytometry analysis, immunofluorescence staining, RT-PCR, real-time PCR, cell differentiation, cytokine array, statistical analysis; data curation and visualization; formal analysis; writing—original draft preparation
Agnieszka Krawczenko	10%	methodology: cell isolation, real-time PCR, cytokine array; formal analysis
Agnieszka Antończyk	5%	methodology: anesthesia, sheep bone marrow aspiration
Krzysztof Buczak	5%	methodology: sheep bone marrow aspiration
Zdzisław Kielbowicz	5%	supervision; funding acquisition
Aleksandra Klimczak	15%	conceptualization; formal analysis; data curation; writing—review and editing; supervision; funding acquisition

Agnieszka Antończyk

07.11.2022 r.

Krzysztof Buczak

Department of Surgery, Faculty of Veterinary Medicine,
Wroclaw University of Environmental and Life Sciences,
pl. Grunwaldzki 51, 50-366 Wroclaw, Poland

Declaration

I hereby declare that my contribution to the following manuscript:

Sandra Gromolak (currently Stammnitz), Agnieszka Krawczenko, Agnieszka Antończyk, Krzysztof Buczak, Zdzisław Kielbowicz, Aleksandra Klimczak. Biological Characteristics and Osteogenic Differentiation of Ovine Bone Marrow Derived Mesenchymal Stem Cells Stimulated with FGF-2 and BMP-2. International Journal of Molecular Sciences. 2020, 21(24):9726

is correctly characterized in the table below.

Contributor	Contribution [%]	Description of main tasks
Sandra Stammnitz	60%	conceptualization; methodology: cell isolation and culture, MTT assay, flow cytometry analysis, immunofluorescence staining, RT-PCR, real-time PCR, cell differentiation, cytokine array, statistical analysis; data curation and visualization; formal analysis; writing—original draft preparation
Agnieszka Krawczenko	10%	methodology: cell isolation, real-time PCR, cytokine array; formal analysis
Agnieszka Antończyk	5%	methodology: anesthesia, sheep bone marrow aspiration
Krzysztof Buczak	5%	methodology: sheep bone marrow aspiration
Zdzisław Kielbowicz	5%	supervision; funding acquisition
Aleksandra Klimczak	15%	conceptualization; formal analysis; data curation; writing—review and editing; supervision; funding acquisition

Buczak

.....

07.11.2022 r.

Zdzisław Kielbowicz

Department of Surgery, Faculty of Veterinary Medicine,
Wroclaw University of Environmental and Life Sciences,
pl. Grunwaldzki 51, 50-366 Wroclaw, Poland

Declaration

I hereby declare that my contribution to the following manuscript:

Sandra Gromolak (currently Stammitz), Agnieszka Krawczenko, Agnieszka Antończyk, Krzysztof Buczak, Zdzisław Kielbowicz, Aleksandra Klimczak. Biological Characteristics and Osteogenic Differentiation of Ovine Bone Marrow Derived Mesenchymal Stem Cells Stimulated with FGF-2 and BMP-2. International Journal of Molecular Sciences. 2020, 21(24):9726

is correctly characterized in the table below.

Contributor	Contribution [%]	Description of main tasks
Sandra Stammitz	60%	conceptualization; methodology: cell isolation and culture, MTT assay, flow cytometry analysis, immunofluorescence staining, RT-PCR, real-time PCR, cell differentiation, cytokine array, statistical analysis; data curation and visualization; formal analysis; writing—original draft preparation
Agnieszka Krawczenko	10%	methodology: cell isolation, real-time PCR, cytokine array; formal analysis
Agnieszka Antończyk	5%	methodology: anesthesia, sheep bone marrow aspiration
Krzysztof Buczak	5%	methodology: sheep bone marrow aspiration
Zdzisław Kielbowicz	5%	supervision; funding acquisition
Aleksandra Klimczak	15%	conceptualization; formal analysis; data curation; writing—review and editing; supervision; funding acquisition

KIEROWNIK
Katedry i Kliniki Chirurgii
Uniwersytetu Przyrodniczego we Wrocławiu

Prof. dr hab. Zdzisław Kielbowicz

07.11.2022 r.

Aleksandra Klimczak

Laboratory of Biology of Stem and Neoplastic Cells,
Hirszfeld Institute of Immunology and Experimental Therapy, Polish Academy of Sciences,
R. Weigla 12, 53-114 Wrocław, Poland


Declaration

I hereby declare that my contribution to the following manuscript:

Sandra Gromolak (currently Stammnitz), Agnieszka Krawczenko, Agnieszka Antończyk, Krzysztof Buczak, Zdzisław Kielbowicz, Aleksandra Klimczak. Biological Characteristics and Osteogenic Differentiation of Ovine Bone Marrow Derived Mesenchymal Stem Cells Stimulated with FGF-2 and BMP-2. International Journal of Molecular Sciences. 2020, 21(24):9726

is correctly characterized in the table below.

Contributor	Contribution [%]	Description of main tasks
Sandra Stammnitz	60%	conceptualization; methodology: cell isolation and culture, MTT assay, flow cytometry analysis, immunofluorescence staining, RT-PCR, real-time PCR, cell differentiation, cytokine array, statistical analysis; data curation and visualization; formal analysis; writing—original draft preparation
Agnieszka Krawczenko	10%	methodology: cell isolation, real-time PCR, cytokine array; formal analysis
Agnieszka Antończyk	5%	methodology: anesthesia, sheep bone marrow aspiration
Krzysztof Buczak	5%	methodology: sheep bone marrow aspiration
Zdzisław Kielbowicz	5%	supervision; funding acquisition
Aleksandra Klimczak	15%	conceptualization; formal analysis; data curation; writing—review and editing; supervision; funding acquisition


.....

07.11.2022 r.

Sandra Starnitz

Laboratory of Biology of Stem and Neoplastic Cells,
Hirsfeld Institute of Immunology and Experimental Therapy, Polish Academy of Sciences,
R. Weigla 12, 53-114 Wrocław, Poland

Declaration

I hereby declare that my contribution to the following manuscript:

Sandra Starnitz, Agnieszka Krawczenko, Urszula Szałaj, Żaneta Górecka, Agnieszka Antończyk, Zdzisław Kiełbowicz, Wojciech Świąszkowski, Witold Łojkowski, Aleksandra Klimczak. Osteogenic Potential of Sheep Mesenchymal Stem Cells Preconditioned with BMP-2 and FGF-2 and Seeded on an nHAP-Coated PCL/HAP/ β -TCP Scaffold. Cells 2022, 11(21):3446

is correctly characterized in the table below.

Contributor	Contribution [%]	Description of main tasks
Sandra Starnitz	50%	conceptualization; methodology: cell isolation and culture on the scaffold, DAPI staining, Picogreen assay, MTT assay, Alizarin Red S staining, ALP activity assay, real-time PCR, immunofluorescence staining, cytokine array, statistical analysis; data curation and visualization; formal analysis; writing—original draft preparation
Agnieszka Krawczenko	5%	methodology: real-time PCR, cytokine array; formal analysis
Urszula Szałaj	5%	methodology: fabrication of the scaffold; data curation and visualization
Żaneta Górecka	5%	methodology: fabrication of the scaffold; data curation
Agnieszka Antończyk	5%	methodology: anesthesia, sheep bone marrow aspiration, data curation and visualization
Zdzisław Kiełbowicz	5%	animal surgery; supervision; formal analysis; funding acquisition
Wojciech Świąszkowski	5%	supervision; formal analysis; funding acquisition
Witold Łojkowski	5%	supervision; formal analysis
Aleksandra Klimczak	15%	conceptualization; formal analysis; data curation; writing—review and editing; supervision; funding acquisition

.....Starnitz.....

07.11.2022 r.

Agnieszka Krawczenko

Laboratory of Biology of Stem and Neoplastic Cells,
Hirszfeld Institute of Immunology and Experimental Therapy, Polish Academy of Sciences,
R. Weigla 12, 53-114 Wrocław, Poland

Declaration

I hereby declare that my contribution to the following manuscript:

Sandra Starnitz, Agnieszka Krawczenko, Urszula Szałaj, Żaneta Górecka, Agnieszka Antończyk, Zdzisław Kielbowicz, Wojciech Świążkowski, Witold Łojkowski, Aleksandra Klimczak. Osteogenic Potential of Sheep Mesenchymal Stem Cells Preconditioned with BMP-2 and FGF-2 and Seeded on an nHAP-Coated PCL/HAP/ β -TCP Scaffold. Cells 2022, 11(21):3446

is correctly characterized in the table below.

Contributor	Contribution [%]	Description of main tasks
Sandra Starnitz	50%	conceptualization; methodology: cell isolation and culture on the scaffold, DAPI staining, Picogreen assay, MTT assay, Alizarin Red S staining, ALP activity assay, real-time PCR, immunofluorescence staining, cytokine array, statistical analysis; data curation and visualization; formal analysis; writing—original draft preparation
Agnieszka Krawczenko	5%	methodology: real-time PCR, cytokine array; formal analysis
Urszula Szałaj	5%	methodology: fabrication of the scaffold; data curation and visualization
Żaneta Górecka	5%	methodology: fabrication of the scaffold; data curation
Agnieszka Antończyk	5%	methodology: anesthesia, sheep bone marrow aspiration, data curation and visualization
Zdzisław Kielbowicz	5%	animal surgery; supervision; formal analysis; funding acquisition
Wojciech Świążkowski	5%	supervision; formal analysis; funding acquisition
Witold Łojkowski	5%	supervision; formal analysis
Aleksandra Klimczak	15%	conceptualization; formal analysis; data curation; writing—review and editing; supervision; funding acquisition

A. Krawczenko

Urszula Szałaj

Affiliation:

1. Institute of High Pressure Physics, Polish Academy of Sciences, Sokołowska 29/37, 01-142 Warsaw, Poland
2. Faculty of Materials Engineering, Warsaw University of Technology, Wołoska 41, 02-507 Warsaw, Poland

Declaration

I hereby declare that my contribution to the following manuscript:

Sandra Stamnitz, Agnieszka Krawczenko, Urszula Szałaj, Żaneta Górecka, Agnieszka Antończyk, Zdzisław Kielbowicz, Wojciech Świąszkowski, Witold Łojkowski, Aleksandra Klimczak. Osteogenic Potential of Sheep Mesenchymal Stem Cells Preconditioned with BMP-2 and FGF-2 and Seeded on an nHAP-Coated PCL/HAP/ β -TCP Scaffold. *Cells* 2022, 11(21):3446

is correctly characterized in the table below.

Contributor	Contribution [%]	Description of main tasks
Sandra Stamnitz	50%	conceptualization; methodology: cell isolation and culture on the scaffold, DAPI staining, Picogreen assay, MTT assay, Alizarin Red S staining, ALP activity assay, real-time PCR, immunofluorescence staining, cytokine array, statistical analysis; data curation and visualization; formal analysis; writing—original draft preparation
Agnieszka Krawczenko	5%	methodology: real-time PCR, cytokine array; formal analysis
Urszula Szałaj	5%	methodology: fabrication of the scaffold; data curation and visualization
Żaneta Górecka	5%	methodology: fabrication of the scaffold; data curation
Agnieszka Antończyk	5%	methodology: anesthesia, sheep bone marrow aspiration, data curation and visualization
Zdzisław Kielbowicz	5%	animal surgery; supervision; formal analysis; funding acquisition
Wojciech Świąszkowski	5%	supervision; formal analysis; funding acquisition

Witold Łojkowski	5%	supervision; formal analysis
Aleksandra Klimczak	15%	conceptualization; formal analysis; data curation; writing—review and editing; supervision; funding acquisition

Witold Łojkowski

07.11.2022 r.

Żaneta Górecka

Division of Materials Design, Faculty of Materials Science and Engineering,
Warsaw University of Technology,
141 Woloska Str., 02-507 Warsaw, Poland

Declaration

I hereby declare that my contribution to the following manuscript:

Sandra Stammnitz, Agnieszka Krawczenko, Urszula Szałaj, Żaneta Górecka, Agnieszka Antończyk, Zdzisław Kielbowicz, Wojciech Świążkowski, Witold Łojkowski, Aleksandra Klimczak. Osteogenic Potential of Sheep Mesenchymal Stem Cells Preconditioned with BMP-2 and FGF-2 and Seeded on an nHAP-Coated PCL/HAP/ β -TCP Scaffold. Cells 2022, 11(21):3446

is correctly characterized in the table below.

Contributor	Contribution [%]	Description of main tasks
Sandra Stammnitz	50%	conceptualization; methodology: cell isolation and culture on the scaffold, DAPI staining, Picogreen assay, MTT assay, Alizarin Red S staining, ALP activity assay, real-time PCR, immunofluorescence staining, cytokine array, statistical analysis; data curation and visualization; formal analysis; writing—original draft preparation
Agnieszka Krawczenko	5%	methodology: real-time PCR, cytokine array; formal analysis
Urszula Szałaj	5%	methodology: fabrication of the scaffold; data curation and visualization
Żaneta Górecka	5%	methodology: fabrication of the scaffold; data curation
Agnieszka Antończyk	5%	methodology: anesthesia, sheep bone marrow aspiration, data curation and visualization
Zdzisław Kielbowicz	5%	animal surgery; supervision; formal analysis; funding acquisition
Wojciech Świążkowski	5%	supervision; formal analysis; funding acquisition
Witold Łojkowski	5%	supervision; formal analysis
Aleksandra Klimczak	15%	conceptualization; formal analysis; data curation; writing—review and editing; supervision; funding acquisition



07.11.2022 r.

Agnieszka Antończyk

Department of Surgery, Faculty of Veterinary Medicine,
Wroclaw University of Environmental and Life Sciences,
pl. Grunwaldzki 51, 50-366 Wroclaw, Poland

Declaration

I hereby declare that my contribution to the following manuscript:

Sandra Stammnitz, Agnieszka Krawczenko, Urszula Szałaj, Żaneta Górecka, Agnieszka Antończyk, Zdzisław Kiełbowicz, Wojciech Świążzkowski, Witold Łojkowski, Aleksandra Klimczak. Osteogenic Potential of Sheep Mesenchymal Stem Cells Preconditioned with BMP-2 and FGF-2 and Seeded on an nHAP-Coated PCL/HAP/ β -TCP Scaffold. Cells 2022, 11(21):3446

is correctly characterized in the table below.

Contributor	Contribution [%]	Description of main tasks
Sandra Stammnitz	50%	conceptualization; methodology: cell isolation and culture on the scaffold, DAPI staining, Picogreen assay, MTT assay, Alizarin Red S staining, ALP activity assay, real-time PCR, immunofluorescence staining, cytokine array, statistical analysis; data curation and visualization; formal analysis; writing—original draft preparation
Agnieszka Krawczenko	5%	methodology: real-time PCR, cytokine array; formal analysis
Urszula Szałaj	5%	methodology: fabrication of the scaffold; data curation and visualization
Żaneta Górecka	5%	methodology: fabrication of the scaffold; data curation
Agnieszka Antończyk	5%	methodology: anesthesia, sheep bone marrow aspiration, data curation and visualization
Zdzisław Kiełbowicz	5%	animal surgery; supervision; formal analysis; funding acquisition
Wojciech Świążzkowski	5%	supervision; formal analysis; funding acquisition
Witold Łojkowski	5%	supervision; formal analysis
Aleksandra Klimczak	15%	conceptualization; formal analysis; data curation; writing—review and editing; supervision; funding acquisition

Agnieszka Antończyk

07.11.2022 r.

Zdzisław Kielbowicz

Department of Surgery, Faculty of Veterinary Medicine,
Wroclaw University of Environmental and Life Sciences,
pl. Grunwaldzki 51, 50-366 Wroclaw, Poland

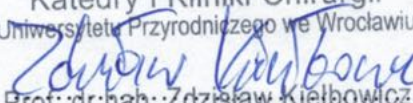
Declaration

I hereby declare that my contribution to the following manuscript:

Sandra Stamnitz, Agnieszka Krawczenko, Urszula Szałaj, Żaneta Górecka, Agnieszka Antończyk, Zdzisław Kielbowicz, Wojciech Świąszkowski, Witold Łojkowski, Aleksandra Klimczak. Osteogenic Potential of Sheep Mesenchymal Stem Cells Preconditioned with BMP-2 and FGF-2 and Seeded on an nHAP-Coated PCL/HAP/ β -TCP Scaffold. Cells 2022, 11(21):3446

is correctly characterized in the table below.

Contributor	Contribution [%]	Description of main tasks
Sandra Stamnitz	50%	conceptualization; methodology: cell isolation and culture on the scaffold, DAPI staining, Picogreen assay, MTT assay, Alizarin Red S staining, ALP activity assay, real-time PCR, immunofluorescence staining, cytokine array, statistical analysis; data curation and visualization; formal analysis; writing—original draft preparation
Agnieszka Krawczenko	5%	methodology: real-time PCR, cytokine array; formal analysis
Urszula Szałaj	5%	methodology: fabrication of the scaffold; data curation and visualization
Żaneta Górecka	5%	methodology: fabrication of the scaffold; data curation
Agnieszka Antończyk	5%	methodology: anesthesia, sheep bone marrow aspiration, data curation and visualization
Zdzisław Kielbowicz	5%	animal surgery; supervision; formal analysis; funding acquisition
Wojciech Świąszkowski	5%	supervision; formal analysis; funding acquisition
Witold Łojkowski	5%	supervision; formal analysis
Aleksandra Klimczak	15%	conceptualization; formal analysis; data curation; writing—review and editing; supervision; funding acquisition

KIEROWNIK
Katedry i Kliniki Chirurgii
Uniwersytetu Przyrodniczego we Wrocławiu

Prof. dr hab. Zdzisław Kielbowicz

07.11.2022 r.

Wojciech Świąszkowski

Division of Materials Design, Faculty of Materials Science and Engineering,
Warsaw University of Technology,
141 Woloska Str., 02-507 Warsaw, Poland

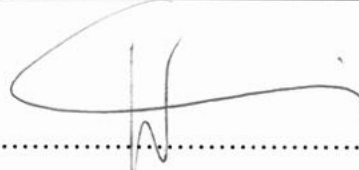
Declaration

I hereby declare that my contribution to the following manuscript:

Sandra Starnitz, Agnieszka Krawczenko, Urszula Szałaj, Żaneta Górecka, Agnieszka Antończyk, Zdzisław Kiełbowicz, Wojciech Świąszkowski, Witold Łojkowski, Aleksandra Klimczak. Osteogenic Potential of Sheep Mesenchymal Stem Cells Preconditioned with BMP-2 and FGF-2 and Seeded on an nHAP-Coated PCL/HAP/ β -TCP Scaffold. Cells 2022, 11(21):3446

is correctly characterized in the table below.

Contributor	Contribution [%]	Description of main tasks
Sandra Starnitz	50%	conceptualization; methodology: cell isolation and culture on the scaffold, DAPI staining, Picogreen assay, MTT assay, Alizarin Red S staining, ALP activity assay, real-time PCR, immunofluorescence staining, cytokine array, statistical analysis; data curation and visualization; formal analysis; writing—original draft preparation
Agnieszka Krawczenko	5%	methodology: real-time PCR, cytokine array; formal analysis
Urszula Szałaj	5%	methodology: fabrication of the scaffold; data curation and visualization
Żaneta Górecka	5%	methodology: fabrication of the scaffold; data curation
Agnieszka Antończyk	5%	methodology: anesthesia, sheep bone marrow aspiration, data curation and visualization
Zdzisław Kiełbowicz	5%	animal surgery; supervision; formal analysis; funding acquisition
Wojciech Świąszkowski	5%	supervision; formal analysis; funding acquisition
Witold Łojkowski	5%	supervision; formal analysis
Aleksandra Klimczak	15%	conceptualization; formal analysis; data curation; writing—review and editing; supervision; funding acquisition



.....

07.11.2022 r.

Witold Łojkowski

Laboratory of Nanostructures and Nanomedicine,
Institute of High Pressure Physics, Polish Academy of Sciences,
Sokolowska 29/37, 01-142 Warsaw, Poland

Declaration

I hereby declare that my contribution to the following manuscript:

Sandra Stannitz, Agnieszka Krawczenko, Urszula Szalaj, Żaneta Górecka, Agnieszka Antończyk, Zdzisław Kielbowicz, Wojciech Świążzkowski, Witold Łojkowski, Aleksandra Klimczak. Osteogenic Potential of Sheep Mesenchymal Stem Cells Preconditioned with BMP-2 and FGF-2 and Seeded on an nHAP-Coated PCL/HAP/ β -TCP Scaffold. *Cells* 2022, 11(21):3446

is correctly characterized in the table below.

Contributor	Contribution [%]	Description of main tasks
Sandra Stannitz	50%	conceptualization; methodology: cell isolation and culture on the scaffold, DAPI staining, Picogreen assay, MTT assay, Alizarin Red S staining, ALP activity assay, real-time PCR, immunofluorescence staining, cytokine array, statistical analysis; data curation and visualization; formal analysis; writing—original draft preparation
Agnieszka Krawczenko	5%	methodology: real-time PCR, cytokine array; formal analysis
Urszula Szalaj	5%	methodology: fabrication of the scaffold; data curation and visualization
Żaneta Górecka	5%	methodology: fabrication of the scaffold; data curation
Agnieszka Antończyk	5%	methodology: anesthesia, sheep bone marrow aspiration, data curation and visualization
Zdzisław Kielbowicz	5%	animal surgery; supervision; formal analysis; funding acquisition
Wojciech Świążzkowski	5%	supervision; formal analysis; funding acquisition
Witold Łojkowski	5%	supervision; formal analysis
Aleksandra Klimczak	15%	conceptualization; formal analysis; data curation; writing—review and editing; supervision; funding acquisition



07.11.2022 r.

Aleksandra Klimczak

Laboratory of Biology of Stem and Neoplastic Cells,
Hirszfeld Institute of Immunology and Experimental Therapy, Polish Academy of Sciences,
R. Weigla 12, 53-114 Wrocław, Poland

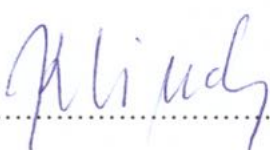
Declaration

I hereby declare that my contribution to the following manuscript:

Sandra Starnitz, Agnieszka Krawczenko, Urszula Szałaj, Żaneta Górecka, Agnieszka Antończyk, Zdzisław Kielbowicz, Wojciech Świążkowski, Witold Łojkowski, Aleksandra Klimczak. Osteogenic Potential of Sheep Mesenchymal Stem Cells Preconditioned with BMP-2 and FGF-2 and Seeded on an nHAP-Coated PCL/HAP/ β -TCP Scaffold. Cells 2022, 11(21):3446

is correctly characterized in the table below.

Contributor	Contribution [%]	Description of main tasks
Sandra Starnitz	50%	conceptualization; methodology: cell isolation and culture on the scaffold, DAPI staining, Picogreen assay, MTT assay, Alizarin Red S staining, ALP activity assay, real-time PCR, immunofluorescence staining, cytokine array, statistical analysis; data curation and visualization; formal analysis; writing—original draft preparation
Agnieszka Krawczenko	5%	methodology: real-time PCR, cytokine array; formal analysis
Urszula Szałaj	5%	methodology: fabrication of the scaffold; data curation and visualization
Żaneta Górecka	5%	methodology: fabrication of the scaffold; data curation
Agnieszka Antończyk	5%	methodology: anesthesia, sheep bone marrow aspiration, data curation and visualization
Zdzisław Kielbowicz	5%	animal surgery; supervision; formal analysis; funding acquisition
Wojciech Świążkowski	5%	supervision; formal analysis; funding acquisition
Witold Łojkowski	5%	supervision; formal analysis
Aleksandra Klimczak	15%	conceptualization; formal analysis; data curation; writing—review and editing; supervision; funding acquisition

.....


07.11.2022 r.

Sandra Stannitz

Laboratory of Biology of Stem and Neoplastic Cells,
Hirszfeld Institute of Immunology and Experimental Therapy, Polish Academy of Sciences,
R. Weigla 12, 53-114 Wrocław, Poland

Declaration

I hereby declare that my contribution to the following manuscript:

Sandra Stannitz, Aleksandra Klimczak. Mesenchymal Stem Cells, Bioactive Factors, and Scaffolds in Bone Repair: From Research Perspectives to Clinical Practice. *Cells*. 2021, 10(8):1925

is correctly characterized in the table below.

Contributor	Contribution [%]	Description of main tasks
Sandra Stannitz	70%	conceptualization; preparation of the tables; writing—original draft preparation
Aleksandra Klimczak	30%	conceptualization; preparation of the figure; writing—review and editing; supervision; funding acquisition

...Stannitz.....

07.11.2022 r.

Aleksandra Klimczak

Laboratory of Biology of Stem and Neoplastic Cells,
Hirszfeld Institute of Immunology and Experimental Therapy, Polish Academy of Sciences,
R. Weigla 12, 53-114 Wrocław, Poland


Declaration

I hereby declare that my contribution to the following manuscript:

Sandra Stammnitz, Aleksandra Klimczak. Mesenchymal Stem Cells, Bioactive Factors, and Scaffolds in Bone Repair: From Research Perspectives to Clinical Practice. *Cells*. 2021, 10(8):1925

is correctly characterized in the table below.

Contributor	Contribution [%]	Description of main tasks
Sandra Stammnitz	70%	conceptualization; preparation of the tables; writing—original draft preparation
Aleksandra Klimczak	30%	conceptualization; preparation of the figure; writing—review and editing; supervision; funding acquisition



.....

Publications



Article

Biological Characteristics and Osteogenic Differentiation of Ovine Bone Marrow Derived Mesenchymal Stem Cells Stimulated with FGF-2 and BMP-2

Sandra Gromolak ¹, Agnieszka Krawczenko ¹, Agnieszka Antończyk ², Krzysztof Buczak ², Zdzisław Kielbowicz ² and Aleksandra Klimczak ^{1,*}

¹ Laboratory of Biology of Stem and Neoplastic Cells, Hirszfeld Institute of Immunology and Experimental Therapy, Polish Academy of Sciences, R. Weigla 12, 53-114 Wrocław, Poland; sandra.gromolak@hirszfeld.pl (S.G.); agnieszka.krawczenko@hirszfeld.pl (A.K.)

² Department of Surgery, Faculty of Veterinary Medicine, Wrocław University of Environmental and Life Sciences, pl. Grunwaldzki 51, 50-366 Wrocław, Poland; agnieszka.antonczyk@upwr.edu.pl (A.A.); krzysztof.buczak@upwr.edu.pl (K.B.); zdzislaw.kielbowicz@upwr.edu.pl (Z.K.)

* Correspondence: aleksandra.klimczak@hirszfeld.pl

Received: 15 November 2020; Accepted: 17 December 2020; Published: 20 December 2020



Abstract: Cell-based therapies using mesenchymal stem cells (MSCs) are a promising tool in bone tissue engineering. Bone regeneration with MSCs involves a series of molecular processes leading to the activation of the osteoinductive cascade supported by bioactive factors, including fibroblast growth factor-2 (FGF-2) and bone morphogenetic protein-2 (BMP-2). In this study, we examined the biological characteristics and osteogenic differentiation potential of sheep bone marrow MSCs (BM-MSCs) treated with 20 ng/mL of FGF-2 and 100 ng/mL BMP-2 in vitro. The biological properties of osteogenic-induced BM-MSCs were investigated by assessing their morphology, proliferation, phenotype, and cytokine secretory profile. The osteogenic differentiation was characterized by Alizarin Red S staining, immunofluorescent staining of osteocalcin and collagen type I, and expression levels of genetic markers of osteogenesis. The results demonstrated that BM-MSCs treated with FGF-2 and BMP-2 maintained their primary MSC properties and improved their osteogenic differentiation capacity, as confirmed by increased expression of osteocalcin and collagen type I and upregulation of osteogenic-related gene markers *BMP-2*, *Runx2*, *osterix*, *collagen type I*, *osteocalcin*, and *osteopontin*. Furthermore, sheep BM-MSCs produced a variety of bioactive factors involved in osteogenesis, and supplementation of the culture medium with FGF-2 and BMP-2 affected the secretome profile of the cells. The results suggest that sheep osteogenic-induced BM-MSCs may be used as a cellular therapy to study bone repair in the preclinical large animal model.

Keywords: bone marrow MSCs; osteogenic differentiation; bone repair; large animal model

1. Introduction

Large bone defects and delayed fracture unions and non-unions, if not repaired effectively by the body, result in pain and lead to morbidity and prolonged, expensive hospitalization [1]. Moreover, bone disorders, such as osteoarthritis and osteoporosis, and the aging of the population constitute serious issues and challenging clinical problems. Thus, researchers are looking for new treatment modalities that will slow or prevent the development of these disorders [2]. Although orthopedic surgery has made great advances, the gold standard for bone defect repair is still dominated by autologous or allogeneic bone grafts. Nevertheless, clinical demands for bone grafts are far above

the available amounts of traditional, natural bone auto- and allo-grafts, especially considering the impending global problem of obesity and aging. Moreover, there are limitations related to bone allografts, such as donor site complications, inferior healing compared to autologous grafts, and risk of disease and infective agent transmission [3].

Recent advances in cell-based therapies for regenerative medicine have supported the development of mesenchymal stem cells (MSCs) as an effective and minimally invasive alternative in bone repair [4]. MSCs are an attractive candidate for clinical approaches because of their ability to self-renew and differentiate into multiple tissues, including bone, cartilage, and fat [5]. They are a key component of the bone repair process, representing the precursors for bone-forming osteoblasts and cartilage-forming chondrocytes and modulating the healing response [4]. The cellular and molecular signals of a bone defect correspond to the beginning stages of fracture healing, which involves, *inter alia*, the trafficking and activation of MSCs. Both innate and adaptive immune responses are modulated by MSCs. Therefore, MSCs not only provide progenitor cells, but also activate other cells involved in tissue regeneration via the paracrine effect, thereby modulating a favorable microenvironment and coordinating bone remodeling [6]. Molecular osteoinductive events in bone regeneration involve a variety of growth factors, cytokines, and chemokine signaling pathways, as well as the upregulation of genes involved in bone formation and mineralization [4,7].

Effective cellular therapy for bone regeneration employs MSCs and growth factors that enhance different steps of differentiation. Bone morphogenetic protein-2 (BMP-2) and fibroblast growth factor-2 (FGF-2) are two molecules that have a synergistic osteogenic effect on MSCs [7–10]. FGF-2 regulates the migration, proliferation, and differentiation of many cell types, including vascular endothelial cells and osteoblasts. There are studies demonstrating the potential of FGF-2 in promoting bone formation and angiogenesis [11–15]. Moreover, FGF-2 increases the BMP-2 osteoinductive potential by upregulating BMP-2 and its receptor expression level [10,16]. BMP-2 is a subtype of the BMP family of growth factors, which are mainly synthesized and secreted by osteoblasts [17]. BMP-2 regulates osteogenesis and induces MSCs to differentiate into cartilage and bone [18,19]. Furthermore, the United States Food and Drug Administration has approved the recombinant human bone morphogenetic protein-2 (rhBMP-2) for clinical applications [20,21]. However, the FGF-2/BMP-2 synergistic effect on bone regeneration is not fully explained, and requires further examination before safe clinical application can be achieved.

In the present study, we introduce the synergistic effect of FGF-2 and BMP-2 on the pro-osteogenic potential of bone marrow-derived mesenchymal stem cells (BM-MSCs) derived from sheep. Whereas rodents are the most widely used animal models for translational medicine, preclinical large animal models provide a better understanding of the mechanism of human diseases. For instance, when investigating musculoskeletal diseases, the thin cartilage and bones of rodents represent an inadequate volume and size of the defects, and the lack of the ability to manage long-term studies makes them less useful for preclinical studies than large animal models [22,23]. Therefore, we decided to use ovine BM-MSCs to study the effect of FGF-2 and BMP-2 on MSC proliferation, phenotype, osteogenesis-related proteins (osteocalcin and collagen type I) expression, multilineage differentiation, and, in particular, early and late osteogenesis-related gene marker expression. We also evaluated the cytokine expression level of BM-MSCs treated with FGF-2, with and without BMP-2. The comprehensive characteristics of ovine BM-MSCs make them good candidates for the study of bone reconstruction in veterinary medicine using a large animal model as a preclinical model in order to assess of the efficacy of cellular therapy in bone regeneration for potential application in clinical practice.

2. Results

2.1. Morphology of Sheep BM-MSCs

The ovine bone marrow-derived mesenchymal stem cells altered their morphology when cultured for 21 days in: (1) complete α MEM, (2) α MEM supplemented with FGF-2, (3) α MEM supplemented with FGF-2 and BMP-2, (4) osteogenic differentiation medium, (5) osteogenic differentiation medium

supplemented with FGF-2, and (6) osteogenic differentiation medium supplemented with FGF-2 and BMP-2. In the α MEM-cultured medium, deprived of additional cytokines, BM-MSCs showed a spindle-shaped morphology, typical for MSCs (Figure 1a). Likewise, in an α MEM medium supplemented with FGF-2, the cells were spindle-shaped, although they were smaller and denser (Figure 1c). However, the largest morphological differences were observed in the cell culture treated with both BMP-2 and FGF-2, where some cells grew into fine mesh-like structures, and some covered the cell monolayer rounded aggregates, resembling bone-like structures (Figure 1e). When BM-MSCs were cultured in an osteogenic differentiation medium, they exhibited calcium deposition, regardless of whether they were additionally stimulated with BMP-2 and/or FGF-2 (Figure 1b,d,f). Interestingly, the crystal formation in the osteogenic differentiation medium supplemented with BMP-2 and/or FGF-2 tended to be smaller, denser, and more dispersed throughout the monolayer (Figure 1d,f).

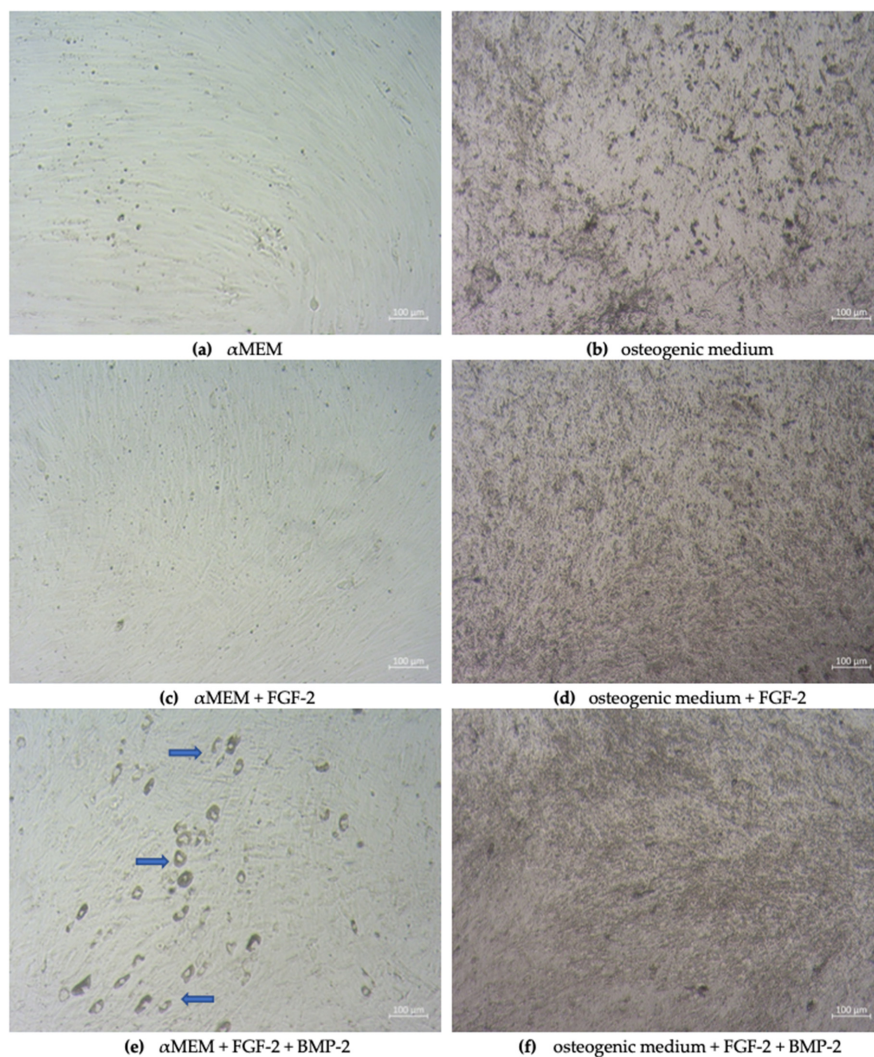


Figure 1. Morphological changes of sheep bone marrow-derived mesenchymal stem cells (BM-MSCs) in different culture conditions. BM-MSCs were cultivated in an α MEM or osteogenic differentiation medium, both supplemented with or without BMP-2 and/or FGF-2 for 21 days. In response to both stimuli (FGF-2 and BMP-2), the cells exhibited different cellular morphology compared to the control culture conditions, i.e., α MEM or osteogenic differentiation medium without any additional cytokines (a,b). Cells treated with FGF-2 were smaller and grew more densely (c). FGF-2 and BMP-2 added to the complete α MEM medium showed an osteogenic differentiation of the cells (e), and when added to the osteogenic differentiation medium, they altered the size and density of calcium acceleration (d,f).

2.2. Cell Proliferation and Doubling Time Analyzed with the MTT Assay

The proliferative activity of sheep BM-MSCs (passage 3) cultured in complete α MEM (control) and α MEM supplemented with BMP-2 and/or FGF-2 was evaluated using the MTT assay. Growth curves in the cells in all culture conditions appeared as a typical “S” curve and showed a latency phase of about 4 h after seeding. After 24 h of incubation, the cells proliferated rapidly and entered the logarithmic phase. After approximately 72 h, the BM-MSCs entered the plateau phase and began to degenerate (Figure 2a). Compared to the untreated cells (cultured in α MEM), the proliferation of the cells treated with BMP-2 and/or FGF-2 began to increase after 24 h, and this stimulatory effect increased during observation. The most efficient proliferative activity was observed in the cells treated with FGF-2, compared to control ($p < 0.005$).

The doubling time of ovine BM-MSCs differed depending on cell culture conditions (Figure 2b). BM-MSCs doubled their cell number significantly faster when cultured in a medium supplemented with BMP-2 and/or FGF-2, compared to the control α MEM without any additional cytokines. BM-MSCs treated with FGF-2 had the strongest cell proliferative ability.

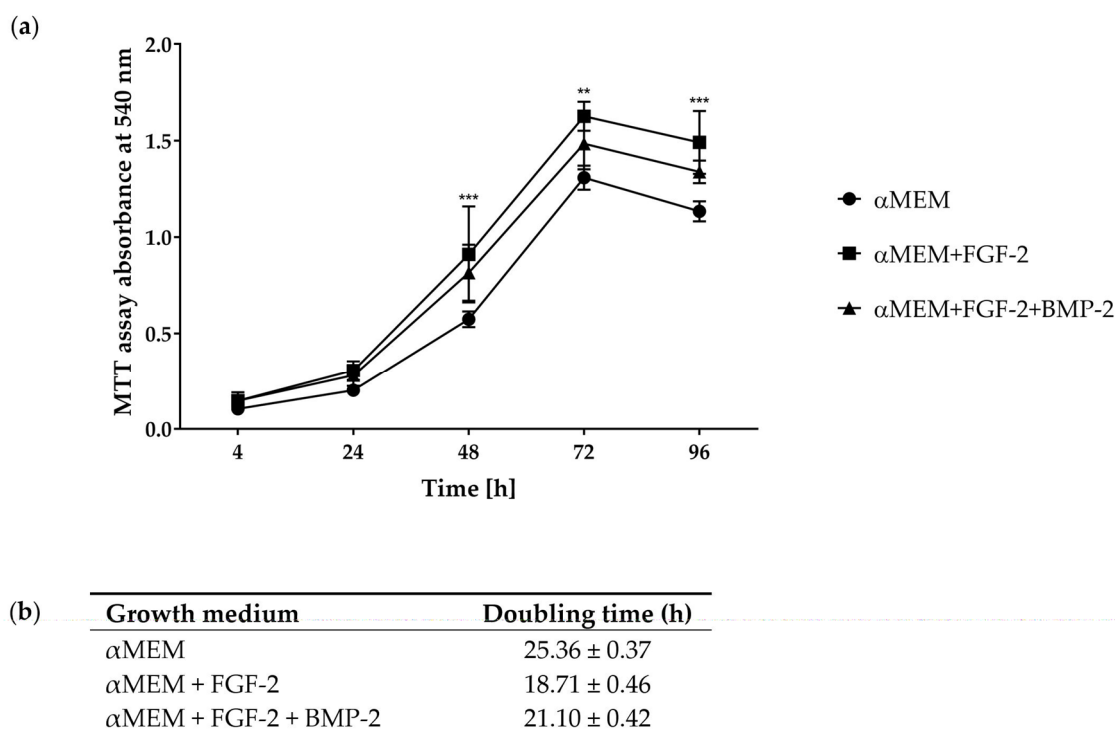


Figure 2. (a) Growth curves of sheep BM-MSCs treated with or without BMP-2 and/or FGF-2 assessed with the MTT assay. Compared to the cell control cultured in α MEM, the proliferation of BM-MSCs treated with BMP-2 and/or FGF-2 increased, whereas the proliferation of cells cultured in α MEM supplemented with FGF-2 was the highest. ** $p < 0.005$, *** $p < 0.0001$. (b) Doubling time of ovine BM-MSCs cultured in growth media supplemented with or without the cytokines FGF-2 and BMP-2 in three independent experiments performed in triplicate.

2.3. Immunophenotype of Sheep BM-MSCs in Different Culture Conditions

BM-MSCs from sheep bone marrow (passage 3) expressed the specific MSC surface markers CD73 and CD105 when cultured in the control medium α MEM and a medium supplemented with BMP-2 and/or FGF-2 on days 7 and 14 (Figure S1a,b in supplementary) and day 21 (Figure 3). The values of positive population ranged between 84% and 99%. The values of CD73 and CD105 for BM-MSCs cultured in α MEM with or without FGF-2 were at the same high level of above 91% of the population, regardless of culture time. On day 7, BM-MSCs cultured with FGF-2 and BMP-2 showed a lower level

of CD73 and CD105 positive cells (84–87%), compared to cells treated with FGF-2 alone or without any supplements (Figure S1a). The percentage of CD73-positive BM-MSCs increased over time for all cell populations cultured in three different conditions. The level of cells with the hematopoietic phenotype CD34 was very low, 1–6% of positive cells, among which the highest level of 5–6% was reported for the cells cultured for 14 days in α MEM with FGF-2 and BMP-2 and for the cells incubated for 21 days in the control medium α MEM. As with CD34, the common hematopoietic marker CD45 was also at a low level between 0–8% during observation. The major histocompatibility complex class II antigen HLA DR was detected at the beginning of the BM-MSCs culture (7 days) in the media supplemented with BMP-2 and/or FGF-2, with values ranging between 38% and 45% of the population, whereas in the control medium α MEM, the value was assessed at 4.5%. The level of HLA-DR-positive cells decreased over time, and on day 21 of culture, was assessed at below 1% in all culture conditions (Figure S1b).

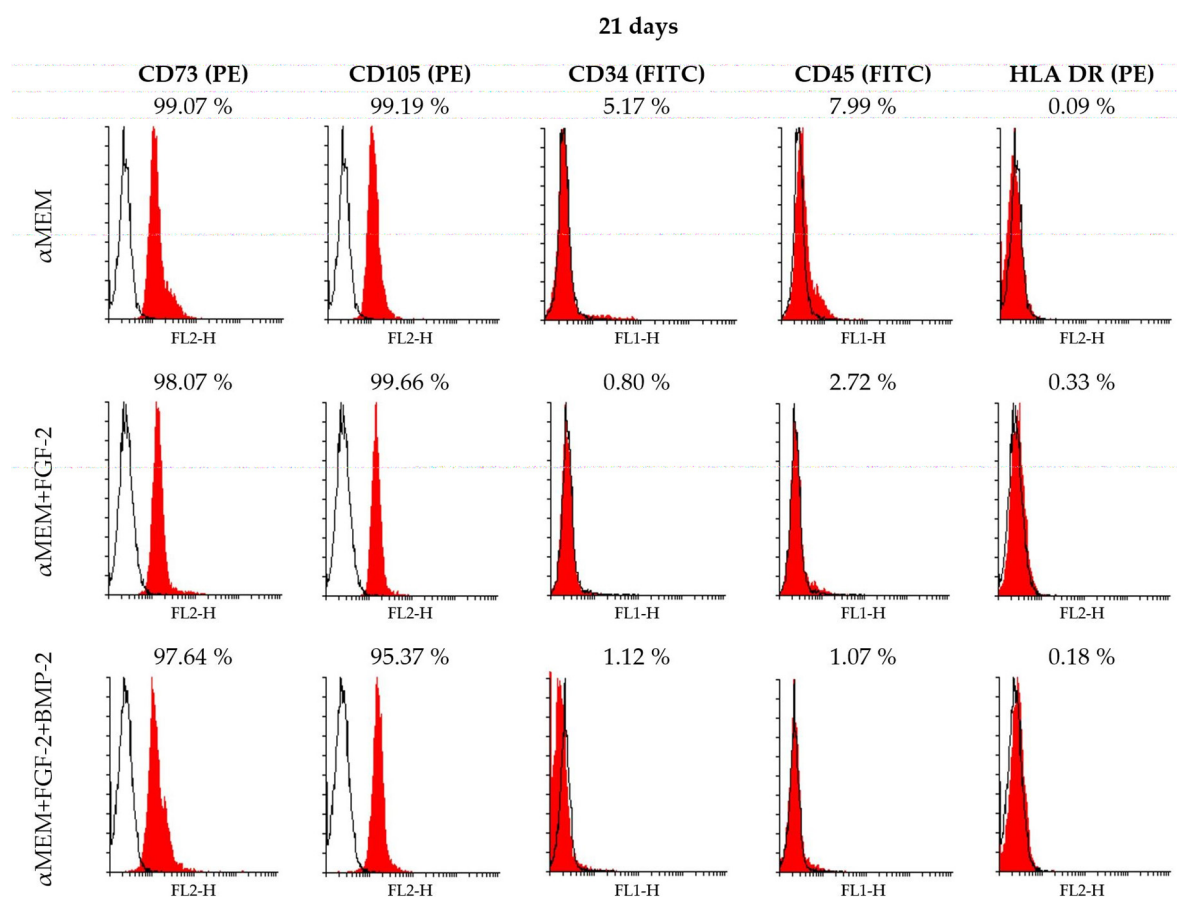


Figure 3. Flow cytometry analysis of BM-MSCs cultured in the control medium α MEM and in a medium supplemented with BMP-2 and/or FGF-2 for 21 days. The expression of the MSC-specific antigens CD73 and CD105 was detected for all cells cultured in different conditions. Cells expressing the hematopoietic markers CD34, CD45, and HLA DR were absent or detected at low levels on day 21 of observation in all culture conditions.

2.4. CD90 Expression Level in Sheep BM-MSCs

As there are no commercially available anti-CD90 antibodies reactive with ovine cells for flow cytometry, CD90 was assessed using reverse transcription polymerase chain reaction (RT-PCR). Differences in the *CD90/GAPDH* relative fold change level depended on the culture medium conditions. Gene expression for the MSC marker *CD90* was detected in all cells treated with or without BMP-2 and/or FGF-2. However, *CD90* expression was associated with culture medium supplementation, and the highest level of *CD90* was observed for BM-MSCs cultured in the complete α MEM medium,

whereas in the BM-MSCs treated with FGF-2 and BMP-2, *CD90* relative fold change was at the lowest level (6.51 vs. 2.95 on day 7; $p < 0.005$). The *CD90* expression remained at a similar level within the cells in the same culture conditions, regardless of incubation time (Figure 4).

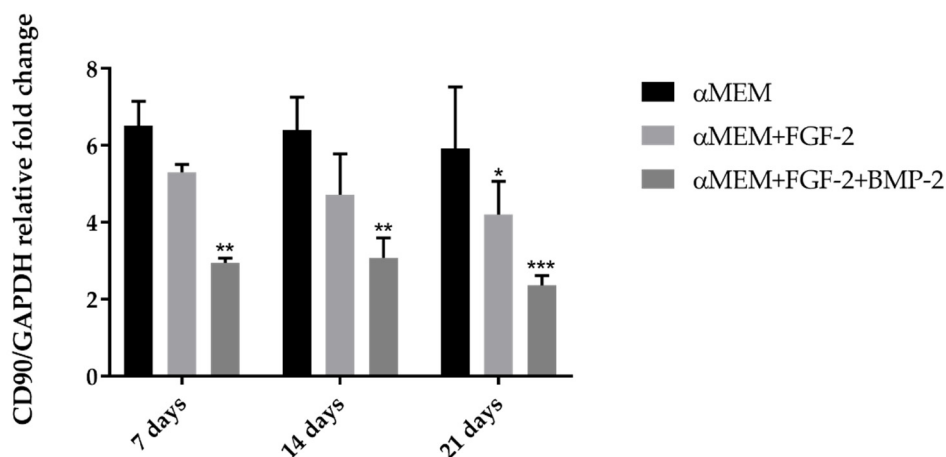


Figure 4. RT-PCR (reverse transcription polymerase chain reaction) analysis for *CD90* gene expression of BM-MSCs cultured in the α MEM medium supplemented with or without BMP-2 and/or FGF-2 for 7, 14, and 21 days. The highest level of *CD90* was observed in cells cultured in the control medium α MEM for all time points. In contrast, BM-MSCs treated with FGF-2 and BMP-2 were characterized with the lowest level of *CD90*. The experiment was assessed three times in duplicate. * $p < 0.05$, ** $p < 0.005$, *** $p < 0.0001$.

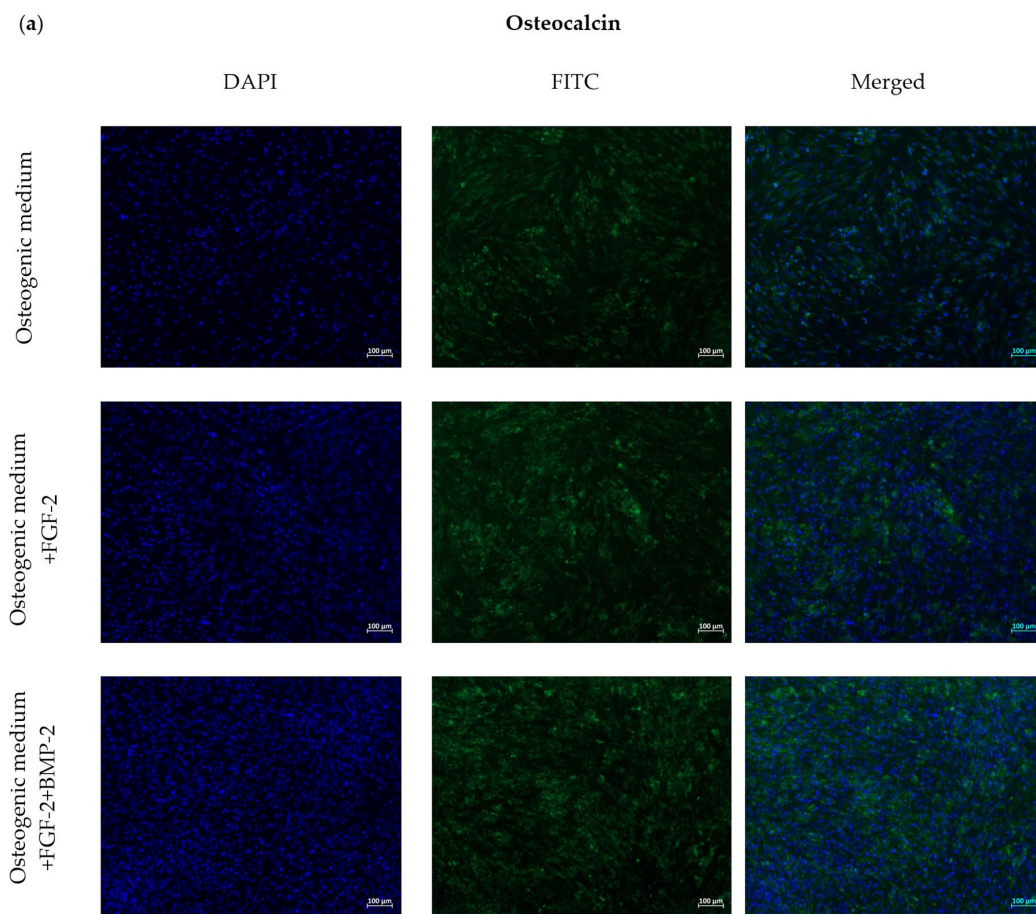
2.5. Assessment of Osteogenic Differentiation Markers

To assess the effect of FGF-2 and BMP-2 on the expression of osteogenesis-related proteins, immunofluorescent staining of osteocalcin and collagen type I was performed after 21 days of BM-MSC culture in an osteogenic differentiation medium as a control and an osteogenic differentiation medium supplemented with BMP-2 and/or FGF-2. The cells treated with BMP-2 and/or FGF-2 showed a moderately enhanced expression of both osteogenic differentiation markers compared to the control cells (Figure 5a,b). The immunofluorescence intensity of osteocalcin and collagen type I was higher in the cells treated with both BMP-2 and FGF-2 than in the cells treated with FGF-2 alone (Figure 5c,d).

2.6. Effect of BMP-2 and FGF-2 on mRNA Expression in Genes Involved in Osteogenic Differentiation

The gene expression of the early osteogenic differentiation markers: *bone morphogenetic protein-2* (*BMP-2*), *runt-related transcription factor 2* (*Runx2*), *osterix* (*Osx*), and *collagen type I* (*Col1*), and late osteogenic markers: *osteocalcin* (*Ocl*) and *osteopontin* (*Opn*), following 7, 14 and 21 days of incubation in the α MEM medium with BMP-2 and/or FGF-2, was analyzed as the effect of BMP-2 on sheep BM-MSCs in osteogenesis. The expression of *BMP-2* increased after 14 days of BM-MSC incubation in both cell culture conditions, compared to control. However, there were no significant differences in the expression level of this gene between 14 and 21 days of cell culture. BM-MSCs cultured 14 days in the medium with FGF-2 and BMP-2 exhibited a higher expression of *BMP-2* than those cultured in the medium with only FGF-2 (Figure 6a, RQ 3.97 vs. 2.34; $p < 0.0001$). The mRNA expression of *Runx2* increased over time from day 7 to 14 in the BM-MSCs cultured in the medium supplemented with FGF-2 and BMP-2 (Figure 6b, RQ 1.84 vs. 6.78; $p < 0.0001$), whereas in the cells cultured only with FGF-2, the expression level of *Runx2* was downregulated over time, but still higher than control. The highest peak in *Osx* gene expression was observed on day 14 in the BM-MSCs treated with FGF-2 and BMP-2 (Figure 6c, RQ 3.33; $p < 0.0001$); afterwards, on day 21, gene expression decreased. In the BM-MSCs treated only with FGF-2, the *Osx* expression level increased after 14 days of incubation and then decreased. In the control, *Osx* gene expression increased over time, and on day 21, it was even slightly

higher than in FGF-2-treated cells. *Col1* gene expression was upregulated in the BM-MSCs treated with FGF-2 or FGF-2 together with BMP-2 over time, and the highest expression level was reported after 21 days of incubation (Figure 6d RQ 5.19 and 4.25; $p < 0.0001$). Interestingly, *Col1* expression was also upregulated in the control on day 14, but decreased afterwards. The gene expression of the late osteogenic marker *Ocl* increased over time for both BM-MSCs treated with FGF-2 alone or FGF-2 with BMP-2; however, at the time point of 21 days, it was higher in the cells incubated with both FGF-2 and BMP-2 (Figure 6e, RQ 7.20 vs. 4.81; $p < 0.0001$). The effect of FGF-2 and BMP-2 on the expression level of the second late osteogenic marker *Opn* also differed from that for FGF-2-only supplementation without BMP-2. *Opn* expression increased over time in both stimulated BM-MSCs. Nevertheless, the BM-MSCs cultured in the medium with FGF-2 and BMP-2 exhibited a significantly higher expression level than those cultured only with FGF-2 (Figure 6f, RQ 4.18 vs. 2.59; $p < 0.0001$).



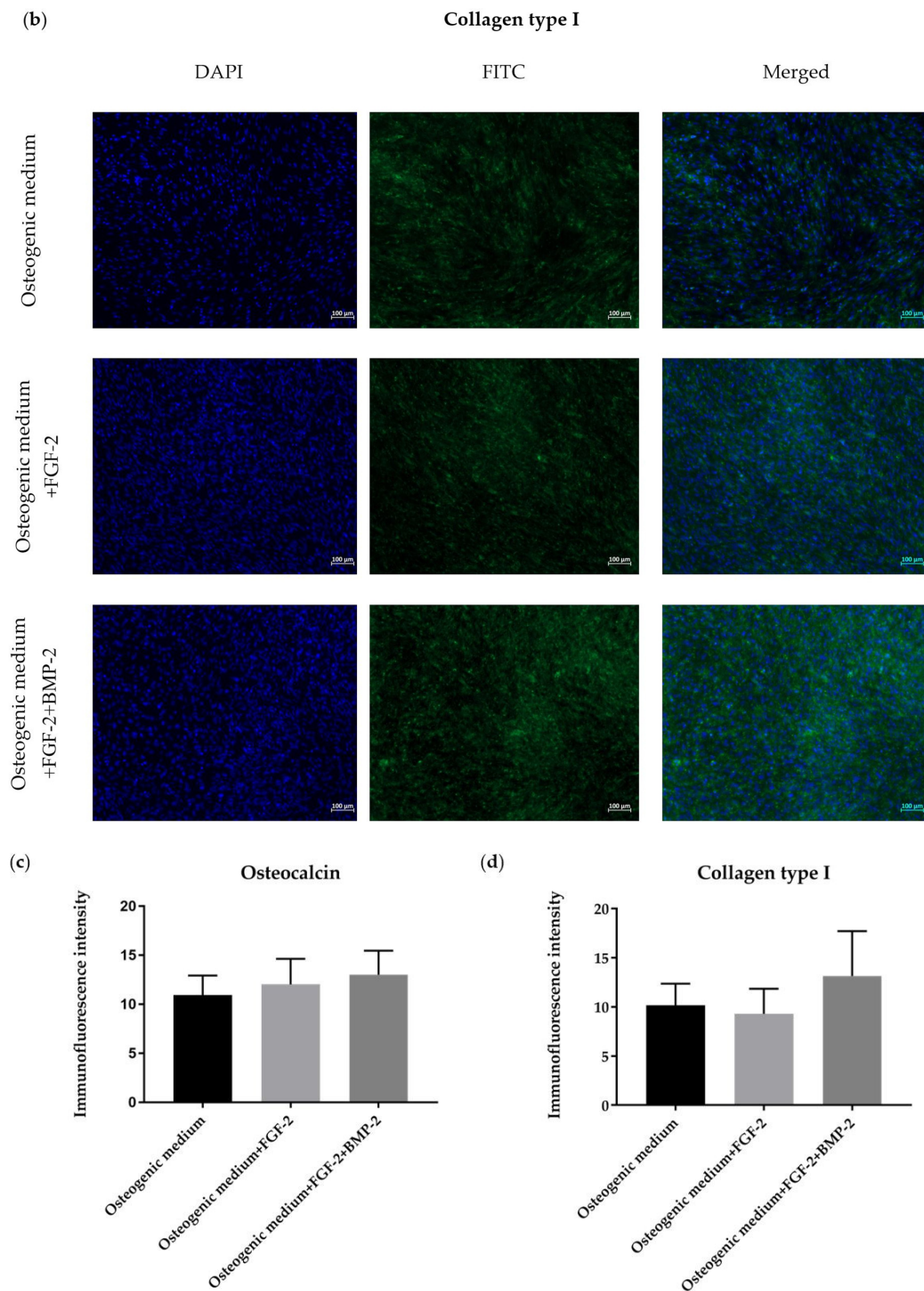


Figure 5. Representative images for the immunofluorescence staining of osteocalcin (Ocl) (a) and collagen type I (Coll) (b), expressed by BM-MSCs cultured in an osteogenic differentiation medium with or without BMP-2 and/or FGF-2 for 21 days. The Ocl and ColI were stained with FITC in green and nuclei in blue with DAPI. Immunofluorescence staining for osteocalcin (c) and collagen type I (d) was quantified using the ImageJ software. FGF-2 and BMP-2 promoted the expression of osteogenic-related proteins, which resulted in a moderately more intense fluorescence in the treated cells compared to the control cells cultured in the osteogenic differentiation medium alone.

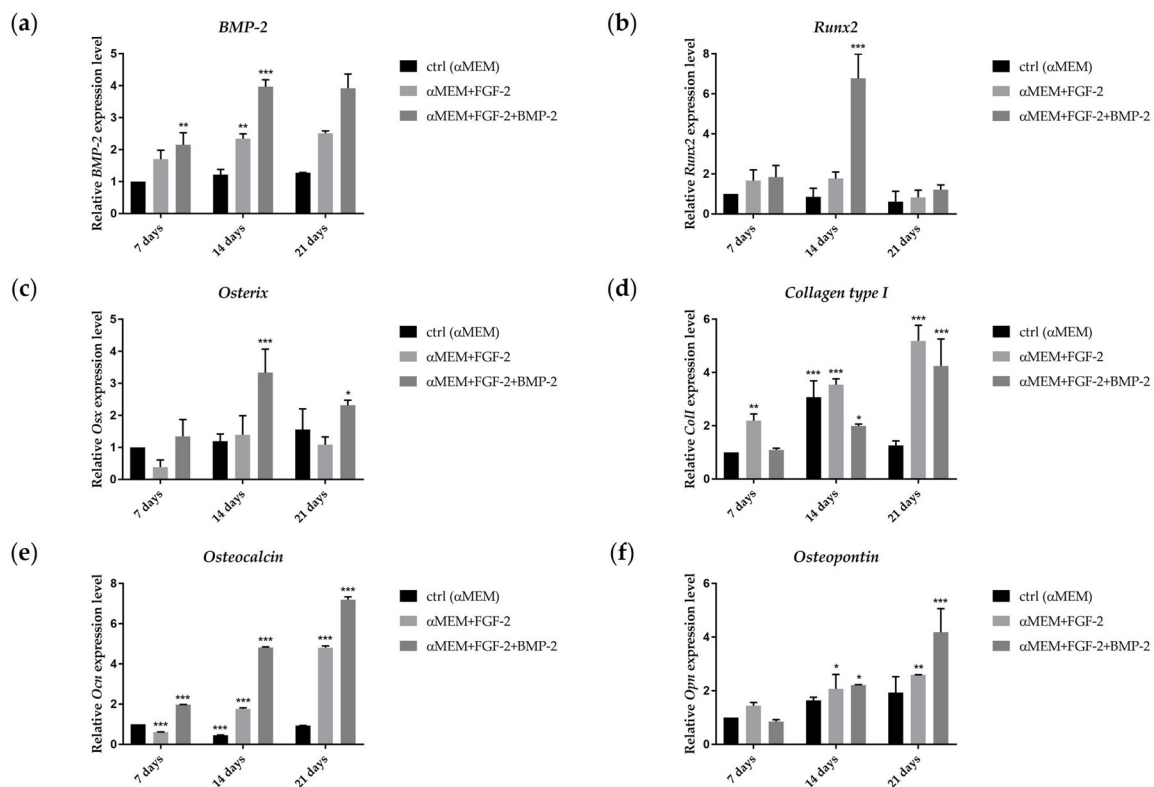


Figure 6. Real-time qRT-PCR analysis for the osteogenic differentiation gene marker of BM-MSCs following treatment with BMP-2 and/or FGF-2 for 7, 14, and 21 days. mRNA for *BMP-2*, *Runx2*, *osterix* (*Osx*), and *collagen type I* (*Coll*) (a–d) characterizes the early stage of osteogenesis; *osteocalcin* (*Ocn*) and *osteopontin* (*Opn*) (e,f) characterize the expression in the late stage of differentiation into osteogenic cells. Three different experiments were performed. * $p < 0.05$, ** $p < 0.005$, *** $p < 0.0001$.

2.7. Differentiation Potential of Sheep BM-MSCs

The capacity of sheep BM-MSCs for multilineage differentiation was confirmed using Alizarin Red S staining for osteogenesis, Oil Red O staining for adipogenesis, and Alcian Blue staining for chondrogenesis. The impact of BMP-2 and FGF-2 on differentiation capacity was also assessed. The cells that were cultured for 21 days in an osteogenic differentiation medium and an osteogenic differentiation medium supplemented with BMP-2 and/or FGF-2 formed a mineralized matrix. The addition of the cytokines FGF-2 or FGF-2 together with BMP-2 did not have a significant impact on the osteogenic differentiation potential. BM-MSCs themselves had the most powerful osteogenesis capacity in comparison to adipogenesis and chondrogenesis; therefore, stimulation by cytokines did not change their osteogenic potential. Interestingly, BM-MSCs differentiate more efficiently into chondrocytes when treated with FGF-2 and/or BMP-2 (Figure 7).

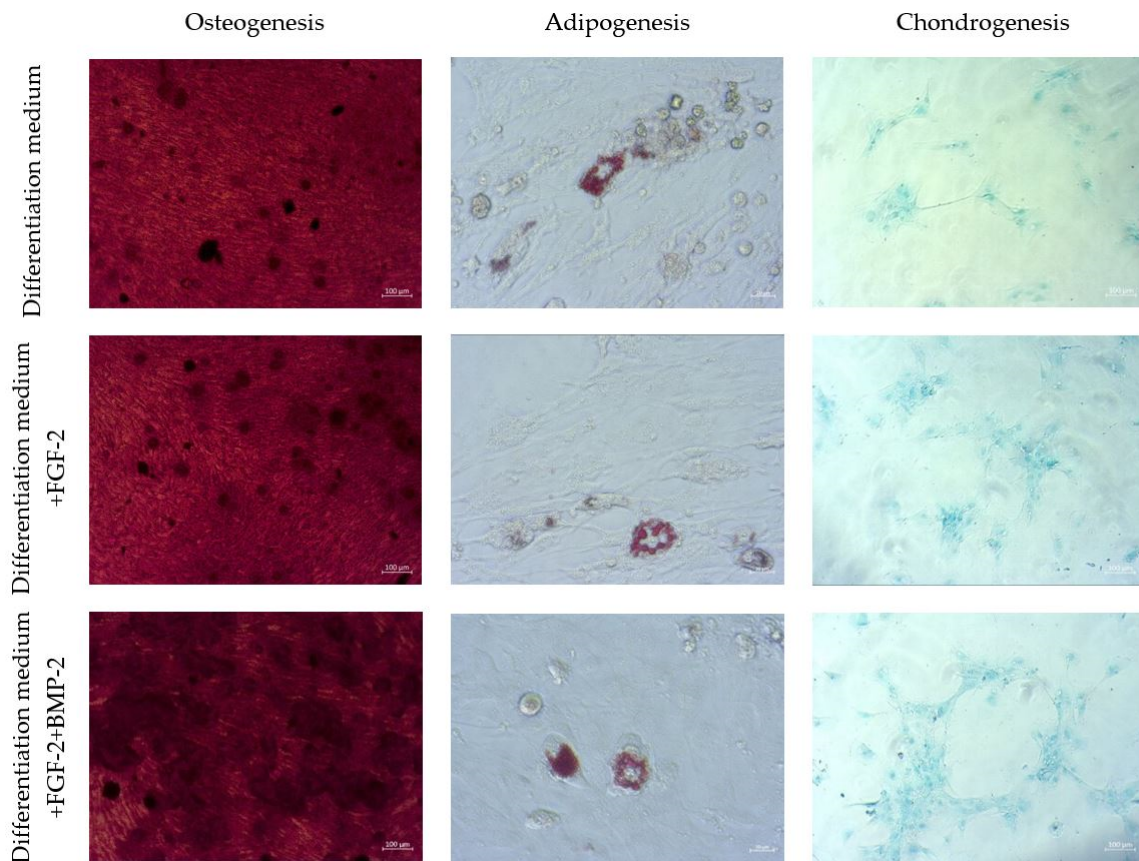


Figure 7. Multilineage differentiation of sheep BM-MSCs. Osteogenic differentiation was assessed using Alizarin Red S staining, adipogenic differentiation using Oil Red O, and chondrogenic differentiation using Alcian Blue staining.

2.8. Secretion Profile of Sheep BM-MSCs

The expression levels of 18 ovine cytokines in the supernatants from BM-MSCs cultured in different media: (1) α MEM, (2) α MEM supplemented with FGF-2, and (3) α MEM supplemented with FGF-2 and BMP-2, were analyzed using the semi-quantitative C-Series Ovine (Sheep) Cytokine Array C1 Kit to determine the impact of culture media on their secretion profile (Figure 8a). Furthermore, changes over time in cytokine expression were also examined, following treatment with BMP-2 and/or FGF-2 for 7, 14 and 21 days (Figure 8b,c). A comparison of cytokine profiles depending on the cell culture medium showed that in all culture conditions, decorin, the cytokine that influences fibrillogenesis, was at the highest relative expression level, which is more than 100% of the internal positive control. In the supernatant of the control cells cultured in the complete α MEM medium, eight cytokines had an expression level of $\geq 10\%$, among which the most abundant were immunomodulatory and pro-angiogenic cytokines, such as: decorin ($>100\%$), regulated on activation, normal T-cell expressed and secreted–RANTES ($\sim 73\%$), interleukin-8–IL-8 ($\sim 42\%$), monokine induced by gamma interferon–MIG ($\sim 21\%$), allograft inflammatory factor–AIF ($\sim 17\%$), tumor necrosis factor α –TNF- α ($\sim 12\%$), secreted frizzled-related protein 3–sFRP-3 ($\sim 12\%$), and vascular endothelial growth factor A–VEGF-A ($\sim 11\%$). After the FGF-2 treatment, the expression levels of MIG, sFRP-3, TNF- α , and VEGF-A increased, whereas the expression level of IL-8 and RANTES decreased. The addition of FGF-2 and BMP-2 to the culture medium reduced the expression level of IL-8, TNF- α , and VEGF-A (Figure 8a).

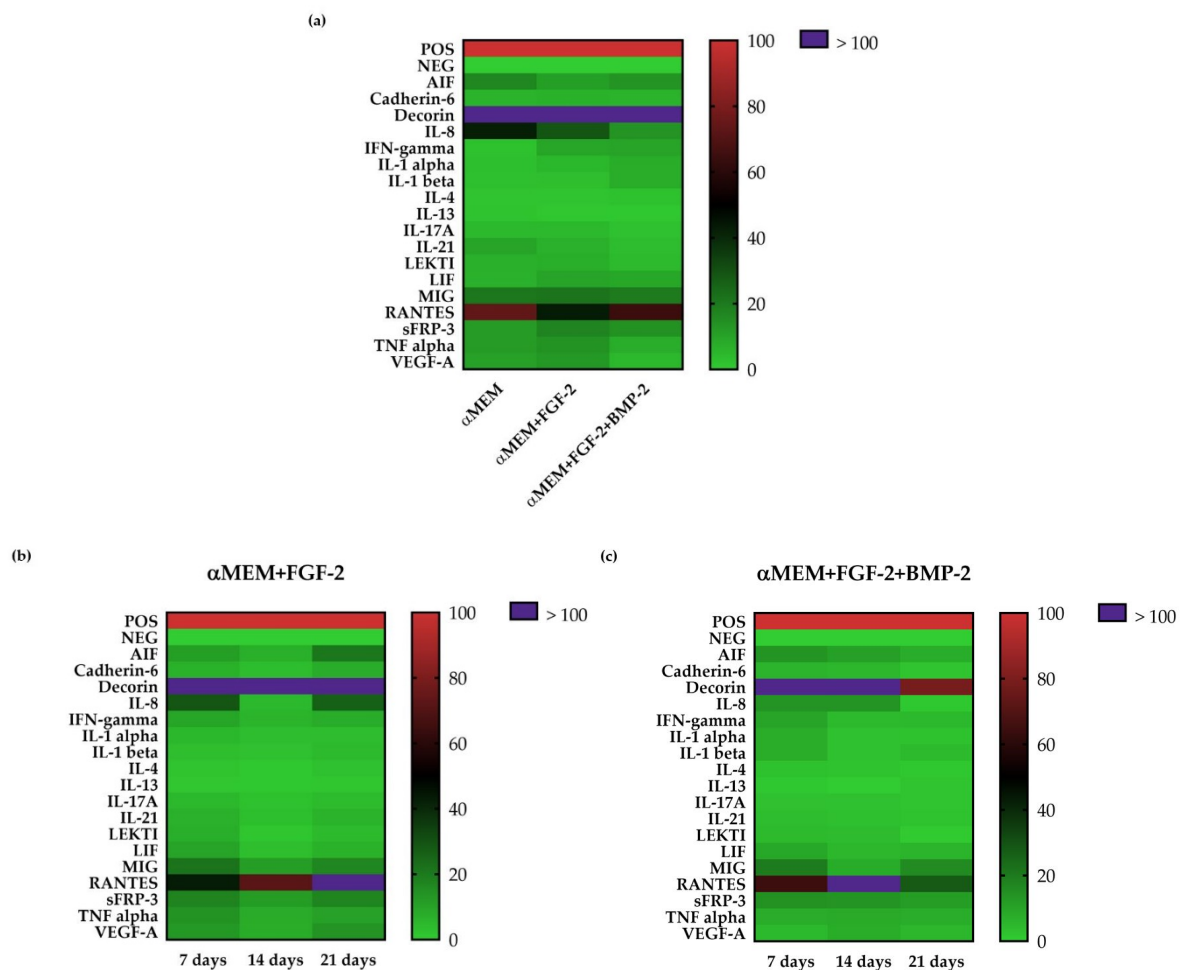


Figure 8. (a) Secretion profile of sheep BM-MSCs using the semi-quantitative C-Series Ovine (Sheep) Cytokine Array C1 Kit, depending on culture conditions. (b) Secretome of BM-MSCs treated with FGF-2 alone, or (c) FGF-2 and BMP-2 after 7, 14 and 21 days of incubation.

Interestingly, the cytokine secretion profile of BM-MSC culture in the treated cells changed over time. In the supernatants from the cell culture treated with FGF-2, the expression level of RANTES increased gradually over time. The expression level of other cytokines remained at the same level in the supernatants collected after 7 and 21 days; however, after 14 days, the expression of most of the examined cytokines was the lowest (Figure 8b). The expression level of AIF, decorin, IL-8, sFRP-3 decreased over time in the supernatants from BM-MSCs treated with FGF-2 and BMP-2. The expression level of RANTES in the collected supernatant was the highest after 14 days (Figure 8c).

3. Discussion

MSC-based therapies are gaining popularity as a therapeutic tool in bone pathologies [24] thanks to their properties of self-renewal, differentiation into osteogenic lineage, secretion of a variety of biological factors, and the ability to regenerate damaged tissues. The application of MSCs in bone engineering can serve as an alternative when standard clinical methods are insufficient, especially for restoring large bone defects or difficult-to-treat non-union fractures. For a safe and efficient bone-healing therapy involving MSCs, it is necessary to characterize in detail the biological properties of MSCs and standardize cell culture conditions [25]. To enable the transition of MSCs from the laboratory to clinical use, large animal models (including sheep) have been widely investigated due to their structural and physiological similarities to humans. Before clinical application, cellular and molecular interactions are studied *in vitro*. Afterwards, small animal models facilitate the initial “proof

of concept," whereas large animal models allow for the examination of the safety, dosing, and efficacy of MSCs prior to clinical application [26]. Although human MSCs have been extensively investigated, sheep MSCs are still poorly characterized [27]. Another problem in research on MSC application in bone diseases is the efficacy of osteogenic differentiation. Consequently, it is crucial to investigate the factors that induce the osteogenic differentiation capacity of MSCs [24]. Previous studies report that bone formation consists of two phases, proliferation and mineralization, which are regulated by specific gene expression [28,29]. In this study, ovine bone marrow-derived MSCs, treated with FGF-2 as a cell proliferation stimulator and BMP-2 as an osteogenic inductor, were investigated in the context of their biological activity for a potential application as a cell-based therapy supporting bone healing in the large animal model.

Our results revealed that the morphology and proliferation of ovine MSCs isolated from bone marrow depended on culture medium supplements, which was previously reported for some supplements (FGF-2, ascorbic acid, epidermal growth factor, and platelet-derived growth factor-BB) in human MSCs [30] and ovine MSCs [31]. However, it has not yet been investigated how FGF-2 and BMP-2 affect the biological properties of ovine MSCs. Major changes in morphology were observed in BM-MSCs cultured in α MEM supplemented with both FGF-2 and BMP-2. In comparison to the morphology of the BM-MSCs cultured in the control medium, which showed a typically fibroblast-like spindle shape, in the cell culture treated with FGF-2 and BMP-2, some osteoblast-like structures were visible in addition to the standard fibroblastic morphology. This observation confirmed the pro-osteogenic function of BMP-2 when applied together with FGF-2 in a cell culture medium, and this phenomenon was also shown earlier for human and mouse MSCs [7]. Supplementation with FGF-2 alone did not result in new osteoblast-like structures; nevertheless, the cells were smaller and grown in a higher cell density. The effect of the osteogenic induction of BMP-2 and FGF-2 was also reported when the cells were cultured in a supplemented osteogenic differentiation medium [7]. The density of calcium deposits and mineralized matrix in the BMP-2- and/or FGF-2-induced cells was moderately higher compared to the cells cultured in an untreated osteogenic differentiation medium. A comparison of cell proliferation curves according to stimuli showed that the highest proliferation rate occurred in α MEM supplemented with FGF-2. This observation is in line with previous reports documenting that FGF-2 increased the proliferation of MSCs and other cell types [32–35]. The addition of both cytokines, FGF-2 and BMP-2, to the culture medium decreased the proliferation of BM-MSCs, although it was still higher than in the cells cultured in the control α MEM medium. This phenomenon, with high probability, is associated with an advanced osteogenic differentiation potential triggered by the complementary action of FGF-2 and BMP-2.

To fulfill the minimal criteria of the International Society for Cellular Therapy (ISCT) relating to the phenotype and tri-lineage differentiation characteristics of MSCs [36], ovine BM-MSCs were characterized for their immunophenotype and multi-lineage differentiation potential. The expression profile of the surface antigens of ovine MSCs has already been reported in some studies [30,31,37–39]; however, there is a lack of data about the effect of FGF-2 and BMP-2 on ovine BM-MSC surface markers. Bearing in mind the restrictions concerning the critical quality of the MSCs that are under consideration for clinical application, it is crucial to analyze whether FGF-2 and BMP-2, which have a positive effect on osteogenic differentiation, do not have a negative effect on the biological properties of MSCs over a period of differentiation time. Therefore, in our study, BM-MSCs treated with osteogenic stimuli were examined during the follow-up period up to 21 days of the cell culture for CD73, CD105, CD34, CD45, and HLA DR expression levels using flow cytometry and for CD90 using RT-PCR. The analysis revealed a high expression level of CD73, CD90, and CD105, and a very low or lack of the expression of CD34, CD45, and HLA DR; this confirmed that the ovine BM-MSCs maintained the naïve MSC phenotype according to ISCT criteria [36]. Moreover, BM-MSCs stimulated with BMP-2 and/or FGF-2 maintained the stability of the basic MSC phenotype, and the level of CD73 and CD105 positive cells increased during observation time, thus confirming the purity of the BM-MSC population. However, our data showed an alteration in the CD90 gene expression performed using the RT-PCR method, depending

on medium supplements and observation time. The highest CD90 gene expression was observed in the control cells cultured in α MEM without any cytokine addition, and the lowest expression was observed in BM-MSCs cultured in α MEM supplemented with FGF-2 and BMP-2 after 21 days of cultivation. This observation suggests that the decrease of CD90 gene expression is a result of FGF-2 and BMP-2 activity. This phenomenon may be the effect of an ongoing osteogenic differentiation of the examined ovine BM-MSCs, as demonstrated in studies on the osteogenic differentiation of human dental pulp stem cells and a decreased expression of the MSC surface marker CD90 [40]. The data showed little variation in the expression level of the negative MSC surface markers, especially HLA DR. Initial analysis, performed on day 7, revealed that the level of cells with the expression of the HLA DR antigen constituted almost half of the population of ovine BM-MSCs treated with BMP-2 and/or FGF-2. However, HLA DR expression decreased to below 0.3% in all examined populations after 21 days of cultivation, which proved that over time, cells with a potential activation ability were removed from the ovine BM-MSC population. Nevertheless, the variability in the expression of HLA DR for human BM-MSCs used in clinical studies has been already described by Grau-Vorster et al. They reported that the multilineage differentiation and immunomodulatory potential of MSCs was independent of their HLA DR expression level [41]. Our results concerning the immunophenotype suggest that BM-MSCs treated with BMP-2 and/or FGF-2 in long-term culture did not lose their characteristic MSC properties.

The FGF-2 and BMP-2 treatment affected osteocalcin and collagen type I expression, as indicated by immunofluorescence intensity. Ovine BM-MSCs showed a moderately high expression of osteocalcin and collagen type I when cultured in the osteogenic differentiation medium supplemented with both FGF-2 and BMP-2. Nevertheless, the addition of FGF-2 alone also slightly increased the expression of osteocalcin and collagen type I at the protein level compared to the osteogenic differentiation medium without any supplements. This is a significant observation that confirms the pro-osteogenic stimulatory effect of FGF-2 and BMP-2 on ovine BM-MSCs. Nevertheless, the differences in immunofluorescence intensity between the cells cultured in an osteogenic medium with or without supplements were rather modest. The reason may have been the impact of the osteogenic differentiation medium on MSCs, which significantly induce cells to differentiate into the osteogenic lineage, regardless of supplement addition. The role of FGF-2 is to enhance the osteogenic potential by stimulating cell proliferation during the early stages of osteogenesis and regulating the BMP-2 osteoinductive potential, whereas BMP-2 is known as one of the strongest inducer of osteogenesis. In physiological conditions, FGF-2 and BMP-2 are produced by osteoblasts and accumulated in the extracellular matrix of the bone [7]. In our study, both cytokines added to α MEM were able to promote the osteogenic differentiation of MSCs by inducing the expression of a range of osteogenic gene markers.

The degree of sheep BM-MSC osteogenic differentiation following FGF-2 and BMP-2 treatment was determined by assessing the expression level of the osteogenic marker genes: *BMP-2*, *Runx2*, *osterix*, *collagen type I*, *osteocalcin*, and *osteopontin*. Our study demonstrated that FGF-2 and BMP-2 treatment upregulated the expression of osteogenic signaling molecules in the sheep BM-MSCs, starting from the early steps of bone formation to the late phase of mineralization. The peak expression of *BMP-2* in BM-MSCs cultured with FGF-2 and BMP-2 was observed after 14 days of differentiation and was higher than in the cells cultured without BMP-2. *BMP-2* has already been described by other researchers as an important regulator of osteogenic differentiation [42,43]. The finding that *BMP-2* increased its own expression may suggest that during the bone healing process, *BMP-2* induces its own expression in response to injury, making it a feedback regulation. It is worth noting that FGF-2 alone also enhanced the relative *BMP-2* expression, but the difference in its expression between days 7, 14, and 21 was rather low.

Runx2 has been reported as the earliest osteogenic marker and a stimulator of *osterix* expression [44,45]. Both genes are involved in osteogenesis as master transcription factors. *Runx2* may affect the early stage of the recruitment of osteoblastic progenitor cells, and *osterix* is involved in the final osteogenic differentiation stage. Furthermore, an overexpression of *osterix* induces the expression of the final osteogenic marker, *osteocalcin* [46]. These observations support the results of the present study.

The relative expression level of *Runx2* increased after 14 days of incubation and was the highest in BM-MSCs treated with FGF-2 and BMP-2, which confirmed the stimulatory effect of FGFs and BMP-2 on *Runx2* expression, as demonstrated by other researchers [19,47]. However, BMP-2 significantly upregulated the *osterix* gene expression on day 14 of culture. In contrast, FGF-2 downregulated the relative *osterix* gene expression in ovine BM-MSCs over the culture period. The same outcome in the gene expression of the late osteogenic markers, *osteocalcin* and *osteopontin*, was observed in BM-MSCs stimulated with FGF-2 and BMP-2. The expression level of these genes increased over time and was the highest after 21 days of incubation. Similar results for *Runx2*, *osterix*, and *osteocalcin* in human BM-MSCs treated with BMP-2 have already been reported [19]. However, in this study, the osteogenic differentiation medium supplemented with BMP-2 was used instead of the complete α MEM.

FGF-2 and BMP-2 are involved in different stages of bone repair. FGF-2 enhances bone formation at the early stage of differentiation based on the proliferation phase, whereas BMP-2 plays a key role in the final stages of mineralization [48]. This hypothesis is supported by the results of our work relating to *collagen type I* and *osteopontin* expression. Collagen is one of the main proteins synthesized by osteoblasts in the early phase of osteogenic differentiation [49]. Relative *collagen type I* gene expression was the highest in the sheep BM-MSCs treated with FGF-2 on day 21. Interestingly, BMP-2, as an active inducer of osteogenic differentiation, enhanced the expression of the late osteogenic marker, *osteopontin*. These findings confirmed that FGF-2 and BMP-2 affect bone formation at different stages of osteogenic differentiation.

To identify the role of BMP-2 and FGF-2 in MSC differentiation, sheep BM-MSCs were cultured in commercial osteo-, adipo-, and chondrogenic differentiation mediums with or without BMP-2 and/or FGF-2. This study showed that BMP-2 and/or FGF-2 did not significantly affect the Alizarin Red S staining intensity. This finding can be explained by the fact that ovine BM-MSCs have a good ability to differentiate into osteoblasts when cultured in an osteogenic differentiation medium. Therefore, the differences between Alizarin Red S stained cells were rather difficult to distinguish, as the intensity of staining in all treated or untreated cells was very high. However, FGF-2 and BMP-2 treatment improved the efficacy of chondrogenic differentiation. The stimulatory effect of BMP-2 on the chondrogenesis of human MSCs has already been reported by other authors [50,51]. Our results confirmed a similar effect of BMP-2 on MSCs obtained from sheep.

MSCs are known for their capability to produce many growth factors, cytokines, and chemokines, which affect immune cells and types of cells that modulate the local environment during regeneration [52]. In this study, 18 cytokines were screened on sheep BM-MSCs following FGF-2 and/or BMP-2 treatment. The cytokine expression pattern differed depending on the cell culture conditions and cultivation time. Firstly, it is worth noting that in all supernatants, the level of decorin was significantly high. Decorin is a bone matrix protein that plays a key role in bone remodeling [53]. Amable and her team have also reported that human MSCs derived from bone marrow and adipose tissue secrete decorin [54]. Moreover, Shu et al. have found that FGF-2 and FGF-18 upregulate the decorin gene expression level in BM-MSCs [55]. Their results support our observation that FGF-2 exerts a stimulatory effect on decorin secretion by ovine BM-MSCs. Our data also showed that the level of proangiogenic and immunomodulatory cytokines, namely VEGF-A, MIG, sFRP-3, and TNF- α , increased in FGF-2-treated BM-MSCs. This observation is in line with a study performed by Gorin et al., who found that FGF-2 enhances the angiogenic properties of the human dental pulp-origin MSC secretome [56]. In contrast, stimulation with both FGF-2 and BMP-2 decreased VEGF-A and TNF- α . Interestingly, IL-8 was downregulated in cells treated with both cytokines, FGF-2 and BMP-2, and its highest level was observed in the control culture without any stimuli. IL-8 is an inflammatory mediator that plays an important role as an enhancer of cell migration in tissue repair. However, Bastidas-Coral et al. demonstrated that IL-8 did not stimulate the osteogenic differentiation of human MSCs [57]. Based on these findings and our observations, we can hypothesize that the upregulation of IL-8 is not needed for osteogenesis.

The role of FGF-2 combined with BMP-2 in the osteo-induction of MSCs and osteoblast-like cells has been investigated by different studies [7,16,48]. For example, it was found that the co-delivery of low doses of FGF-2 and BMP-2 is more efficient in the bone formation of old human and mouse cell cultures than BMP-2 treatment alone [7]. Although the effect of stimulation with FGF-2 and BMP-2 on the osteogenic differentiation of mouse and human MSCs remains to be researched, the primary MSCs obtained from large animals have not yet been investigated for their osteogenic potential following FGF-2 and BMP-2 treatment. It is important to fully understand the response to osteogenic stimuli of ovine cells in vitro before undertaking in vivo experiments on the large animal model in order to test different strategies of enhancing the regeneration of large bone defects. Our results suggest that treatment with FGF-2 and BMP-2 significantly improves the osteogenic potential of ovine BM-MSCs on both the molecular and the protein level.

4. Materials and Methods

4.1. BM-MSC Isolation and Culture

The study was approved by the institutional Animal Ethics Committee at the Institute of Immunology and Experimental Therapy PAS (No 63/2017 from 21 of June 2017). Six adult sheep weighing from 42 to 54 kg were used in the study. A 15-gauge bone marrow aspiration needle (15 G × 15 mm, Perfectus, Medax, Italy) was used to aspirate 10 mL of bone marrow from the iliac crest into a 20 mL heparinized syringe. All procedures were performed under general inhalant anesthesia with oxygen volatilized isoflurane (IsoVet, Piramal Healthcare, UK). Analgesia was provided with fentanyl (Fentanyl WZF, Warsaw, Poland). Bone marrow aspirations were performed by experienced surgeons at the Department and Clinic of Surgery, Faculty of Veterinary Medicine, Wrocław University of Environmental and Life Sciences. Mononuclear cells were isolated using the Lymphoflot gradient (Bio-Rad, Dreieich, Germany, cat. no. 824012) during 30 min of centrifugation at 400 g at room temperature (RT). Next, the isolated mononuclear cells of bone marrow-origin were collected and washed two times in PBS. Cell suspensions were seeded in 75 cm² (T75) culture flasks and cultured in Minimum Essential Medium α -transformation- α MEM (IET PAS, Wrocław, Poland) supplemented with 10% fetal bovine serum, FBS (Biowest, Riverside, Montana, MT, USA, cat. no. S1810-500), 2 mM L-glutamine (Biowest, Riverside, Montana, MT, USA, cat. no. X0550-100), and 1% penicillin/streptomycin (Merck, Saint Louis, MO, USA, cat. no. P0781). The cells were incubated in a humidified atmosphere at 37 °C with a 5% CO₂. To ensure an effective adherence of MSCs, the culture medium was first changed after 7 days of incubation, after which the complete medium was replaced every three days. When the plastic adherent bone marrow-derived mesenchymal stem cells (BM-MSCs) reached 80% confluence, they were harvested using the Accutase Cell Detachment Solution (Corning, Manassas, VA, USA, cat. no. 25-058-CI). Accutase was deactivated with an equal volume of the complete culture medium and centrifuged at 200 g for 5 min at RT, resuspended in the culture medium, and plated again in T75 culture flasks at a density of 1×10^4 cells/mL for the experiments.

4.2. BMP-2 and FGF-2 Supplementation

To determine the osteogenic stimulatory effect of BMP-2 and FGF-2 on BM-MSCs, the cells were treated with 100 ng/mL of BMP-2 (Stem Cell Technologies, Grenoble, France, cat. no. 78004.1) and/or 20 ng/mL FGF-2 (Merck, Saint Louis, MO, USA, cat. no. F0291). BM-MSCs cultured in the α MEM complete medium were used as a control. The supplemented and control media were changed every three days. The experiments on osteogenic induced BM-MSCs were performed after 7, 14, and 21 days of incubation.

4.3. Cell Proliferation and Doubling Time Calculation

The proliferative activity of BM-MSCs cultured with BMP-2 and/or FGF-2 was analyzed using the MTT assay. The cells were seeded in triplicate at a density of 2×10^3 cells/well in 96-well plates.

Cells were allowed to attach to the plates for the first 4 h, after which 10 μ L of a 4 mg/mL MTT (Merck, Saint Louis, MO, USA, cat. no. M2128) solution was added. After incubation, over the next 4 h at 37 $^{\circ}$ C, the medium was aspirated and 100 μ L of DMSO (POCH, Gliwice, Poland, cat. no. 363550117) was added to solubilize the purple formazan crystals. Optical density was measured at 540 nm with a Wallac Victor2 microplate reader (Perkin Elmer LAS, Waltham, MA, USA). The cell proliferation was analyzed after 24, 48, 72, and 96 h. The medium in each well was replaced after three days. The MTT proliferation assay was repeated three times.

To calculate the cell doubling time (DT), the following formula was used:

$$DT = T \cdot \frac{\ln 2}{\ln \frac{N_T}{N_0}} \quad (1)$$

where T is the incubation time (hours), N_T is the number of cells after the incubation time, and N_0 is the number of cells initially harvested. The incubation time point was 48 h, based on the exponential phase. The number of cells after the incubation time was obtained from the growth curve from the MTT assay. The standard curve was plotted to determine the relationship between cell number and absorbance at 540 nm.

4.4. Flow Cytometry

BM-MSCs cultured in three different media: α MEM, α MEM + FGF-2, and α MEM + FGF-2 + BMP-2 at different time points of incubation, 7 and 21 days, were analyzed for the basic MSC surface markers using flow cytometry and a FACS Calibur platform (BD Bioscience, Cambridge, UK). Briefly, cells were harvested with the Accutase Cell Detachment Solution (Corning, Manassas, VA, USA), washed in PBS (IIET PAS, Wroclaw, Poland), and resuspended in PBS at a concentration of 2×10^6 cells/mL. For direct flow cytometry, 50 μ L of BM-MSCs and an appropriate amount of a conjugated primary antibody (Table S1) were added to the FACS tubes and incubated for 30 min at 4 $^{\circ}$ C in the dark. Then, the cells were washed in 1 mL of PBS. After centrifugation, the cells were resuspended in 100 μ L of PBS and analyzed. For indirect labelling, 50 μ L of BM-MSCs were incubated with the primary antibody at 4 $^{\circ}$ C for 30 min. Next, the cells were washed and resuspended in a solution of a diluted fluorochrome-labeled secondary antibody in 3% BSA/PBS (Gibco, Carlsbad, CA, USA) and incubated in the dark at 4 $^{\circ}$ C for 30 min. After incubation, the cells were washed, resuspended in 100 μ L PBS, and analyzed using FACS Calibur (Becton Dickinson, San Jose, CA, USA). The data from the flow cytometry experiments were visualized using the Flowing Software version 2.5.1. All used antibodies and their dilutions are listed in Table S1 in the supplementary materials.

4.5. Immunofluorescence Staining

To detect osteogenesis-related proteins, collagen type I, and osteocalcin, the BM-MSCs were cultured in 96-well plates at a density of 1×10^3 cells/well in an α MEM- and α MEM-medium supplemented with BMP-2 and/or FGF-2. The α MEM-medium was used as a control. For immunostaining, performed after 7, 14 and 21 days of incubation, the culture media were aspirated, and the cells were washed with PBS. Next, BM-MSCs were fixed in 100 μ L of 3.7% paraformaldehyde for 20 min at RT and washed again in PBS. The cells were then covered with 50 μ L of 3% BSA/PBS to block the nonspecific bindings and incubated for 1.5 h at 37 $^{\circ}$ C. Afterwards, the blocking solution was removed, 50 μ L of diluted primary antibodies, rabbit anti-collagen type I, and mouse anti-osteocalcin (Table S1) were added to the wells for 24 h of incubation at 40 $^{\circ}$ C. Next, each well was washed with PBS three times, and the cells were incubated with 50 μ L of secondary goat anti-rabbit or goat anti-mouse FITC-conjugated solutions (Table S1) for 30 min in the dark at RT. After incubation with secondary antibodies, the wells were washed three times in PBS. For nuclei staining, DAPI (Vector Labs, Burlingame, CA, USA, cat. no. H-1200) was used for 20 min of incubation in the dark at RT, after which the cells were washed with PBS. Immunofluorescence staining was visualized using an Axio Observer inverted fluorescence

microscope (Zeiss, Jena, Germany) equipped with a system for image acquisition and digitalization and analyzed using the Zeiss Zen Blue software.

4.6. RT-PCR (Reverse Transcription Polymerase Chain Reaction)

To evaluate the expression of the surface marker CD90, RNA was extracted and purified from the BM-MSCs cultured in α MEM with or without BMP-2 and/or FGF-2 for 7, 14, and 21 days using the NucleoSpin[®] RNA Kit (Macherey-Nagel, Düren, Germany, cat. no. 740955.50) according to the manufacturer's instructions. Next, the reverse transcription of 1 μ g of total RNA from each sample was performed to prepare cDNA using the RevertAid First Strand cDNA Synthesis Kit (Thermo Fisher, Vilnius, Lithuania, cat. no. K1622). To ensure a good quality of DNA examination, PCR for β -actin was performed on 2% agarose gel with ethidium bromide. The synthesized cDNAs were subjected to PCR using DreamTaq DNA Polymerase (Thermo Fisher, Vilnius, Lithuania, cat. no. EP0702). The PCR primer sequences and reaction parameters are shown in Table S2 in the supplementary materials. The PCR products were analyzed and visualized with 2% agarose gel electrophoresis using a G:BOX system (Syngene, Cambridge, UK). RT-PCR was normalized by the housekeeping gene GAPDH, and the gel bands were quantified using the ImageJ software (National Institutes of Health, Bethesda, Maryland, USA).

4.7. Real-Time qRT-PCR

Extraction and reverse transcription of total RNA from the BM-MSCs treated with 100 ng/mL BMP-2 and/or 20 ng/mL FGF-2 for 7, 14 and 21 days was performed as previously described in the RT-PCR methodology. Real-time PCR was conducted with the Power SYBR Green PCR Master Mix (Life Technologies, Warrington, UK) using the ViiA 7 Real-Time PCR System (Applied Biosystems, Foster City, CA, USA). The reactions were carried out in triplicate with the program running: initial denaturation at 95 °C for 10 min, followed by 40 cycles of denaturation at 95 °C for 15 s, annealing at the T_m (°C) of the primers listed in Table S2 for 1 min, and extension at 72 °C for 40 s. All PCR product quantifications were normalized to the housekeeping gene GAPDH. The relative mRNA expression level was calculated using the $2^{-\Delta\Delta CT}$ method, where the threshold cycle (CT) from the triplicate runs was averaged and calibrated to GAPDH CT.

4.8. Multilineage Differentiation

To examine the multilineage differentiation potential of sheep BM-MSCs, the cells were seeded in a 24-well plate at a density of 1×10^4 cells/well and allowed to attach. After overnight incubation, the culture media were changed to the osteogenic, adipogenic, and chondrogenic differentiation media (PromoCell, Heidelberg, Germany, cat. no. C-28013, C-28012, C-28016) with or without BMP-2 and/or FGF-2 in a volume of 400 μ L/well for the induced cells and α MEM for the control cells. The media were refreshed every three days. After 14 days of incubation for chondrogenesis and 21 days for osteogenesis and adipogenesis, the differentiation potential was assessed through visualization with appropriate staining. To perform the staining, the differentiation media were removed, the cells were washed with PBS and fixed for 20 min at RT in a 3.7% formaldehyde (Merck, Saint Louis, MO, USA, cat. no. 104003). Next, the formaldehyde was removed, the cells were washed with PBS again and stained at RT with 200 μ L Alizarin Red S for 10 min for osteogenic differentiation, Oil Red O for 15 min for adipogenic differentiation, and Alcian Blue for 40 min for chondrogenic differentiation (Merck, Saint Louis, MO, USA, cat. no. A5533, O0625, A3157).

4.9. Sheep Cytokine Array

To evaluate the impact of FGF-2 and BMP-2 on the cytokine secretory profile of sheep BM-MSCs, the cells were cultured in the α MEM medium supplemented with 2 mM L-glutamine and 1% penicillin/streptomycin without FBS and with the addition of: (1) FGF-2 and (2) FGF-2 with BMP-2 for 7, 14 and 21 days. The cells were seeded in T75 cell culture flasks at a density of 1.9×10^4 /cm²,

in the complete α MEM medium first, and incubated for 24 h. Next, the media were changed for α MEM without FBS supplemented with BMP-2 and/or FGF-2. The media were changed every three days. After the time points, the supernatants were collected into 15 mL tubes. To remove cellular debris, the supernatants were centrifuged at 1200 rpm for 10 min at RT, placed into the new tubes, centrifuged once again at 1600 rpm for 10 min at RT, placed into the new tubes and stored in -20°C . The secretory profile of BM-MSC cytokines was examined using the semi-quantitative C-Series Ovine (Sheep) Cytokine Array C1 Kit (Ray-Bio[®], Norcross, GA, USA, cat. no. AAO-CYT-1-8) according to the manufacturer's protocol. Briefly, membranes were placed into the wells of the incubation tray and incubated at RT for 30 min with 2 mL of blocking buffer. Next, the samples were aspirated and 1 mL of supernatants were added for overnight incubation at 4°C . The next step was to wash the membranes and incubate them with 1 mL of biotinylated antibody cocktail for 2 h at RT. The second wash was performed to remove the unbound antibody, after which 1 mL of HRP-Streptavidin was incubated with the membranes at RT for 2 h. At the end, the membranes were washed and detected with chemiluminescence using an X-ray film. The differences in relative protein expression were measured using the ImageJ and the Protein Array Analyzer plugin. Next, the data were analyzed in Microsoft Excel-based Analysis Software Tool for the Ovine Cytokine Array C1 kit (Ray-Bio[®], Norcross, GA, USA). The results are presented on heat maps created in GraphPad Prism version 7 (GraphPad Software, Inc., San Diego, California, USA).

4.10. Statistical Analysis

All statistical analyses were calculated with the GraphPad Prism version 7. The one-way analysis of variance (one-way ANOVA) with Dunnett's test for multiple comparison procedures was used to compare the obtained data. p -values < 0.05 were considered as statistically significant. All experiments were conducted at least in three independent analyses.

5. Conclusions

In this study, we showed that MSCs from sheep bone marrow had a great osteogenic potential when stimulated with FGF-2 and BMP-2. After long-term treatment, the cells still maintained the characteristic phenotype of MSCs and expanded more efficiently compared to the culture in the control medium without cytokines. FGF-2 and BMP-2 enhanced osteogenic differentiation, as confirmed by Alizarin Red S staining and by osteocalcin and collagen type I expression. Furthermore, FGF-2 and BMP-2 upregulated the gene expression of the early osteogenic markers, including *BMP-2*, *osterix*, and *Runx2*, and the late osteogenic markers, *osteocalcin* and *osteopontin*. Our findings demonstrated that sheep BM-MSCs produced a variety of growth factors, cytokines, and chemokines involved in osteogenesis, and supplementation of the culture medium with FGF-2 and BMP-2 affected the secretome profile of the cells.

The improvement of the osteogenic potential of MSCs is very important in research on an innovative treatment for many bone diseases. Co-administration of FGF-2 and BMP-2 seems to be a promising strategy for bone regeneration in *in vivo* studies on sheep MSCs. Therefore, the next step in this project is to develop a safe cell-based therapy for large bone defects in the sheep model with osteo-induced BM-MSCs as a preclinical model for cellular therapy in bone regeneration and further potential clinical application.

Supplementary Materials: Supplementary materials can be found at <http://www.mdpi.com/1422-0067/21/24/9726/s1>.

Author Contributions: Conceptualization, A.K. (Aleksandra Klimczak) and S.G.; methodology, S.G., A.K. (Agnieszka Krawczenko), A.A. and K.B.; formal analysis, S.G., A.K. (Agnieszka Krawczenko) and A.K. (Aleksandra Klimczak); investigation, S.G. and A.K. (Agnieszka Krawczenko); data curation, S.G. and A.K. (Aleksandra Klimczak); writing—original draft preparation, S.G.; writing—review and editing, A.K. (Aleksandra Klimczak); visualization, S.G.; supervision, A.K. (Aleksandra Klimczak) and Z.K.; funding acquisition, A.K. (Aleksandra Klimczak) and Z.K. All authors have read and agreed to the published version of the manuscript.

Funding: This research was supported by THE NATIONAL CENTER FOR RESEARCH AND DEVELOPMENT, STRATEGMED3/306888/3/NCBR/2017.

Acknowledgments: We are grateful to Maria Paprocka for her support in flow cytometry and Aleksandra Bielawska-Pohl for her support in statistical analysis.

Conflicts of Interest: The authors declare no conflict of interest. The funders had no role in the design of the study; in the collection, analyses, or interpretation of data; in the writing of the manuscript, or in the decision to publish the results.

Abbreviations

AIF	allograft inflammatory factor
BM-MSCs	bone marrow derived mesenchymal stem cells
BMP-2	bone morphogenetic protein 2
ColI	collagen type I
DMSO	dimethyl sulfoxide
FGF-2	fibroblast growth factor 2
HLA DR	Human Leukocyte Antigen–DR isotype
IL-8	interleukin-8
MIG	monokine induced by gamma interferon
MSCs	mesenchymal stem cells
Ocl	osteocalcin
Opn	osteopontin
Osx	osterix
RANTES	Regulated on Activation, Normal T-cell Expressed and Secreted
Runx2	Runt related transcription factor 2
sFRP-3	secreted frizzled-related protein 3
TNF- α	tumor necrosis factor α
VEGF-A	vascular endothelial growth factor A
α MEM	Minimum Essential Medium α -transformation

References

1. Tseng, S.S.; Lee, M.A.; Reddi, A.H. Nonunions and the potential of stem cells in fracture-healing. *J. Bone Jt. Surg. Am.* **2008**, *90* (Suppl. 1), 92–98. [[CrossRef](#)]
2. Loeser, R.F. Age-related changes in the musculoskeletal system and the development of osteoarthritis. *Clin. Geriatr. Med.* **2010**, *26*, 371–386. [[CrossRef](#)]
3. Wang, W.; Yeung, K.W.K. Bone grafts and biomaterials substitutes for bone defect repair: A review. *Bioact. Mater.* **2017**, *2*, 224–247. [[CrossRef](#)]
4. Knight, M.N.; Hankenson, K.D. Mesenchymal Stem Cells in Bone Regeneration. *Adv. Wound Care (New Rochelle)* **2013**, *2*, 306–316. [[CrossRef](#)]
5. Undale, A.H.; Westendorf, J.J.; Yaszemski, M.J.; Khosla, S. Mesenchymal stem cells for bone repair and metabolic bone diseases. *Mayo Clin. Proc.* **2009**, *84*, 893–902. [[CrossRef](#)]
6. Lin, W.; Xu, L.; Zwingenberger, S.; Gibon, E.; Goodman, S.B.; Li, G. Mesenchymal stem cells homing to improve bone healing. *J. Orthop. Transl.* **2017**, *9*, 19–27. [[CrossRef](#)] [[PubMed](#)]
7. Kuhn, L.T.; Ou, G.; Charles, L.; Hurley, M.M.; Rodner, C.M.; Gronowicz, G. Fibroblast growth factor-2 and bone morphogenetic protein-2 have a synergistic stimulatory effect on bone formation in cell cultures from elderly mouse and human bone. *J. Gerontol. A Biol. Sci. Med. Sci.* **2013**, *68*, 1170–1180. [[CrossRef](#)] [[PubMed](#)]
8. Behr, B.; Sorkin, M.; Lehnhardt, M.; Renda, A.; Longaker, M.T.; Quarto, N. A comparative analysis of the osteogenic effects of BMP-2, FGF-2, and VEGFA in a calvarial defect model. *Tissue Eng. Part A* **2012**, *18*, 1079–1086. [[CrossRef](#)] [[PubMed](#)]
9. Charles, L.F.; Woodman, J.L.; Ueno, D.; Gronowicz, G.; Hurley, M.M.; Kuhn, L.T. Effects of low dose FGF-2 and BMP-2 on healing of calvarial defects in old mice. *Exp. Gerontol.* **2015**, *64*, 62–69. [[CrossRef](#)] [[PubMed](#)]
10. Gronowicz, G.; Jacobs, E.; Peng, T.; Zhu, L.; Hurley, M.; Kuhn, L.T. Calvarial Bone Regeneration Is Enhanced by Sequential Delivery of FGF-2 and BMP-2 from Layer-by-Layer Coatings with a Biomimetic Calcium Phosphate Barrier Layer. *Tissue Eng. Part A* **2017**, *23*, 1490–1501. [[CrossRef](#)] [[PubMed](#)]

11. Charoenlarp, P.; Rajendran, A.K.; Iseki, S. Role of fibroblast growth factors in bone regeneration. *Inflamm. Regen.* **2017**, *37*, 10. [[CrossRef](#)] [[PubMed](#)]
12. Coffin, J.D.; Homer-Bouthiette, C.; Hurley, M.M. Fibroblast Growth Factor 2 and Its Receptors in Bone Biology and Disease. *J. Endocr. Soc.* **2018**, *2*, 657–671. [[CrossRef](#)] [[PubMed](#)]
13. Kyllonen, L.; D'Este, M.; Alini, M.; Eglin, D. Local drug delivery for enhancing fracture healing in osteoporotic bone. *Acta Biomater.* **2015**, *11*, 412–434. [[CrossRef](#)] [[PubMed](#)]
14. Lei, L.; Wang, S.; Wu, H.; Ju, W.; Peng, J.; Qahtan, A.S.; Chen, C.; Lu, Y.; Peng, J.; Zhang, X.; et al. Optimization of release pattern of FGF-2 and BMP-2 for osteogenic differentiation of low-population density hMSCs. *J. Biomed. Mater. Res. A* **2015**, *103*, 252–261. [[CrossRef](#)] [[PubMed](#)]
15. Li, P.; Bai, Y.; Yin, G.; Pu, X.; Huang, Z.; Liao, X.; Chen, X.; Yao, Y. Synergistic and sequential effects of BMP-2, bFGF and VEGF on osteogenic differentiation of rat osteoblasts. *J. Bone Miner. Metab.* **2014**, *32*, 627–635. [[CrossRef](#)] [[PubMed](#)]
16. Song, R.; Wang, D.; Zeng, R.; Wang, J. Synergistic effects of fibroblast growth factor-2 and bone morphogenetic protein-2 on bone induction. *Mol. Med. Rep.* **2017**, *16*, 4483–4492. [[CrossRef](#)]
17. Smith, D.M.; Cooper, G.M.; Mooney, M.P.; Marra, K.G.; Losee, J.E. Bone morphogenetic protein 2 therapy for craniofacial surgery. *J. Craniofac. Surg.* **2008**, *19*, 1244–1259. [[CrossRef](#)]
18. Sun, J.; Li, J.; Li, C.; Yu, Y. Role of bone morphogenetic protein-2 in osteogenic differentiation of mesenchymal stem cells. *Mol. Med. Rep.* **2015**, *12*, 4230–4237. [[CrossRef](#)]
19. Marupanthorn, K.; Tantrawatpan, C.; Kheolamai, P.; Tantikanlayaporn, D.; Manochantr, S. Bone morphogenetic protein-2 enhances the osteogenic differentiation capacity of mesenchymal stromal cells derived from human bone marrow and umbilical cord. *Int. J. Mol. Med.* **2017**, *39*, 654–662. [[CrossRef](#)]
20. Kawaguchi, H.; Jingushi, S.; Izumi, T.; Fukunaga, M.; Matsushita, T.; Nakamura, T.; Mizuno, K.; Nakamura, T.; Nakamura, K. Local application of recombinant human fibroblast growth factor-2 on bone repair: A dose-escalation prospective trial on patients with osteotomy. *J. Orthop. Res.* **2007**, *25*, 480–487. [[CrossRef](#)]
21. Burkus, J.K.; Gornet, M.F.; Dickman, C.A.; Zdeblick, T.A. Anterior lumbar interbody fusion using rhBMP-2 with tapered interbody cages. *J. Spinal. Disord. Tech.* **2002**, *15*, 337–349. [[CrossRef](#)] [[PubMed](#)]
22. Harding, J.; Roberts, R.M.; Mirochnitchenko, O. Large animal models for stem cell therapy. *Stem Cell Res. Ther.* **2013**, *4*, 23. [[CrossRef](#)] [[PubMed](#)]
23. Futrega, K.; Music, E.; Robey, P.G.; Gronthos, S.; Crawford, R.W.; Saifzadeh, S.; Klein, T.J.; Doran, M.R. Characterisation of ovine bone marrow-derived stromal cells (oBMSC) and evaluation of chondrogenically induced micro-pellets for cartilage tissue repair in vivo. *bioRxiv* **2020**. [[CrossRef](#)]
24. Oryan, A.; Kamali, A.; Moshiri, A.; Baghaban Eslaminejad, M. Role of Mesenchymal Stem Cells in Bone Regenerative Medicine: What Is the Evidence? *Cells Tissues Organs.* **2017**, *204*, 59–83. [[CrossRef](#)]
25. Murphy, M.B.; Moncivais, K.; Caplan, A.I. Mesenchymal stem cells: Environmentally responsive therapeutics for regenerative medicine. *Exp. Mol. Med.* **2013**, *45*, e54. [[CrossRef](#)] [[PubMed](#)]
26. Hotham, W.E.; Henson, F.M.D. The use of large animals to facilitate the process of MSC going from laboratory to patient-‘bench to bedside’. *Cell Biol. Toxicol.* **2020**, *36*, 103–114. [[CrossRef](#)] [[PubMed](#)]
27. Haddouti, E.M.; Randau, T.M.; Hilgers, C.; Masson, W.; Walgenbach, K.J.; Pflugmacher, R.; Burger, C.; Gravius, S.; Schildberg, F.A. Characterization and Comparison of Human and Ovine Mesenchymal Stromal Cells from Three Corresponding Sources. *Int. J. Mol. Sci.* **2020**, *21*, 2310. [[CrossRef](#)]
28. Mundy, G.R.; Chen, D.; Zhao, M.; Dallas, S.; Xu, C.; Harris, S. Growth regulatory factors and bone. *Rev. Endocr. Metab. Disord.* **2001**, *2*, 105–115. [[CrossRef](#)]
29. Mundy, G.R. Regulation of bone formation by bone morphogenetic proteins and other growth factors. *Clin. Orthop. Relat. Res.* **1996**, *324*, 24–28. [[CrossRef](#)]
30. Gharibi, B.; Hughes, F.J. Effects of medium supplements on proliferation, differentiation potential, and in vitro expansion of mesenchymal stem cells. *Stem Cells Transl. Med.* **2012**, *1*, 771–782. [[CrossRef](#)]
31. Adamzyk, C.; Emonds, T.; Falkenstein, J.; Tolba, R.; Jahnen-Dechent, W.; Lethaus, B.; Neuss, S. Different Culture Media Affect Proliferation, Surface Epitope Expression, and Differentiation of Ovine MSC. *Stem Cells Int.* **2013**, *2013*, 387324. [[CrossRef](#)] [[PubMed](#)]
32. Kottakis, F.; Polytarchou, C.; Foltopoulou, P.; Sanidas, I.; Kampranis, S.C.; Tschlis, P.N. FGF-2 regulates cell proliferation, migration, and angiogenesis through an NDY1/KDM2B-miR-101-EZH2 pathway. *Mol. Cell* **2011**, *43*, 285–298. [[CrossRef](#)] [[PubMed](#)]

33. Yamachika, E.; Tsujigiwa, H.; Matsubara, M.; Hirata, Y.; Kita, K.; Takabatake, K.; Mizukawa, N.; Kaneda, Y.; Nagatsuka, H.; Iida, S. Basic fibroblast growth factor supports expansion of mouse compact bone-derived mesenchymal stem cells (MSCs) and regeneration of bone from MSC in vivo. *J. Mol. Histol.* **2012**, *43*, 223–233. [[CrossRef](#)] [[PubMed](#)]
34. Cartland, S.P.; Genner, S.W.; Zahoor, A.; Kavurma, M.M. Comparative Evaluation of TRAIL, FGF-2 and VEGF-A-Induced Angiogenesis in Vitro and In Vivo. *Int. J. Mol. Sci.* **2016**, *17*, 2025. [[CrossRef](#)] [[PubMed](#)]
35. Lee, J.G.; Jung, E.; Heur, M. Fibroblast growth factor 2 induces proliferation and fibrosis via SNAI1-mediated activation of CDK2 and ZEB1 in corneal endothelium. *J. Biol. Chem.* **2018**, *293*, 3758–3769. [[CrossRef](#)] [[PubMed](#)]
36. Dominici, M.; Le Blanc, K.; Mueller, I.; Slaper-Cortenbach, I.; Marini, F.; Krause, D.; Deans, R.; Keating, A.; Prockop, D.; Horwitz, E. Minimal criteria for defining multipotent mesenchymal stromal cells. The International Society for Cellular Therapy position statement. *Cytotherapy* **2006**, *8*, 315–317. [[CrossRef](#)] [[PubMed](#)]
37. McCarty, R.C.; Gronthos, S.; Zannettino, A.C.; Foster, B.K.; Xian, C.J. Characterisation and developmental potential of ovine bone marrow derived mesenchymal stem cells. *J. Cell Physiol.* **2009**, *219*, 324–333. [[CrossRef](#)]
38. Khan, M.R.; Chandrashekran, A.; Smith, R.K.; Dudhia, J. Immunophenotypic characterization of ovine mesenchymal stem cells. *Cytom. A* **2016**, *89*, 443–450. [[CrossRef](#)]
39. Vivas, D.; Caminal, M.; Oliver-Vila, I.; Vives, J. Derivation of Multipotent Mesenchymal Stromal Cells from Ovine Bone Marrow. *Curr. Protoc. Stem Cell Biol.* **2018**, *44*, 2B.9.1–2B.9.22. [[CrossRef](#)]
40. Okajcekova, T.; Strnadel, J.; Pokusa, M.; Zahumenska, R.; Janickova, M.; Halasova, E.; Skovierova, H. A Comparative in Vitro Analysis of the Osteogenic Potential of Human Dental Pulp Stem Cells Using Various Differentiation Conditions. *Int. J. Mol. Sci.* **2020**, *21*, 2280. [[CrossRef](#)]
41. Grau-Vorster, M.; Laitinen, A.; Nystedt, J.; Vives, J. HLA-DR expression in clinical-grade bone marrow-derived multipotent mesenchymal stromal cells: A two-site study. *Stem Cell Res. Ther.* **2019**, *10*, 164. [[CrossRef](#)] [[PubMed](#)]
42. Dumic-Cule, I.; Peric, M.; Kucko, L.; Grgurevic, L.; Pecina, M.; Vukicevic, S. Bone morphogenetic proteins in fracture repair. *Int. Orthop.* **2018**, *42*, 2619–2626. [[CrossRef](#)] [[PubMed](#)]
43. Onishi, T.; Ishidou, Y.; Nagamine, T.; Yone, K.; Imamura, T.; Kato, M.; Sampath, T.K.; ten Dijke, P.; Sakou, T. Distinct and overlapping patterns of localization of bone morphogenetic protein (BMP) family members and a BMP type II receptor during fracture healing in rats. *Bone* **1998**, *22*, 605–612. [[CrossRef](#)]
44. Tsao, Y.T.; Huang, Y.J.; Wu, H.H.; Liu, Y.A.; Liu, Y.S.; Lee, O.K. Osteocalcin Mediates Biomineralization during Osteogenic Maturation in Human Mesenchymal Stromal Cells. *Int. J. Mol. Sci.* **2017**, *18*, 159. [[CrossRef](#)] [[PubMed](#)]
45. Ryoo, H.M.; Lee, M.H.; Kim, Y.J. Critical molecular switches involved in BMP-2-induced osteogenic differentiation of mesenchymal cells. *Gene* **2006**, *366*, 51–57. [[CrossRef](#)] [[PubMed](#)]
46. Lee, K.S.; Kim, H.J.; Li, Q.L.; Chi, X.Z.; Ueta, C.; Komori, T.; Wozney, J.M.; Kim, E.G.; Choi, J.Y.; Ryoo, H.M.; et al. Runx2 is a common target of transforming growth factor beta1 and bone morphogenetic protein 2, and cooperation between Runx2 and Smad5 induces osteoblast-specific gene expression in the pluripotent mesenchymal precursor cell line C2C12. *Mol. Cell Biol.* **2000**, *20*, 8783–8792. [[CrossRef](#)]
47. Kim, H.J.; Kim, J.H.; Bae, S.C.; Choi, J.Y.; Kim, H.J.; Ryoo, H.M. The protein kinase C pathway plays a central role in the fibroblast growth factor-stimulated expression and transactivation activity of Runx2. *J. Biol. Chem.* **2003**, *278*, 319–326. [[CrossRef](#)]
48. Hughes-Fulford, M.; Li, C.-F. The role of FGF-2 and BMP-2 in regulation of gene induction, cell proliferation and mineralization. *J. Orthop. Surg. Res.* **2011**, *6*, 8. [[CrossRef](#)]
49. Persson, M.; Lehenkari, P.P.; Berglin, L.; Turunen, S.; Finnila, M.A.J.; Risteli, J.; Skrifvars, M.; Tuukkanen, J. Osteogenic Differentiation of Human Mesenchymal Stem cells in a 3D Woven Scaffold. *Sci. Rep.* **2018**, *8*, 10457. [[CrossRef](#)]
50. Vanhatupa, S.; Ojansivu, M.; Autio, R.; Juntunen, M.; Miettinen, S. Bone Morphogenetic Protein-2 Induces Donor-Dependent Osteogenic and Adipogenic Differentiation in Human Adipose Stem Cells. *Stem Cells Transl. Med.* **2015**, *4*, 1391–1402. [[CrossRef](#)]

51. Legendre, F.; Ollitrault, D.; Gomez-Leduc, T.; Bouyoucef, M.; Hervieu, M.; Gruchy, N.; Mallein-Gerin, F.; Leclercq, S.; Demoor, M.; Galera, P. Enhanced chondrogenesis of bone marrow-derived stem cells by using a combinatory cell therapy strategy with BMP-2/TGF-beta1, hypoxia, and COL1A1/HtrA1 siRNAs. *Sci. Rep.* **2017**, *7*, 3406. [[CrossRef](#)] [[PubMed](#)]
52. Kraskiewicz, H.; Paprocka, M.; Bielawska-Pohl, A.; Krawczenko, A.; Panek, K.; Kaczynska, J.; Szyposzynska, A.; Psurski, M.; Kuroпка, P.; Klimczak, A. Can supernatant from immortalized adipose tissue MSC replace cell therapy? An in vitro study in chronic wounds model. *Stem Cell Res. Ther.* **2020**, *11*, 29. [[CrossRef](#)] [[PubMed](#)]
53. Takeuchi, Y.; Kodama, Y.; Matsumoto, T. Bone matrix decorin binds transforming growth factor-beta and enhances its bioactivity. *J. Biol. Chem.* **1994**, *269*, 32634–32638. [[PubMed](#)]
54. Amable, P.R.; Teixeira, M.V.; Carias, R.B.; Granjeiro, J.M.; Borojevic, R. Protein synthesis and secretion in human mesenchymal cells derived from bone marrow, adipose tissue and Wharton's jelly. *Stem Cell Res. Ther.* **2014**, *5*, 53. [[CrossRef](#)] [[PubMed](#)]
55. Shu, C.; Smith, S.M.; Little, C.B.; Melrose, J. Use of FGF-2 and FGF-18 to direct bone marrow stromal stem cells to chondrogenic and osteogenic lineages. *Future Sci. OA* **2016**, *2*, FSO142. [[CrossRef](#)]
56. Gorin, C.; Rochefort, G.Y.; Bascetin, R.; Ying, H.; Lesieur, J.; Sadoine, J.; Beckouche, N.; Berndt, S.; Novais, A.; Lesage, M.; et al. Priming Dental Pulp Stem Cells With Fibroblast Growth Factor-2 Increases Angiogenesis of Implanted Tissue-Engineered Constructs Through Hepatocyte Growth Factor and Vascular Endothelial Growth Factor Secretion. *Stem Cells Transl. Med.* **2016**, *5*, 392–404. [[CrossRef](#)]
57. Bastidas-Coral, A.P.; Bakker, A.D.; Zandieh-Doulabi, B.; Kleverlaan, C.J.; Bravenboer, N.; Forouzanfar, T.; Klein-Nulend, J. Cytokines TNF-alpha, IL-6, IL-17F, and IL-4 Differentially Affect Osteogenic Differentiation of Human Adipose Stem Cells. *Stem Cells Int.* **2016**, *2016*, 1318256. [[CrossRef](#)]

Publisher's Note: MDPI stays neutral with regard to jurisdictional claims in published maps and institutional affiliations.



© 2020 by the authors. Licensee MDPI, Basel, Switzerland. This article is an open access article distributed under the terms and conditions of the Creative Commons Attribution (CC BY) license (<http://creativecommons.org/licenses/by/4.0/>).

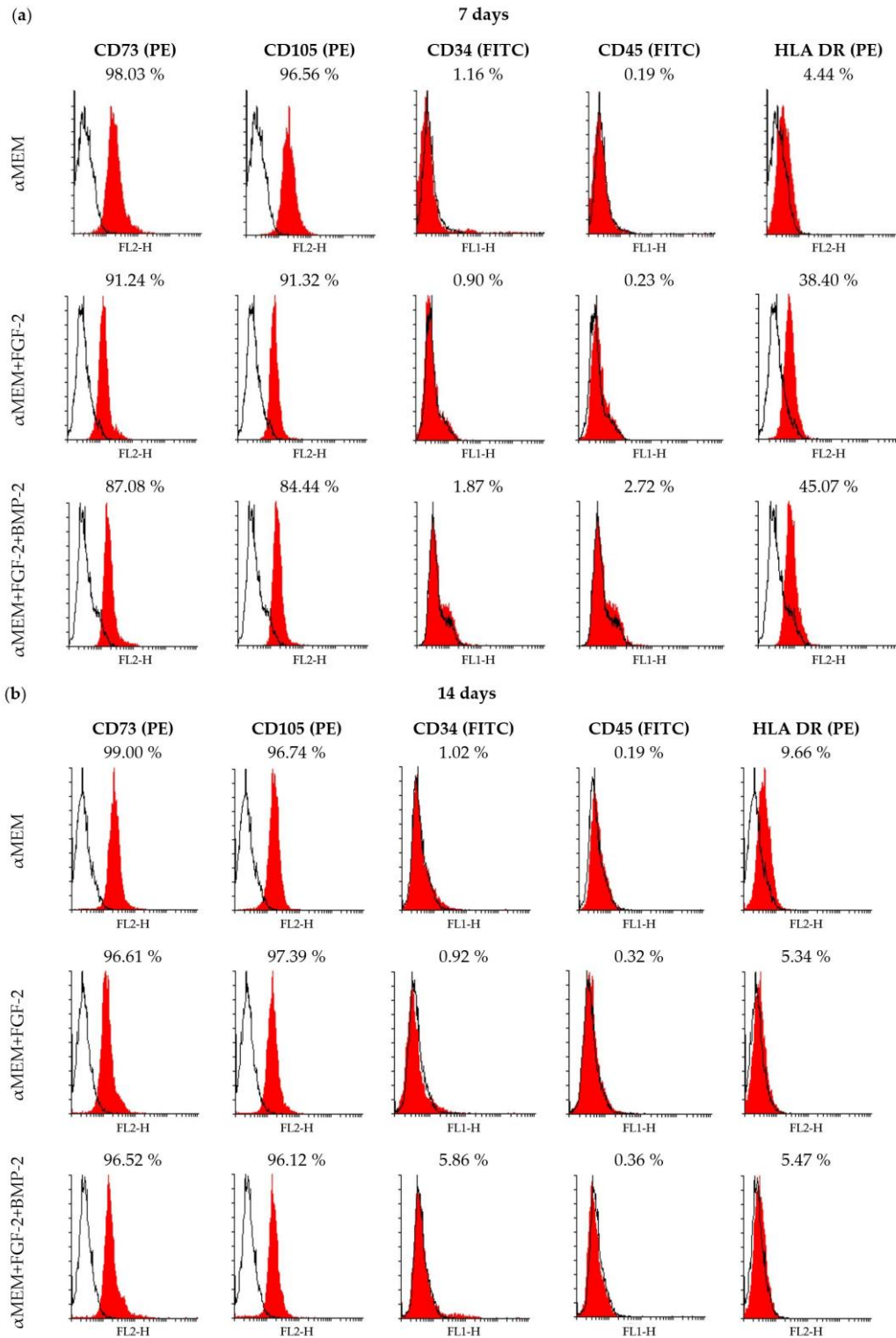


Figure S1. Flow cytometry analysis of BM-MSCs cultured in the control medium α MEM and in a medium supplemented with BMP-2 and/or FGF-2 for 7 and 14 days (a, b). Cell surface markers of BM-MSCs are similar in all culture conditions and incubation times.

Table S1. Antibodies used for flow cytometry and immunofluorescence.

Antigen	Antibody clone	Company	Dilution
Direct flow cytometry			
CD 73 PE	TY/23	BD Pharmingen, California, USA	1:5
CD 105 PE	MJ7/18	BD Pharmingen, California, USA	1:5
HLA-DR PE	37.68	Novus Biologicals, Abingdon, UK	1:250
Isotype control PE		Abcam, Cambridge, UK	1:50
Indirect flow cytometry			
CD34	EP373Y	Abcam, Cambridge, UK	1:250
CD45	CACTB51A	Novus Biologicals, Abingdon, UK	1:250
Goat Anti-Rabbit FITC		Abcam, Cambridge, UK	1:500
Goat Anti-Mouse FITC		Abcam, Cambridge, UK	1:500
Immunofluorescence staining			
Anti-Collagen I	Rabbit polyclonal	Abcam, Cambridge, UK	1:100
Anti-Osteocalcin	OCG3	Abcam, Cambridge, UK	1:100

Table S2. Primers used in PCR assays.

Gene	Primer Sequences (5'-3')	Fragment size (bp)	Cycles	T_m (°C)
RT-PCR assay				
<i>GAPDH</i>	F: CCTGCACCACCAACTGCTTG R: TTGAGCTCAGGGATGACCTTG	224	30	55
<i>CD90</i>	F: AGGACACAGGAAGCCACAAG R: CCCTCACTCTCCATCAGGTC	311	30	56
qRT-PCR assay				
<i>GAPDH</i>	F: GCAAGTTCCACGGCACAG R: GGTTACGCCCATCACAA	249	40	58
<i>BMP-2</i>	F: ATGGTTTCGTGGTGGAGGTAG R: ACTTGAGGCGTTTCCGCTGTT	210	40	58
<i>Runx2</i>	F: TCGCCTCACAAACAACCA R: AGGGACCTGCGGAGATTA	102	40	53
<i>Osterix</i>	F: CAGCGGCGTGCAGTAAAT R: CTGGGAACGAGTGGGAAAA	240	40	56
<i>Collagen type I</i>	F: CAAGAAGAAGACATCCCACC R: AGATCACGTCATCGCACA	133	40	55
<i>Osteocalcin</i>	F: AGATGCAAAGCCTGGTGATGC R: CTCCTGGAAGCCGATGTGGT	211	40	60
<i>Osteopontin</i>	F: TCCCACTGACATTCCAACAA R: CTGTGGCATCTGGACTCTCA		40	60

Article

Osteogenic Potential of Sheep Mesenchymal Stem Cells Preconditioned with BMP-2 and FGF-2 and Seeded on an nHAP-Coated PCL/HAP/ β -TCP Scaffold

Sandra Stammitz ¹, Agnieszka Krawczenko ¹, Urszula Szałaj ², Żaneta Górecka ³, Agnieszka Antończyk ⁴, Zdzisław Kielbowicz ⁴, Wojciech Świąszkowski ³, Witold Łojkowski ² and Aleksandra Klimczak ^{1,*}

¹ Laboratory of Biology of Stem and Neoplastic Cells, Hirszfeld Institute of Immunology and Experimental Therapy, Polish Academy of Sciences, R. Weigla 12, 53-114 Wrocław, Poland

² Laboratory of Nanostructures and Nanomedicine, Institute of High Pressure Physics, Polish Academy of Sciences, Sokolowska 29/37, 01-142 Warsaw, Poland

³ Division of Materials Design, Faculty of Materials Science and Engineering, Warsaw University of Technology, 141 Woloska Str., 02-507 Warsaw, Poland

⁴ Department of Surgery, Faculty of Veterinary Medicine, Wrocław University of Environmental and Life Sciences, pl. Grunwaldzki 51, 50-366 Wrocław, Poland

* Correspondence: aleksandra.klimczak@hirszfeld.pl

Citation: Stammitz, S.; Krawczenko, A.; Szałaj, U.; Górecka, Ż.; Antończyk, A.; Kielbowicz, Z.; Świąszkowski, W.; Łojkowski, W.; Klimczak, A. Osteogenic Potential of Sheep Mesenchymal Stem Cells Preconditioned with BMP-2 and FGF-2 and Seeded on an nHAP-Coated PCL/HAP/ β -TCP Scaffold. *Cells* **2022**, *11*, 3446. <https://doi.org/10.3390/cells11213446>

Academic Editor: Tong-Chuan He

Received: 22 September 2022

Accepted: 28 October 2022

Published: 31 October 2022

Publisher's Note: MDPI stays neutral with regard to jurisdictional claims in published maps and institutional affiliations.



Copyright: © 2022 by the authors. Licensee MDPI, Basel, Switzerland. This article is an open access article distributed under the terms and conditions of the Creative Commons Attribution (CC BY) license (<https://creativecommons.org/licenses/by/4.0/>).

Abstract: Mesenchymal stem cells (MSCs) attract interest in regenerative medicine for their potential application in bone regeneration. However, direct transplantation of cells into damaged tissue is not efficient enough to regenerate large bone defects. This problem could be solved with a biocompatible scaffold. Consequently, bone tissue engineering constructs based on biomaterial scaffolds, MSCs, and osteogenic cytokines are promising tools for bone regeneration. The aim of this study was to evaluate the effect of FGF-2 and BMP-2 on the osteogenic potential of ovine bone marrow-derived MSCs seeded onto an nHAP-coated PCL/HAP/ β -TCP scaffold in vitro and its in vivo biocompatibility in a sheep model. In vitro analysis revealed that cells preconditioned with FGF-2 and BMP-2 showed a better capacity to adhere and proliferate on the scaffold than untreated cells. BM-MSCs cultured in an osteogenic medium supplemented with FGF-2 and BMP-2 had the highest osteogenic differentiation potential, as assessed based on Alizarin Red S staining and ALP activity. qRT-PCR analysis showed increased expression of osteogenic marker genes in FGF-2- and BMP-2-treated BM-MSCs. Our pilot in vivo research showed that the implantation of an nHAP-coated PCL/HAP/ β -TCP scaffold with BM-MSCs preconditioned with FGF-2 and BMP-2 did not have an adverse effect in the sheep mandibular region and induced bone regeneration. The biocompatibility of the implanted scaffold-BM-MSC construct with sheep tissues was confirmed by the expression of early (collagen type I) and late (osteocalcin) osteogenic proteins and a lack of an elevated level of proinflammatory cytokines. These findings suggest that FGF-2 and BMP-2 enhance the osteogenic differentiation potential of MSCs grown on a scaffold, and that such a tissue engineering construct may be used to regenerate large bone defects.

Keywords: mesenchymal stem cells; scaffold; tissue engineering construct; bone regeneration

1. Introduction

Bone, as a particularly dynamic connective tissue, undergoes continuous remodeling, during which osteoclasts remove damaged bone cells, then osteoblasts take part in the formation of new bone tissue. This process enables optimal adaptation of the bone structure to functional demands [1]. Although bone tissue has a tremendous regenerative capacity and is able to heal itself without fibrotic scar formation (contrary to most other tissues in the human body), approximately 5–10% of fractures are prone to healing

abnormally [2]. Indeed, bone disorders are a daily occurrence in today's clinical practice, contributing to a health, economic, and social burden on our aging population [3]. The most challenging pathological conditions are large traumatic bone damage and extensive bone loss due to tumor resection or failed surgery [4]. The clinical gold standard in orthopedic surgery is the autologous bone graft. However, there are limitations, such as deficient bone supply and donor site morbidity, that make it necessary to look for alternative methods. Although allografts or xenografts admittedly solve these problems, the drawbacks of these methods are immune reactions, risk of infectious agent transmission, high costs, and donor scarcity [5]. Therefore, more efficient alternatives to bone grafting are needed.

Technological advances have provided orthopedic implants made of biomaterials that reconstruct the damaged bone. These bioactive materials are able to elicit controlled action and reaction within the biological environment. However, biomaterials alone only serve as guidance for bone tissue, rather than as an osteoinductive agent, which means that immature cells are not recruited or stimulated to differentiate into osteogenic cells. In order to ensure not only structural but also functional integrity in complex skeletal defects, tissue engineering constructs composed of cells, scaffolds, and bioactive factors are required [6]. Mesenchymal stem cells (MSCs) are useful in the field of regenerative medicine because of their (1) multiple differentiation capability, (2) availability in large amounts, (3) usability in both autologous and allogenic transplants, (4) painless isolation methods, and (5) conformity with Good Manufacturing Practice guidelines (GMP) [7]. In addition to the capacity of MSCs to differentiate into bone tissue cells, they are also able to secrete bioactive factors, which impact other cells by regulating their significant biological functions, such as migration, proliferation, communication, and differentiation. The MSC secretome may be affected by specific culture conditions, such as medium composition or biomaterial properties [8]. Therefore, growth factors, such as fibroblast growth factor 2 (FGF-2) and osteogenic differentiating factors, such as bone morphogenetic proteins (BMPs), can be used to enhance the MSC osteogenic potential. BMPs and FGFs are among the main regulators in the bone healing cascade [9]. Although FGFs do not directly stimulate osteogenic differentiation, they modulate it by increasing osteoblast proliferation as well as inducing angiogenesis in the bone defect site [10]. BMPs are currently considered to be the proteins with the most beneficial effect on the repair of large bone defects [11]. They are involved in skeletal development and the osteogenic differentiation of MSCs and bone formation [12]. Furthermore, the Food and Drug Administration (FDA) has approved BMP-2 for clinical use in bone fracture treatment [13]. FGF-2 and BMP-2 were found to display a synergistic effect on MSC osteogenic differentiation [14–16].

In bone tissue engineering, scaffolds with osteoinductive and osteoconductive properties have been designed to provide 3D culture conditions for MSCs and enhance their regenerative properties, resulting in bone tissue formation [17]. Scaffolds play a crucial role in bone regeneration, acting as the extracellular matrix, which enables cells to grow in a three-dimensional environment and interact with other cells [18]. A safe and successful clinical application of biomaterials requires a scaffold with the appropriate properties, including biocompatibility, osteogenic stimulation, mechanical properties, and no immune response while being implanted into the host bone [19,20]. Biodegradable scaffolds consisting of composites, such as polymers combined with ceramics, display better physicochemical properties than non-composite scaffolds. For example, FDA-approved polycaprolactone (PCL) combined with ceramics, such as tricalcium phosphate (TCP) and hydroxyapatite (HA), shows both the controlled degradation kinetic potential of polymers and the considerable bioactive potential of ceramics [21].

Although many studies have been conducted in the field of bone regeneration, further investigation is needed for successful human clinical trials. In particular, the optimization of MSC culture methods on an appropriate scaffold and stimulation with bioactive factors in order to obtain a tissue engineering construct with optimal bone healing properties is required for the reconstruction of large bone tissue defects. It is worth mentioning

that selecting an appropriate animal model for in vivo research is crucial in order to provide proof of concept for new bone tissue engineering techniques. Rodents are the most commonly used animal model. However, large animal models are more advantageous due to their body weight, bone size, and structural similarity to humans [22]. An adequate simulation of the biomechanics of human large bone defects based on animal models, such as mice or rats, is impossible. In addition, immunological responses in large animal models are closer to human responses [23] than in small animal models. Therefore, to mimic human clinical settings, the use of large animal models is absolutely essential [24].

Our previous study demonstrated that FGF-2 and BMP-2 enhance the osteogenic potential of sheep bone marrow-derived MSCs (BM-MSCs) in vitro [25]. In this study, we developed a bone tissue engineering construct consisting of an ovine BM-MSC and a nanohydroxyapatite-coated polycaprolactone/hydroxyapatite/ β -tricalcium phosphate (nHAP-coated PCL/HAP/ β -TCP) scaffold. We investigated the induced osteogenic effect of the bioactive factors FGF-2 and BMP-2 on this construct in vitro, after which we applied the construct in vivo to test its biocompatibility and regenerative potential in a large animal sheep model.

2. Materials and Methods

2.1. Biomaterial Characterization

Fabrication of a 3D Printed Scaffold

Composite scaffolds were tested. The composite material for scaffold fabrication was prepared from poly(ϵ -caprolactone) (PCL, PURASORB PC12, Corbion, Amsterdam, the Netherlands), hydroxyapatite (HAP, $\text{Ca}_5(\text{OH})(\text{PO}_4)_3$, Merck, Kenilworth, NJ, USA) and tricalcium phosphate (TCP, powder < 4 μm , 100% Beta-TCP, $\text{Ca}_3(\text{PO}_4)_2$, Progentix) using the solvent casting method as with the previous studies [26–28]. The mass ratio of PCL:HAP:TCP was 9:4.5:4.5, respectively. The scaffolds were fabricated with a BioScaffold printer (SYSENG, Germany) at a temperature of 110 $^\circ\text{C}$ using the G23 nozzle (ID 0.33 mm). The layers were printed with the 0° – 90° pattern and a 0.27 mm layer thickness. The distance between the parallel fibers was set at 1.1 mm. Lastly, the obtained fiber diameter was $342.9 \pm 19.5 \mu\text{m}$, and the pore size was $718 \pm 19.8 \mu\text{m}$. The fabricated scaffolds had a cylindrical shape with a diameter of 6 mm and a height of 3 mm. The scaffolds were additionally coated with nano-hydroxyapatite (GoHAP), as previously described [29]. Nano-hydroxyapatite GoHAP Type 3 was produced by the Institute of High Pressure Physics, PAS, was used to form layers on the surface of the scaffolds (GoHAP nano-hydroxyapatite layers) [29–32]. Nano-hydroxyapatite GoHAP is a synthetic bone mineral that is highly similar to the hydroxyapatite naturally present in the bones. The mean particle size of GoHAP was $16 \pm 3 \text{ nm}$, the specific surface was $140 \pm 15 \text{ nm}^2$, and the Ca/P ratio was 1.61. The GoHAP nano-hydroxyapatite layers were deposited on the 3D-printed scaffolds using the sonocoating method described in [33,34]. The morphology of the nano-hydroxyapatite GoHAP layers was tested using a SEM (Ultra Plus, Carl Zeiss Meditec AG, Jena, Germany) with a secondary electron (SE) detector. The thickness of the layer shown in the SEM images was measured using the ImageJ software, version 1.53k. The number of individual layer thickness measurements was 68. As a control, pristine PCL scaffolds were fabricated at a temperature of 100 $^\circ\text{C}$. All scaffolds were sterilized with 25 kGy of a Cobalt 60 gamma radiation source before the in vitro and in vivo experiments.

2.2. Sheep Bone Marrow-Derived Stem Cell (BM-MSC) Cultures on the Scaffold

The BM-MSCs collected from the same sheep were used in in vitro research and as autologous cells in in vivo experiments. BM-MSCs were isolated from the ovine iliac crest as previously described. A phenotype analysis of the sheep BM-MSCs confirmed the presence of specific MSC surface markers: $\text{CD}73^+$, $\text{CD}90^+$, and $\text{CD}105^+$, as introduced in our previous paper [25]. In this study, BM-MSCs were thawed at passage 1 or 2, seeded for expansion, and then used for both in vitro and in vivo experiments at passage 2 or 3. Cells

were cultured in the Minimum Essential Medium α -transformation, α MEM (IET PAS, Wroclaw, Poland), supplemented with 10% fetal bovine serum, FBS (Biowest, Riverside, Montana, MT, USA, cat. no. S1810-500), 1% penicillin/streptomycin (Merck, Saint Louis, MO, USA, cat. no. P0781), 2 mM L-glutamine (Biowest, Riverside, Montana, MT, USA, cat. no. X0550-100) and incubated at 37 °C in 5% CO₂ and 95% air. The medium was replaced two times a week. Prior to the in vitro cell seeding, the scaffold was placed in an appropriate culture plate well and washed with the culture medium for 30 min. Next, the medium was aspirated and the trypsinized BM-MSCs were seeded at a density of 5×10^4 in 20 μ L of the medium (for experiments lasting 21 days) or a 5×10^5 cells/scaffold for the MTT and Picogreen assay. The cells were incubated for one hour at 37 °C to allow diffusion into and adhesion to the scaffold before the addition of the culture medium to each well. The experiments were conducted in three different medium conditions: (1) α MEM (control), (2) α MEM supplemented with 20 ng/mL FGF-2 (Merck, Saint Louis, MO, USA, cat. no. F0291), and (3) α MEM supplemented with 20 ng/mL FGF-2 and 100 ng/mL BMP-2 (Stem Cell Technologies, Grenoble, France, cat. no. 78004.1).

2.3. DAPI Staining for the Observation of BM-MSC Adhesion on a Scaffold

For the recognition of cell attachment to the scaffold, the DAPI staining method was used. BM-MSCs at a density of 5×10^4 cells/scaffold were seeded onto scaffolds in a 48-well plate and cultured for 21 days in 500 μ L of the α MEM medium supplemented with 20 ng/mL FGF-2 only or 20 ng/mL FGF-2 and 100 ng/mL BMP-2, and in an osteogenic differentiation medium (PromoCell, Heidelberg, Germany, cat. no. C-28013) with FGF-2 only or FGF-2 and BMP-2. The media were changed every three days. After three weeks, the culture media were aspirated, and the cell-scaffold constructs were washed with PBS (IET PAS, Wroclaw, Poland) and fixed with 3.7% formaldehyde (Merck, Saint Louis, MO, USA, cat. no. 104003) for 30 min. Excess formalin was removed, and the scaffolds were washed again in PBS. Next, the cell nuclei were stained with DAPI (Vector Labs, Burlingame, CA, USA, cat. no. H-1200) for 20 min in the dark at RT. The scaffolds were rinsed three times with PBS to remove excess DAPI, and the cells were visualized using an Axio Observer fluorescence microscope (Zeiss, Jena, Germany).

2.4. Quantification of BM-MSCs on the Scaffold

To determine the effect of medium supplementation with FGF-2 only or with a combination of FGF-2 and BMP-2 on the capacity of the cells to adhere to the scaffold, the cells were quantified on the scaffold using the Picogreen solution from the Quant-it Picogreen kit (Invitrogen Life Technologies, France, cat. no. P7589), which binds double-stranded DNA. First, scaffolds in duplicates were placed in the V-bottom wells of a 96-well plate and incubated for 30 min at 37 °C with 200 μ L of the α MEM medium (control) or with FGF-2 only or with FGF-2 and BMP-2. Next, the medium was aspirated, and 5×10^5 cells in 20 μ L of the medium with or without cytokines were seeded onto the scaffolds. After three hours of incubation, the scaffolds with the adhered cells were removed. To the remaining BM-MSCs at the bottom of the V-shape wells, 200 μ L of a lysis solution was added, containing the Tris-EDTA buffer (Sigma-Aldrich, St. Louis, MO, USA, cat. no. T9285-100ML), 0.1% Triton X-100 (Sigma-Aldrich, St. Louis, MO, USA, cat. no. T8787-50ML), and 0.2 mg/mL proteinase K (Ambion RNA by Life Technologies, Waltham, MA, USA, cat. no. AM2548). The suspensions were incubated at 52 °C overnight, after which they underwent three heat shocks at -80 °C and RT, followed by sonication for 10 min. Meanwhile, a standard cell range from 0 to 5×10^5 of BM-MSCs was prepared. DNA samples from the cell standard range and non-adherent cells were labelled with Picogreen in a 96-well plate and incubated for 10 min in the dark. Fluorescence was read at 520 nm using an EnSpire 2300 Multilabel Reader (Perkin Elmer LAS, Waltham, MA, USA). To quantify the cells, a standard curve was used. The experiment was repeated three times.

2.5. BM-MSC Viability on the Scaffold

The viability of BM-MSCs cultured with FGF-2 only or with a mixture of FGF-2 and BMP-2 on the scaffolds was analyzed using the MTT assay. The cells were seeded in duplicate at a density of 5×10^5 BM-MSCs/scaffold in 20 μ L of the medium in 96-well plates. The cells were allowed to attach to the scaffold for the first hour, after which 200 μ L of the medium was added. Cell proliferation was analyzed after 1, 3, 5, and 7 days. Next, 20 μ L of a 4 mg/mL MTT solution (Merck, Saint Louis, MO, USA, cat. no. M2128) were added. After incubation, over the next 4 h at 37 °C, the medium was aspirated, and 200 μ L of DMSO (POCH, Gliwice, Poland, cat. no. 363550117) was added to solubilize the purple formazan crystals. Absorbance was quantified at 570 nm with a Wallac Victor2 microplate reader (Perkin Elmer LAS, Waltham, MA, USA). The medium in each well was replaced every two days. The MTT assay was repeated three times.

2.6. Alizarin Red S Staining Quantification

Alizarin Red S staining was performed to evaluate the osteogenic differentiation of BM-MSCs untreated or treated with FGF-2 only or with a combination of FGF-2 and BMP-2 and seeded on a scaffold. BM-MSCs at a density of 5×10^4 /scaffold were seeded in 20 μ L of the medium in 96-well plates. After one hour of incubation, 200 μ L of an osteogenic differentiation medium (PromoCell, Heidelberg, Germany, cat. no. C-28013) alone or supplemented with FGF-2 only or with FGF-2 and BMP-2 was added. The media were refreshed three times a week. After 7, 14, and 21 days of incubation, the differentiation potential was quantified based on Alizarin Red S staining using the cetylpyridinium chloride, CPC (Sigma-Aldrich, St. Louis, MO, USA, cat. no. C0732-100G) extraction method. For staining, the differentiation medium was removed, and the BM-MSC-scaffold constructs were washed with PBS and fixed for 20 min at RT in 3.7% formaldehyde. Next, the formaldehyde was aspirated, and the constructs were washed with PBS again and stained with 200 μ L Alizarin Red S for 10 min at RT. For CPC extraction, PBS was removed from the wells, and the cells on the scaffold were incubated for two hours at 37 °C with 200 μ L of a 10% CPC solution. The dye was transferred to a new 96-well plate and read at 405 nm with a Wallac Victor2 reader.

2.7. Alkaline Phosphatase Activity

To measure ALP activity, p-nitrophenyl phosphate, pNPP (Sigma-Aldrich, St. Louis, MO, USA, cat. no. P7998-100ML), was used as an ALP substrate. BM-MSCs were cultured on a scaffold following the same procedure as in the Alizarin Red S staining Section 2.6. On days 7, 14, and 21 of incubation, the BM-MSC-scaffold constructs were washed with PBS, and 200 μ L of pNPP were added. After one hour of incubation at 37 °C, the yellow product was transferred to a fresh 96-well plate in order to measure absorbance at 405 nm using a Wallac Victor2 reader.

2.8. qRT-PCR for Osteogenic Gene Expression

To analyze the impact of FGF-2 and BMP-2 on the osteogenic gene expression of the tissue engineering construct consisting of an nHAP-coated PCL/HAP/ β -TCP scaffold and BM-MSCs, the constructs were cultured for 21 days in a 6-well plate in the α MEM control medium, or supplemented with FGF-2 only or with FGF-2 and BMP-2. The samples were collected after 7, 14, and 21 days into 2 mL Matrix M tubes with beads (MP Biomedicals, Solon, OH, USA, cat. nos. 6923050 and 6540034) with 1 mL of the TRIzol reagent (Ambion RNA by Life Technologies, Waltham, MA, USA, cat. no. 15596026) and homogenized using a FastPrep-24 tissue and cell homogenizer (MP Biomedicals, Solon, OH, USA). Total RNA was extracted and purified with the NucleoSpin RNA Kit (Macherey-Nagel, Düren, Germany, cat. no. 740955.50) according to the manufacturer's instructions for RNA purification in combination with TRIzol lysis. A reverse transcription of total RNA in the amount of 1 μ g from each sample was conducted using the RevertAid First Strand cDNA Synthesis Kit (Thermo Fisher, Vilnius, Lithuania, cat. no. K1622). Real-time PCR was

performed with the Power SYBR Green PCR Master Mix (Life Technologies, Warrington, UK, cat. no. 4367659), and the rate of dye incorporation was analyzed using the ViiA 7 Real-Time PCR System (Applied Biosystems, Foster City, CA, USA). The reactions were carried out three times with two biological replicates with the following program settings: initial denaturation at 95 °C for 10 min, followed by 40 cycles of denaturation at 95 °C for 15 s, annealing at the T_m (°C) of the primers listed in Table 1 for one minute, and extension at 72 °C for 40 s. The levels of the housekeeping gene GAPDH transcript were used to normalize all PCR product quantifications (ΔCT), and the relative mRNA expression level was obtained using the $2^{-\Delta\Delta CT}$ calculation method.

Table 1. Primer sequences for qRT-PCR.

Gene	Primer Sequences (5'-3')	Fragment Size (bp)	Cycles	T_m (°C)	GenBank Accession no.
<i>GAPDH</i>	F: GCAAGTTCCACGGCACAG R: GGTCACGCCCATCACAA	249	40	58	AF030943.1
<i>BMP-2</i>	F: ATGGTTTCGTGGTGGAGGTAG R: ACTTGAGGCGTTCCGCTGTT	210	40	58	AF508028.1
<i>Runx2</i>	F: TCGCCTCACAAACAACCA R: AGGGACCTGCGGAGATTA	102	40	53	DY517479.1
<i>Osterix</i>	F: CAGCGGCGTG CAGTAAAT R: CTGGGAACGAGTGGGAAAA	240	40	56	BC151270.1
<i>Collagen type I</i>	F: CAAGAAGAAGACATCCCACC R: AGATCACGTCATCGCACA	133	40	55	AF129287.1
<i>Osteocalcin</i>	F: AGATGCAAAGCCTGGTGATGC R: CTCCTGGAAGCCGATGTGGT	211	40	60	DQ418490.1
<i>Osteopontin</i>	F: TCCCCTGACATTCCAACAA R: CTGTGGCATCTGGACTCTCA	196	40	60	AF152416.1

2.9. Animal Surgery

The study was approved by the local Animal Ethics Committee at the Institute of Immunology and Experimental Therapy PAS (no. 63/2017). Preliminary research in vivo using four adult sheep weighing from 42 to 54 kg was performed primarily to assess the biocompatibility and osteogenic potential of the scaffold-BM-MSCs construct in the mandibular region of a large animal model. Moreover, this region was used to assess the feasibility of the treatment method for critical-sized mandibular bone defects. In the small ruminant model, the mandibular angle is the optimal site to create artificial, critical bone defects due to the specific anatomy and physiology of this species. Creating the defect more cranially would damage the tooth roots, disrupting the physiological chewing process and leading to the animal's death. All surgical procedures were performed by experienced surgeons at the Department and Clinic of Surgery, Faculty of Veterinary Medicine, Wrocław University of Environmental and Life Sciences.

2.9.1. Anesthesia and Analgesia

All sheep received medetomidine (0.01 mg/kg, Cepetor, CP-Pharma Handelsges), butorphanol (0.1 mg/kg, Butomidol Richter Pharma AG, Oberösterreich, Austria), and a combination of tiletamine and zolazepam (2 mg/kg, Zoletil 100, Virbac, Carros, France) intramuscularly (im). General anesthesia was induced with propofol (Propofol-Lipuro®, 10 mg/mL, B. Braun Melsungen AG, Melsungen, Germany) at an initial dose of 2 mg/kg to effect, in order to permit tracheal intubation. The anesthesia was maintained with isoflurane (IsoVet, Piramal Healthcare, Morpeth, UK) in oxygen. After a bolus of fentanyl (Fentanyl WZF, Polfa Warszawa, Poland; 3 mcg/kg), analgesia was continued with a constant rate infusion of fentanyl (CRI—0.3 mcg/kg/min). Postoperative pain was managed with meloxicam (0.2 mg/kg sc, Metacam, Boehringer Ingelheim Vetmedica GmbH,

Ingelheim am Rhein, Germany), metamizole (50 mg/kg iv, Injectio Pyralgini Biowet Puławy, Biowet Puławy Sp. z o.o., Puławy, Poland), and buprenorphine (0.02 mg/kg im, Bupaq Multidose, Richter Pharma AG, Austria). Intravenous fluids (crystalloids) were given in each case at a rate of 10 mL/kg/h. Throughout the surgical procedure, the vital parameters of the animals (heart rate, respiratory rate, end-tidal CO₂, blood pressure, oxygen saturation, and temperature) were monitored continuously (Datex-Ohmeda S5 monitor, Helsinki, Finland).

2.9.2. Surgical Procedure for Scaffold Implantation

Two incisions of up to 8 cm in length were made on the right and left side over the mandibular surface. Before the scaffold implantation, 20×10^6 of autologous BM-MSCs treated with FGF-2 ($n = 2$) or FGF-2 and BMP-2 ($n = 2$) were resuspended in 2 mL of 0.9% NaCl and seeded on each scaffold using a 3-mL syringe with a 27-gauge needle. After dissecting through the masseter muscle, a facial vein was isolated, and the scaffold was implemented around the vessel in a manner that enabled blood to flow through the vessel (Figure 1a). To confirm the location of the scaffold and patency of a blood vessel, a computed tomography (CT) scan (Siemens Somatom Emotion 16) with iodine-based contrast (Iomeron 400, Bracco Imaging Deutschland GmbH, Konstanz, Germany) was performed after the implantation (Figure 1b). After the surgery, the sheep were observed for a period of 6 months. Wound healing, the general health of the animals, and signs of inflammation were monitored.

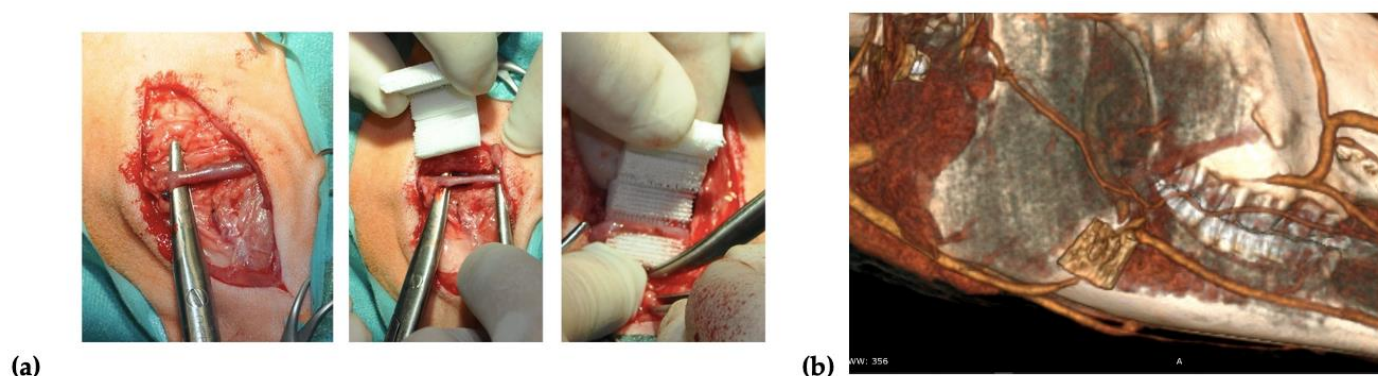


Figure 1. (a) Scaffold implantation in the masseter muscles, around the facial vein. (b) A tomography scan performed immediately after the implantation procedure.

2.10. Collagen Type I and Osteocalcin Immunofluorescence Staining

Sections prepared from the nHAP-coated PCL/HAP/ β -TCP scaffolds implanted with BM-MSCs treated with FGF-2 alone ($n = 2$) or FGF-2 and BMP-2 ($n = 2$) were retrieved from recipient sheep 6 months after surgery. The formalin-fixed paraffin-embedded slides were placed in a 60 °C oven for an hour. Next, the sections were deparaffinized with xylene (CHEMPUR, Piekary Sl., Poland, cat. no. 115208603) twice, and washed with 100% ethanol (CHEMPUR, Piekary Sl., Poland, cat. no. 113964800), 70% ethanol, and 40% ethanol, every wash lasting 10 min. After the washes, the sections were immersed in miliQ water. Antigens were retrieved using a 10 mM sodium citrate buffer, pH 6.0 (IIET PAS, Wroclaw, Poland) for 20 min at 98 °C. Afterwards, the slides were cooled to RT, washed twice with PBS, and proceeded with immunostaining. Each section was incubated overnight at 4 °C with 150 μ L of 1:100 diluted primary antibody, rabbit anti-collagen type I (Abcam, Cambridge, UK, cat. no. AB34710), or mouse anti-osteocalcin (Abcam, Cambridge, UK, cat. no. AB13420). Next, each slide was washed with PBS three times and incubated for 30 min in the dark at RT with 150 μ L of 1:500 diluted secondary goat anti-rabbit (Abcam, Cambridge, UK, cat. no. AB6717) or goat anti-mouse (Abcam, Cambridge, UK, cat. no. AB6785) FITC-conjugated solutions. After three PBS washes, DAPI (Vector

Labs, Burlingame, CA, USA, cat. no. H-1200) was used for nuclei staining for 20 min of incubation in the dark at RT. Finally, the sections were washed with PBS and the immunofluorescence staining was visualized using an Axio Observer inverted fluorescence microscope (Zeiss, Jena, Germany) and analyzed using the Zeiss Zen Blue software, version 2.6.

2.11. *Ovine Cytokine Array*

To assess the biocompatibility of the implanted scaffold covered with BM-MSCs, the activity of trophic factors promoting osteogenesis and the expression of proinflammatory cytokines associated with the immune response were examined. Serum samples from the sheep undergoing the implantation of the nHAP-coated PCL/HAP/ β -TCP scaffold covered with BM-MSCs and treated with FGF-2- ($n = 2$) or FGF-2 and BMP-2 ($n = 2$) were collected one week prior to and also one, two, and four weeks after surgery. The C-Series Ovine (Sheep) Cytokine Array C1 Kit (Ray-Bio®, Norcross, GA, USA, cat. no. AAO-CYT-1-8) was used to evaluate the relative level of cytokines in the sheep serum. Firstly, the samples were centrifuged at 3000 rpm for 10 min at RT and diluted five times with a blocking buffer, included in the Array Kit. The experiment was conducted according to the manufacturer's protocol. The data were obtained with the Protein Array Analyzer plugin for the ImageJ software. The differences in the relative protein expression of the serum samples were presented on heat maps created using the GraphPad Prism version 7 (GraphPad Software, Inc., San Diego, California, USA).

2.12. *Statistical Analysis*

Statistical analysis was performed with the GraphPad Prism 9 software, version 9.2.0, using one-way analysis of variance (one-way ANOVA) with Dunnett's test for multiple comparison. A p -value < 0.05 was considered statistically significant.

3. Results

3.1. *Biomaterial Characterization*

The sonocoating method [33,34] allowed for the deposition of a bioactive layer consisting of nano-hydroxyapatite nanoparticles (GoHAP Type 3) on the surface of the 3D-printed scaffold. SEM imaging showed that the GoHAP nano-hydroxyapatite layers deposited on the scaffold surface were homogeneous. Moreover, the GoHAP nano-hydroxyapatite layers were present not only on the outer surface of the scaffold (Figure 2A,B), but also on the surface of the scaffold pores, as demonstrated by the cross-sectional imaging of the coated scaffold (Figure 2C–F). The average thickness of the GoHAP nano-hydroxyapatite layer was about 220 ± 70 nm.

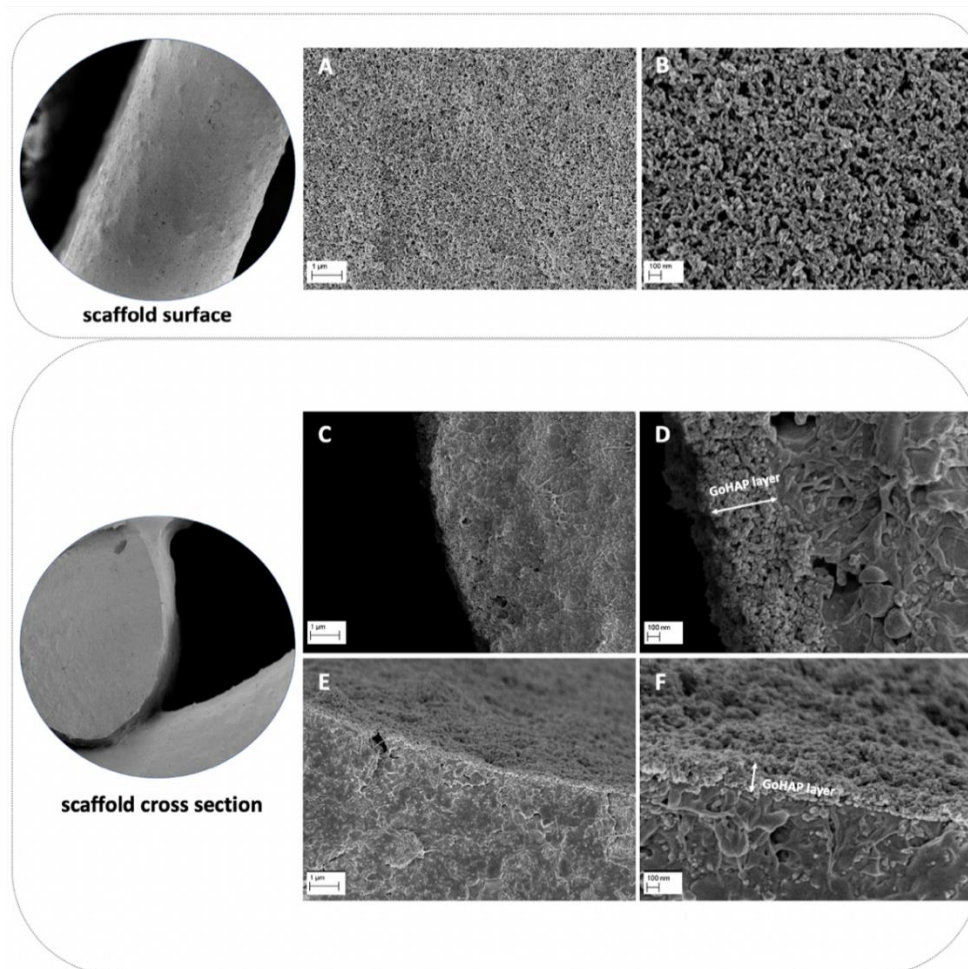


Figure 2. SEM images of the obtained nano-hydroxyapatite GoHAP layers on nHAP-coated PCL/HAP/ β -TCP scaffolds: (A,B) outer fiber surface of the scaffold; (C–F) cross-section of the inner fibers of the scaffold.

3.2. BM-MSCs Attachment and Spreading on the nHAP-Coated PCL/HAP/ β -TCP Scaffold

The attachment and spread of BM-MSCs on the nHAP-coated PCL/HAP/ β -TCP scaffold was observed microscopically at the following time points: 7, 14, and 21 days. The capacity for cell adhesion was compared between (a) the control medium α MEM, (b) α MEM supplemented with FGF-2, and (c) α MEM supplemented with FGF-2 and BMP-2. In all three media, the cells readily adhered to the scaffolds (Figure 3). Untreated BM-MSCs began to gather around the cross-bar segments of the scaffold after 14 days of incubation. However, by day 21, there were still large unfilled spaces between the scaffold bars (Figure 3a). In contrast, BM-MSCs cultured in α MEM and FGF-2 showed a more favorable adhesion to the scaffold. After 21 days, they covered a sizable space around the scaffold bars (Figure 3b). Nevertheless, the best capacity to attach and spread on the scaffold was observed for the cells treated with FGF-2 and BMP-2. Migrating BM-MSCs started to spread between the scaffold bars on day 7, and after 14 days, the cells covered a larger area between the bars compared to the cells cultured with FGF-2. However, on day 21, FGF-2- and BMP-2-treated cells filled the space between the scaffold bars to an extent comparable to that of FGF-2-treated BM-MSCs (Figure 3c). Together, these observations indicated that ovine BM-MSCs maintained good adhesion ability and material affinity on the nHAP-coated PCL/HAP/ β -TCP scaffold and that pretreatment with FGF-2 and BMP-2 promoted this capacity.

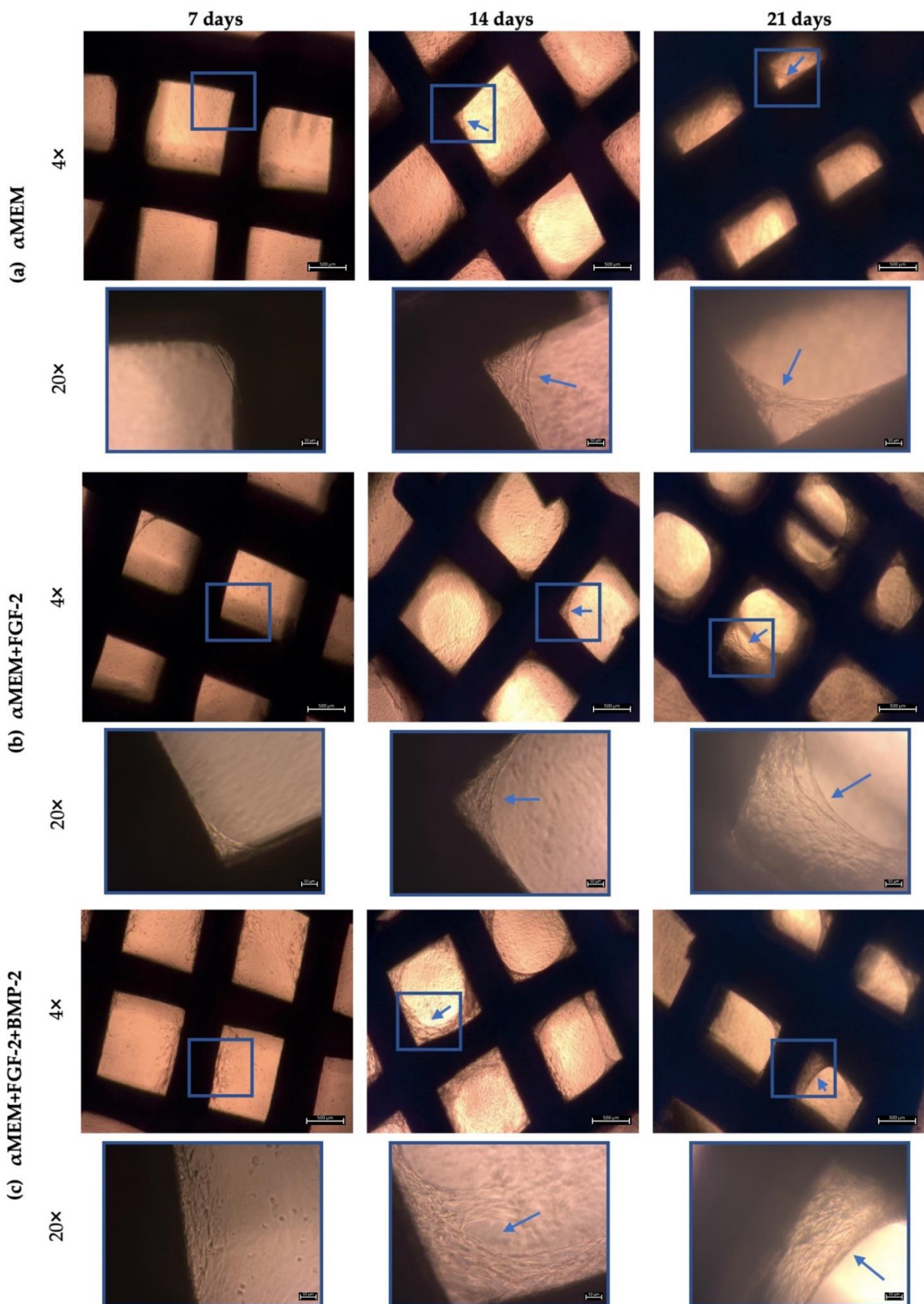


Figure 3. Morphology of sheep BM-MSCs on days 7, 14, and 21, cultured on the nHAP-coated PCL/HAP/ β -TCP scaffold in different culture media. In response to FGF-2 and BMP-2 stimulation, the cells attached differently to the scaffold. (a) BM-MSCs cultured in α MEM started to grow over the space between the scaffold structures on day 14; marked with blue arrows in the picture. (b) FGF-2-treated BM-MSCs created a specific 3D structure on the scaffold on day 21. This 3D cell structure covered a larger area than with the untreated cells. (c) BM-MSCs stimulated with FGF-2 and BMP-2 had the best ability to adhere to the scaffold surface after 14 days of incubation and maintained this ability on day 21 of observation. Under each picture, a higher magnification (20 \times) was added to show the area marked with the blue frame.

3.3. BM-MSC Adhesion on the nHAP-Coated PCL/HAP/ β -TCP Scaffold Analyzed with DAPI Staining

nHAP-coated PCL/HAP/ β -TCP scaffolds were seeded with BM-MSCs in a control medium α MEM and an osteogenic medium (Figure 4a,b) for 21 days. Furthermore, to investigate the impact of FGF-2 and BMP-2 on the ability of the cells to adhere to the scaffold, the culture media were supplemented with FGF-2 alone or FGF-2 and BMP-2. DAPI staining enabled the visualization of the cell nuclei on the scaffold bars, which are not visible with light microscopy. All analyzed culture media conditions promoted cell adhesion to the scaffold surface. The supplementation of FGF-2 seemed to not play a significant role in cell proliferation on the scaffold (Figure 4c,d). In contrast, supplementation of both the control medium and the osteogenic medium with both FGF-2 and BMP-2 stimulated the cells not only to proliferate on the scaffold surface but also to fill the space between the scaffold bars with a network of cells (Figure 4e,f).

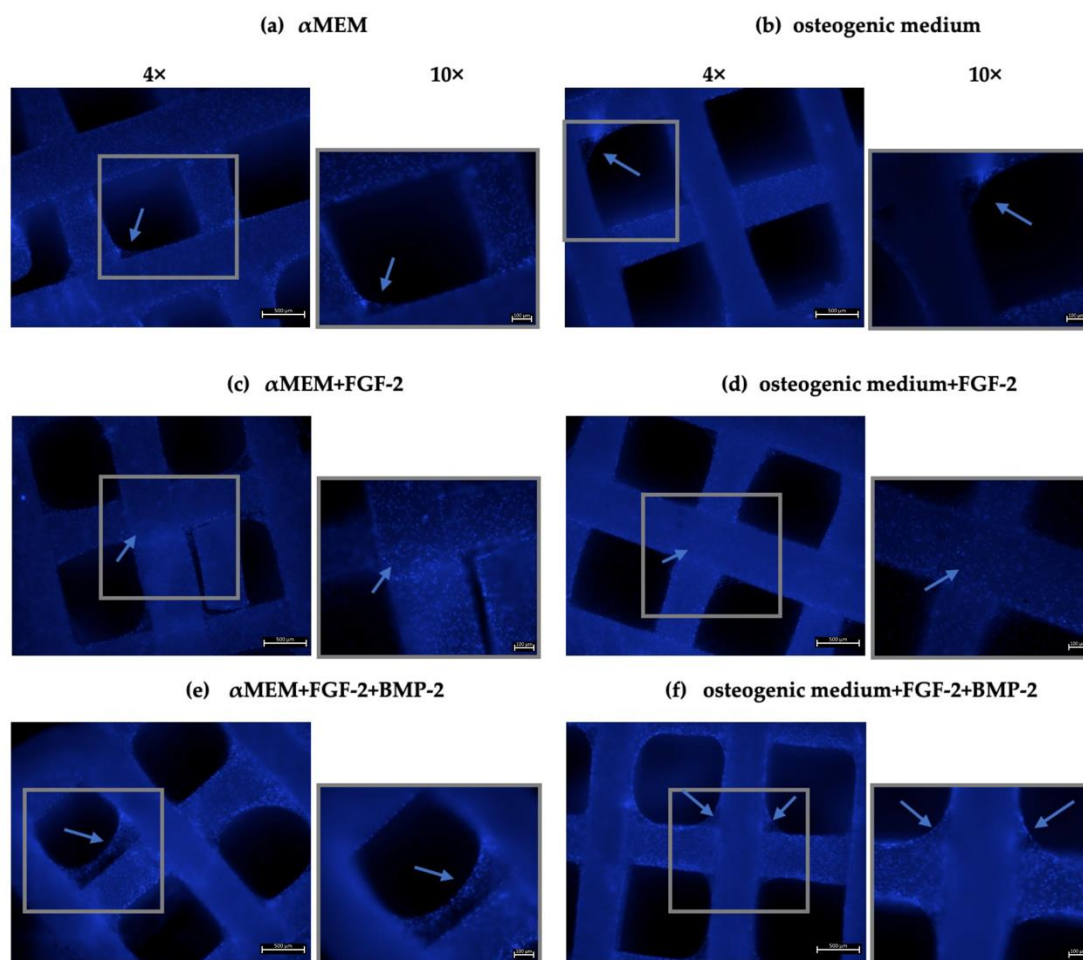


Figure 4. Ovine BM-MSC nuclei stained with DAPI (blue) on an nHAP-coated PCL/HAP/ β -TCP scaffolds 21 days after seeding, cultured in (a) α MEM, (b) osteogenic medium, (c) α MEM + FGF-2, (d) osteogenic medium + FGF-2, (e) α MEM + FGF-2 + BMP-2 and (f) osteogenic medium + FGF-2 + BMP-2. The BM-MSCs maintained good material affinity on the scaffold, as indicated by the number of nuclei on the cross-bar segments of the scaffold. However, stimulation with FGF-2 and BMP-2 increased cell proliferation not only on the scaffold bars but also in the space between the bars. A higher magnification (10 \times) was added next to each picture in order to show the area marked with the gray frame.

3.4. Number of Cell on the Scaffold Analyzed with the Picogreen Assay

The adhesion capacity of BM-MSCs to the nHAP-coated PCL/HAP/ β -TCP scaffold was evaluated through the quantification of total DNA, labelled with Picogreen. After 3 h of incubation of 5×10^5 cells on the scaffold, the number of cells that adhered to the scaffold was assessed in the α MEM medium supplemented with only FGF-2 or FGF-2 and BMP-2 and compared to the control medium α MEM. The number of BM-MSCs cultured with FGF-2 alone or FGF-2 and BMP-2 on the scaffold was significantly higher compared to the control. In the control medium α MEM, out of the 5×10^5 seeded cells, less than 10^5 cells adhered to the scaffold, whereas in α MEM and FGF-2, over 2.5×10^5 BM-MSCs attached to the scaffold. Nevertheless, supplementation with both FGF-2 and BMP-2 resulted in the highest adherence of the BM-MSCs to the scaffold, as indicated by the adhesion of 3.5×10^5 cells to the scaffold ($p < 0.0001$, Figure 5).

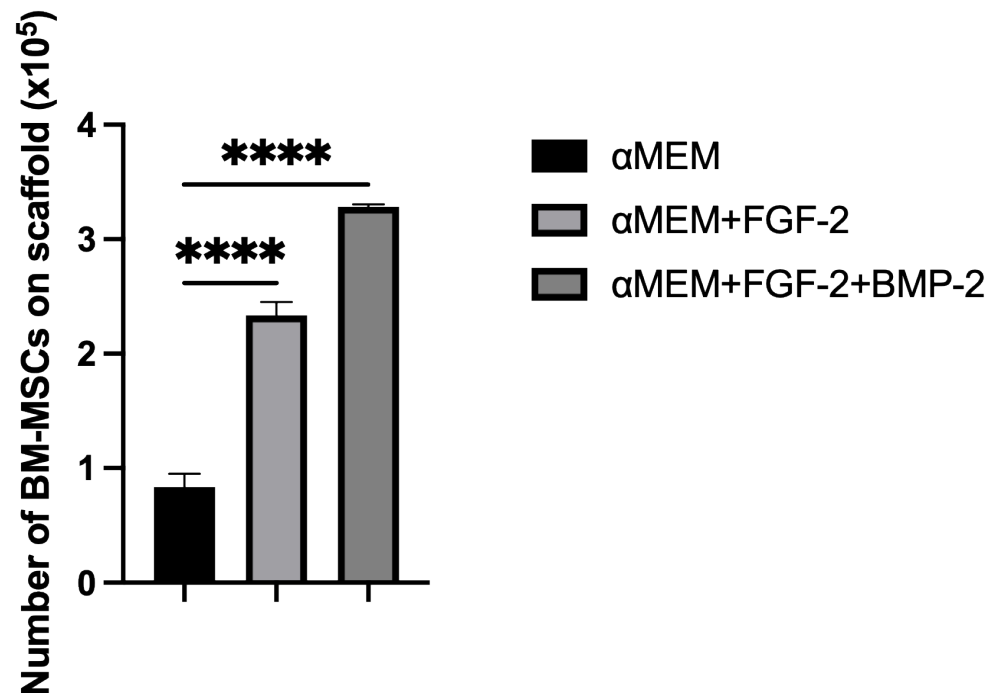


Figure 5. Number of BM-MSCs on an nHAP-coated PCL/HAP/ β -TCP scaffold 3 h post-seeding in α MEM with or without FGF-2 alone or FGF-2 and BMP-2. Cells treated with FGF-2 adhered better to the scaffold than untreated cells. However, the highest number of cells that adhered to the scaffold was observed in the medium supplemented with both FGF-2 and BMP-2. The experiment was conducted in three independent assays, each in triplicate. **** $p < 0.0001$.

3.5. Cell Proliferation and Viability

The impact of FGF-2 and BMP-2 on BM-MSCs proliferation and viability on the nHAP-coated PCL/HAP/ β -TCP scaffold was evaluated with the use of an MTT assay. During 7 days of incubation, the proliferation rate of sheep BM-MSCs growing on scaffold increased over time, independently of the culture medium. These results indicates that

nHAP-coated PCL/HAP/ β -TCP scaffold is not toxic for the cells and stimulates cell proliferation. Nevertheless, FGF-2 was found to have the most beneficial effect on the BM-MSCs proliferation capacity until day 5 of cell culture ($p < 0.001$, Figure 6). The addition of both FGF-2 and BMP-2 to the medium resulted in a greater proliferation rate compared to the untreated cells. However, the rate was not higher than in FGF-2-only treated cells. On day 7, the proliferation ability was almost the same in all the culture media.

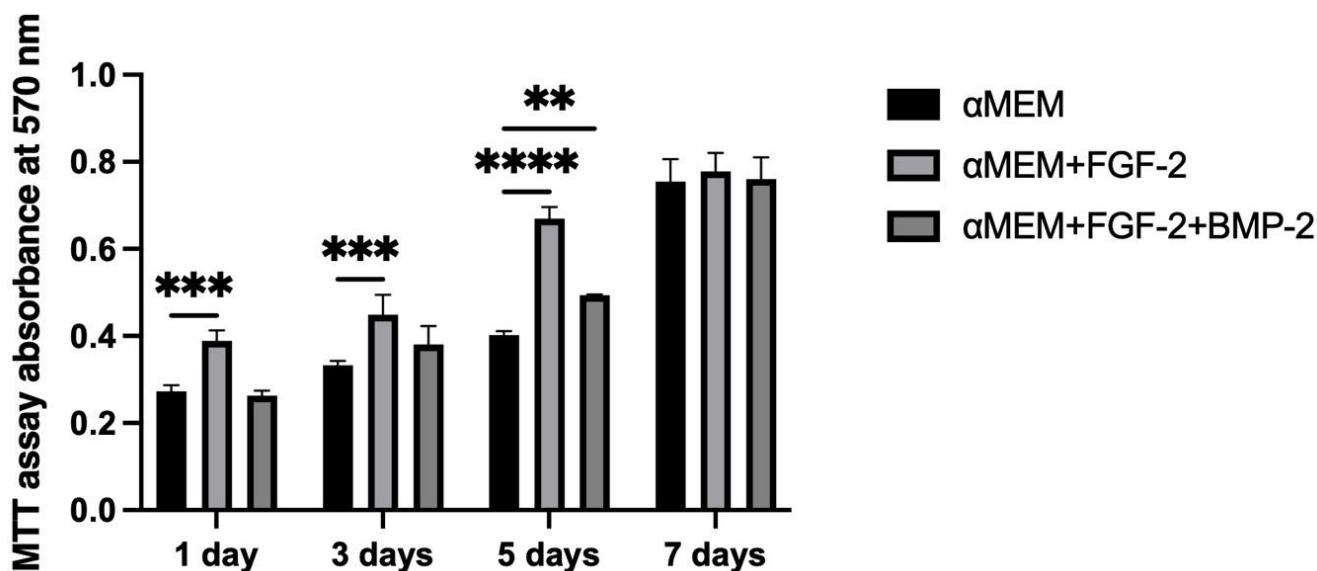


Figure 6. Ability of BM-MSCs to proliferate on the scaffold in α MEM supplemented with only FGF-2 or both FGF-2 and BMP-2, assessed with MTT over 7 days of incubation. The proliferation rate of the cells increased over time. The highest cell proliferation on the scaffold was observed for BM-MSCs treated with FGF-2 only, and the lowest proliferation was observed for untreated cells up to day 5. The MTT assay was performed in three independent experiments in triplicate each. ** $p < 0.005$, *** $p < 0.001$, **** $p < 0.0001$.

3.6. Osteogenic Differentiation with Alizarin Red S Staining

A semi-quantitative analysis of the osteogenic differentiation capacity of BM-MSCs growing on the nHAP-coated PCL/HAP/ β -TCP scaffold was conducted through CPC extraction of Alizarin Red S-stained mineral particles. The absorbance of the extracted solution was measured on days 7, 14, and 21 in an osteogenic medium with or without FGF-2 alone or with FGF-2 and BMP-2. The results showed that the osteogenic differentiation capacity increased over time in all culture conditions. Supplementation with FGF-2 only had a very low impact on osteogenesis after 21 days of cell treatment compared to control (Figure 7, absorbance at 405 nm 1.62 vs. 1.40). However, on day 21, supplementation with both FGF-2 and BMP-2 had the highest impact on BM-MSCs osteogenesis compared to untreated and FGF-2-only treated cells (absorbance at 405 nm 2.56 vs. 1.40 and 1.62, $p < 0.0001$).

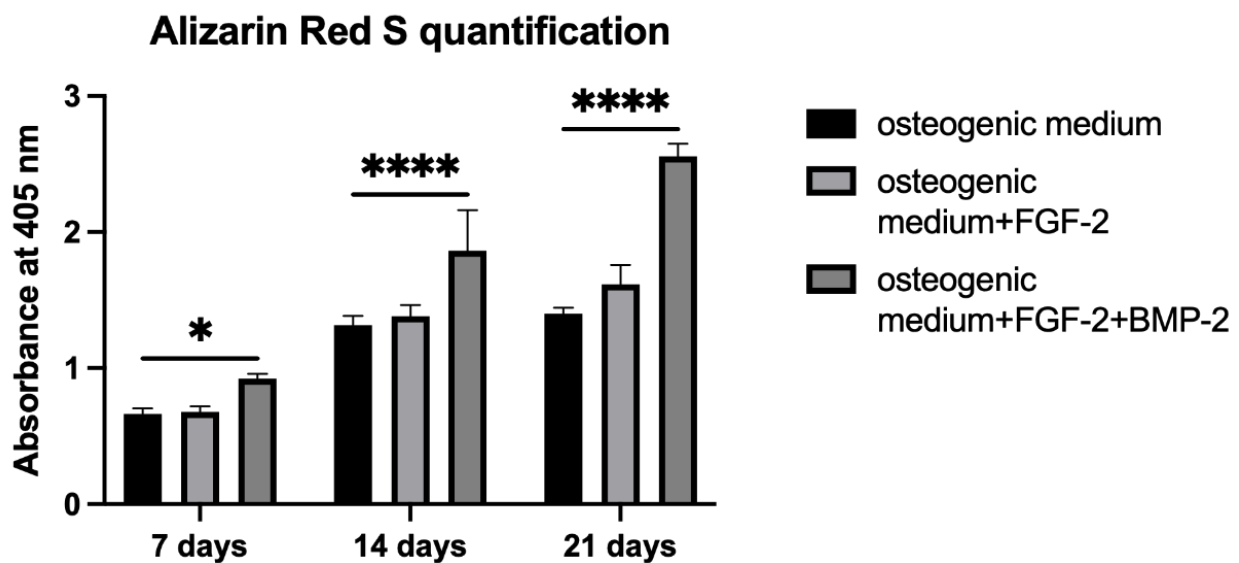


Figure 7. Quantification of Alizarin Red S staining of BM-MSCs growing on a scaffold using the CPC extraction method. Cells cultured in an osteogenic medium supplemented with both FGF-2 and BMP-2 had the greatest osteogenic differentiation potential compared to untreated or FGF-2-only treated cells. Alizarin Red S was quantified in three independent experiments in duplicate each. * $p < 0.05$, **** $p < 0.0001$.

3.7. ALP Activity

An analysis of ALP activity showed that BM-MSCs growing on the scaffold required 21 days for a significant increase in the ALP rate, independently of culture media. Between 7 and 14 days of cell incubation, there were no significant differences in ALP activity across all groups. However, on day 21, ALP activity increased significantly, even for untreated cells, compared to 14 days of incubation (Figure 8, absorbance at 405 nm 0.75 vs. 0.15). Nonetheless, FGF-2 and BMP-2 stimulated osteogenic differentiation through an increase in ALP activity more than untreated cells (on day 21, absorbance 1.01 vs. 0.75, $p < 0.005$).

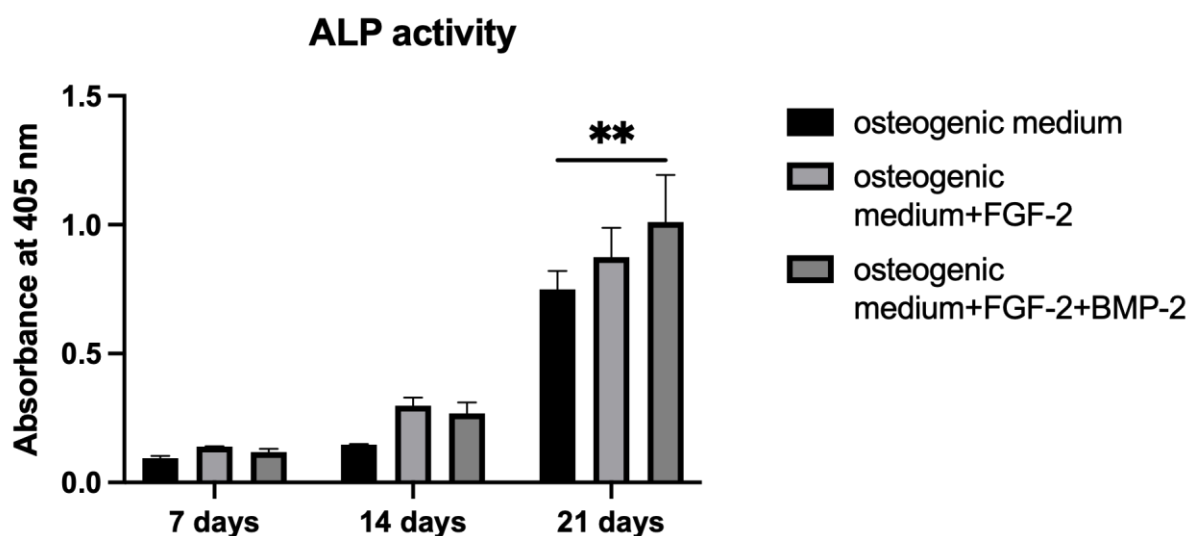


Figure 8. ALP activity of BM-MSCs grown on an nHAP-coated PCL/HAP/ β -TCP scaffold treated or untreated with only FGF-2 or FGF-2 and BMP-2. ALP activity measured at 405 nm significantly increased for all culture conditions on day 21. The highest ALP activity was observed for FGF-2- and BMP-2-treated cells. The ALP assay was repeated in three independent experiments in duplicate each. ** $p < 0.005$.

3.8. Expression of Osteogenic Genes in BM-MSCs Grown on the nHAP-Coated PCL/HAP/ β -TCP Scaffold Depending on FGF-2 and BMP-2 Stimulation

On days 7, 14, and 21, following treatment with FGF-2 alone or FGF-2 and BMP-2, samples of sheep BM-MSCs grown on the nHAP-coated PCL/HAP/ β -TCP scaffold were collected for real-time PCR. The influence of cytokines on BM-MSCs osteogenic differentiation was evaluated based on the relative expression levels of early osteogenesis gene markers: *Runx2*, *osterix* (*Osx*), *BMP-2*, and *collagen type I* (*Col1*) and late osteogenesis gene markers: *osteopontin* (*Opn*) and *osteocalcin* (*Ocn*). Relative expression of *Runx2* increased over time for BM-MSCs grown on the scaffold and treated with FGF-2 alone or FGF-2 and BMP-2. The highest peak was observed for the cells treated with FGF-2 and BMP-2 after 21 days (RQ 2.39 vs. 1.29 in control; $p < 0.0001$) (Figure 9a). For the untreated cells or cells treated with FGF-2 only, there was no significant difference in the relative expression of *Runx2*, and the expression was at a similar level regardless of the time-point of observation. Treatment with FGF-2 and BMP-2 significantly upregulated the mRNA level of *osterix* from day 14 to 21 (RQ 7.82 vs. 15.74) (Figure 9b), whereas between day 7 and 14, there was no significant difference (RQ 7.51 vs. 7.82). The relative expression of *osterix* for untreated or FGF-2-treated cells increased over time and was the highest after 21 days of incubation (RQ 2.31 and 2.28); however, it was much lower compared to FGF-2- and BMP-2-treated cells. Interestingly, the relative expression of *BMP-2* was upregulated over time in all cases; however, the highest peak was observed after 21 days for FGF-2-alone treated cells, and not for FGF-2- and BMP-2-treated BM-MSCs (RQ 4.92 vs. 4.28) (Figure 9c). Interestingly, on day 14, FGF-2- and BMP-2-treated cells showed the highest relative expression of *BMP-2* (RQ 3.03 vs. 1.33 in control; $p < 0.0001$). The relative mRNA expression of *collagen type I* decreased after 14 days of incubation in all culture conditions to slightly increase after 21 days; however, it was still lower than on day 7 for all groups (RQ on day 7, 14, and 21 for control 1.00, 0.48, and 0.83, respectively) (Figure 9d). Untreated BM-MSCs showed a higher expression of *Col1* than FGF-2 alone- or FGF-2- and BMP-2-treated cells across all analyzed time points. The relative expression level of the late osteogenic marker *osteopontin* increased over time in all groups. However, the increase in the control group was negligible, with the value remaining stable at an RQ of about 1.00 (Figure 9e). BM-MSCs grown on the nHAP-coated PCL/HAP/ β -TCP scaffold with FGF-2 and BMP-2 for 21 days showed the highest expression of *Opn* (RQ 1.43 vs. 1.09 in control; $p < 0.0001$). Differences in the second late osteogenic gene expression marker, *osteocalcin*, were more prominent. On day 7, cells treated with FGF-2 and BMP-2 showed the highest relative expression of *Ocn* (RQ 2.13 vs. 1.00 in control; $p < 0.001$) (Figure 9f). On day 14, *Ocn* expression increased for all culture conditions and was similar for FGF-2 alone- or FGF-2- and BMP-2-treated cells (RQ 3.95 and 4.07). However, after 21 days, it was higher in BM-MSCs cultured with FGF-2 than in BM-MSCs treated with both FGF-2 and BMP-2 (RQ 8.13 vs. 6.24).

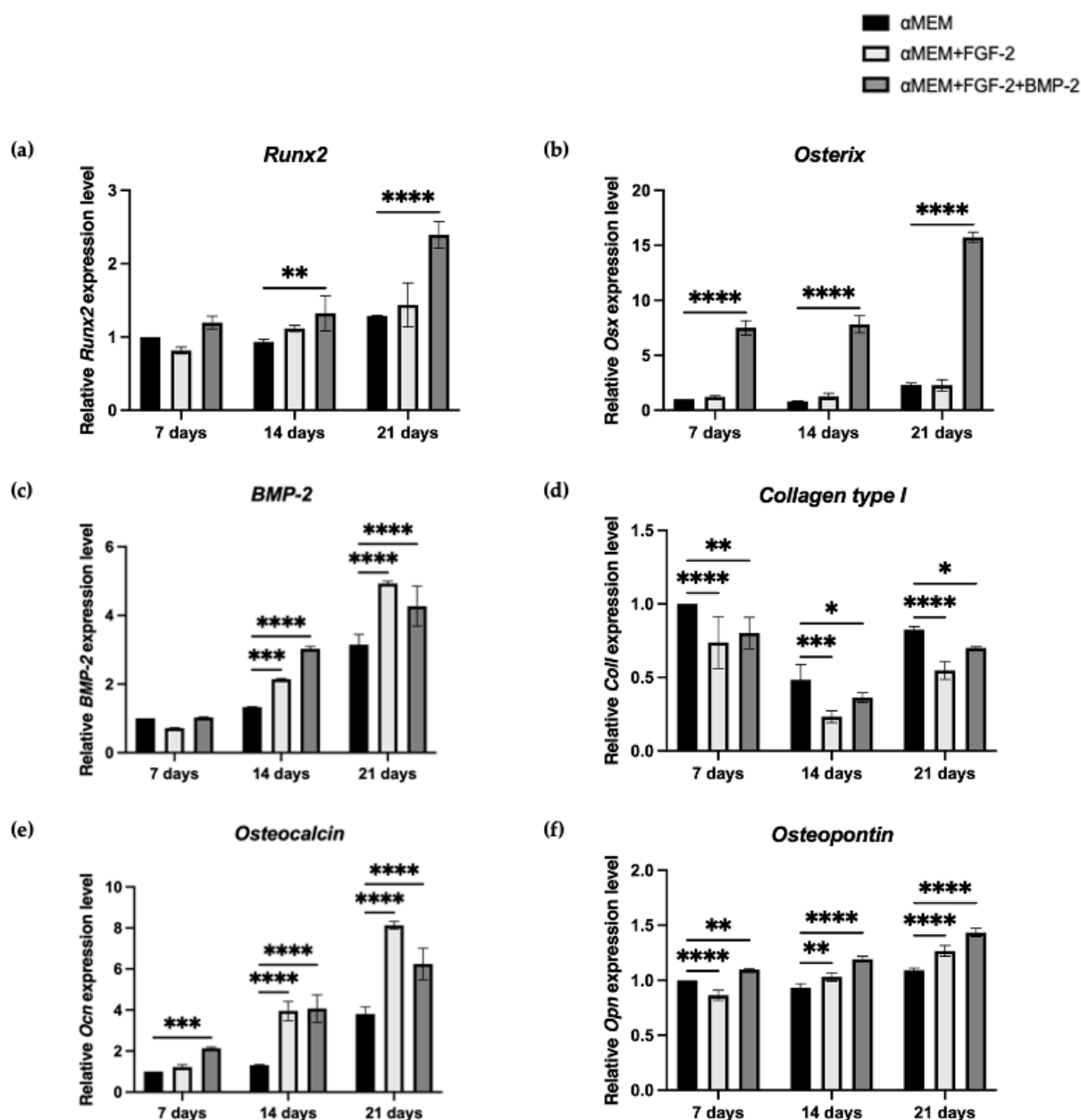


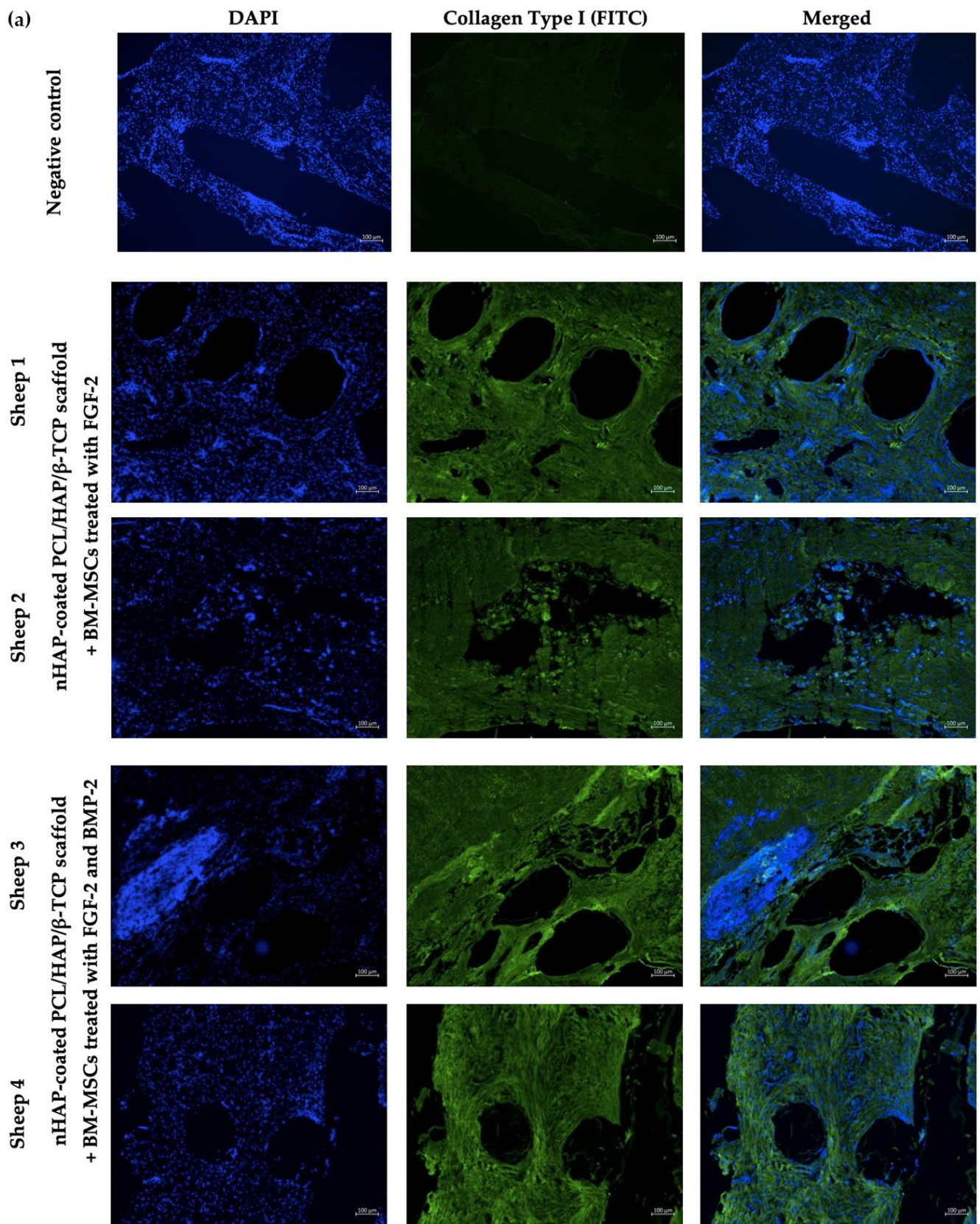
Figure 9. Relative expression of the early osteogenic differentiation gene markers (a) *Runx2*, (b) *osterix* (*Osx*), (c) *BMP-2*, and (d) *collagen type I* (*Coll*) and late osteogenic gene markers (e) *osteocalcin* (*Ocn*) and (f) *osteopontin* (*Opn*), analyzed with real-time PCR in ovine BM-MSCs grown on an nHAP-coated PCL/HAP/ β -TCP scaffold with or without FGF-2 alone or with FGF-2 and BMP-2 for 21 days. Three independent experiments were each performed in duplicate. * $p < 0.05$, ** $p < 0.005$, *** $p < 0.001$, **** $p < 0.0001$.

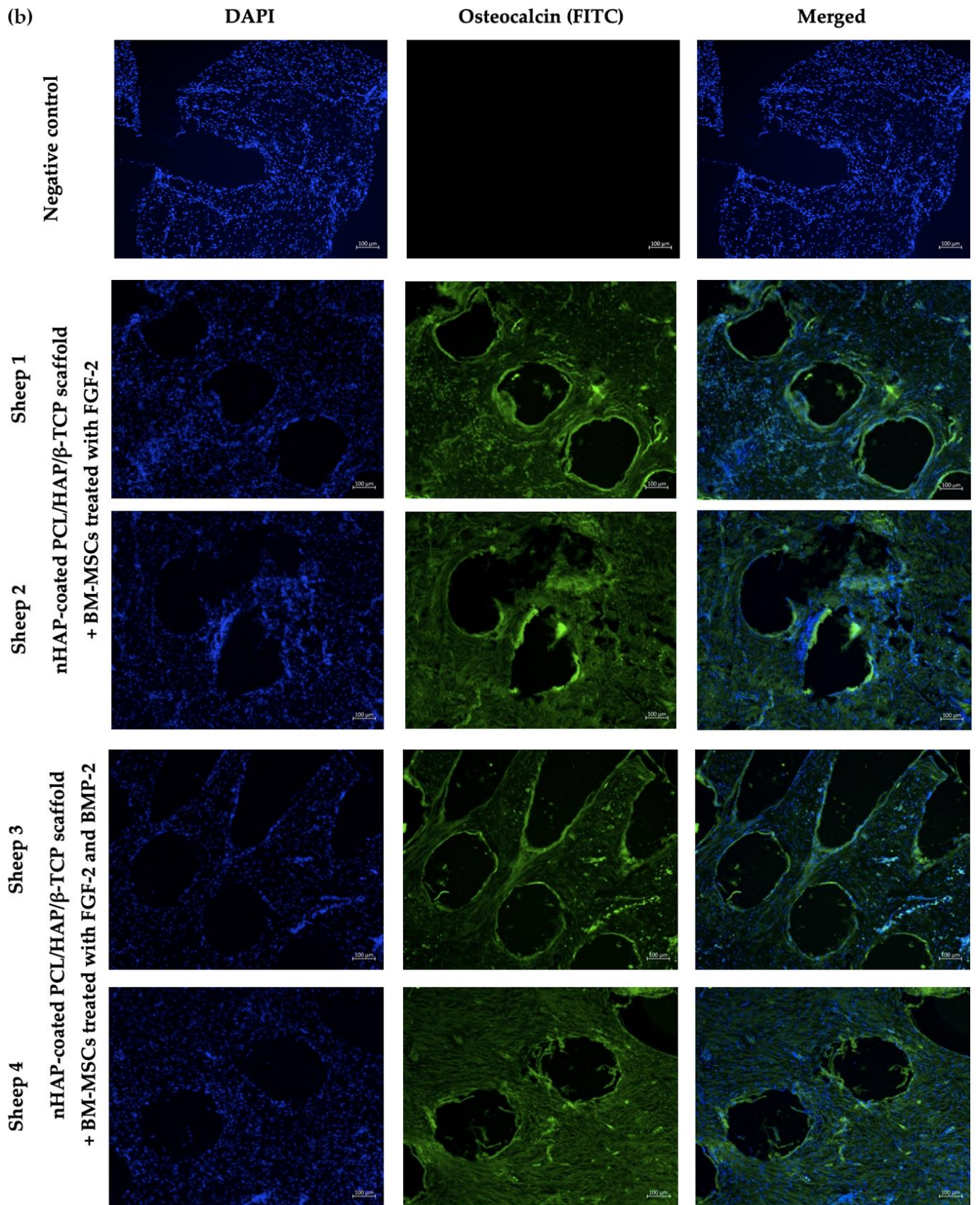
3.9. Clinical Assessment

After the implantation of the nHAP-coated PCL/HAP/ β -TCP scaffolds, the animals were monitored for wound healing, general health, and signs of inflammation. The implanted scaffolds were well tolerated in all animals, with only minor side effects associated with wound healing, such as temporary swelling over two days after surgery. No fever or other undesired signs of inflammation were observed.

3.10. Immunofluorescent Staining of Osteocalcin and Collagen Type I

The *in vivo* osteogenic differentiation potential of the BM-MSCs treated with only FGF-2 or FGF-2 and BMP-2 together with the nHAP-coated PCL/HAP/ β -TCP scaffold grafted into the ovine mandible was evaluated using immunofluorescent staining for the early osteogenic marker collagen type I and for the late osteogenic marker osteocalcin. Sections were obtained from two sheep 6 months after the surgical implantation of the nHAP-coated PCL/HAP/ β -TCP scaffold and FGF-2-treated BM-MSCs, and from two sheep that received the nHAP-coated PCL/HAP/ β -TCP scaffold and BM-MSCs treated with FGF-2 and BMP-2. The presence of bone-specific proteins was verified with FITC green fluorescence. It was found that BM-MSCs treated with FGF-2-treated and treated with FGF-2 and BMP-2, grafted with the nHAP-coated PCL/HAP/ β -TCP scaffold into the mandible site, showed the production of both collagen type I and osteocalcin (Figure 10a,b). The average fluorescence intensity graphs showed slight autofluorescence in the negative control for collagen type I (Figure 10c) and even smaller autofluorescence for osteocalcin (Figure 10d).





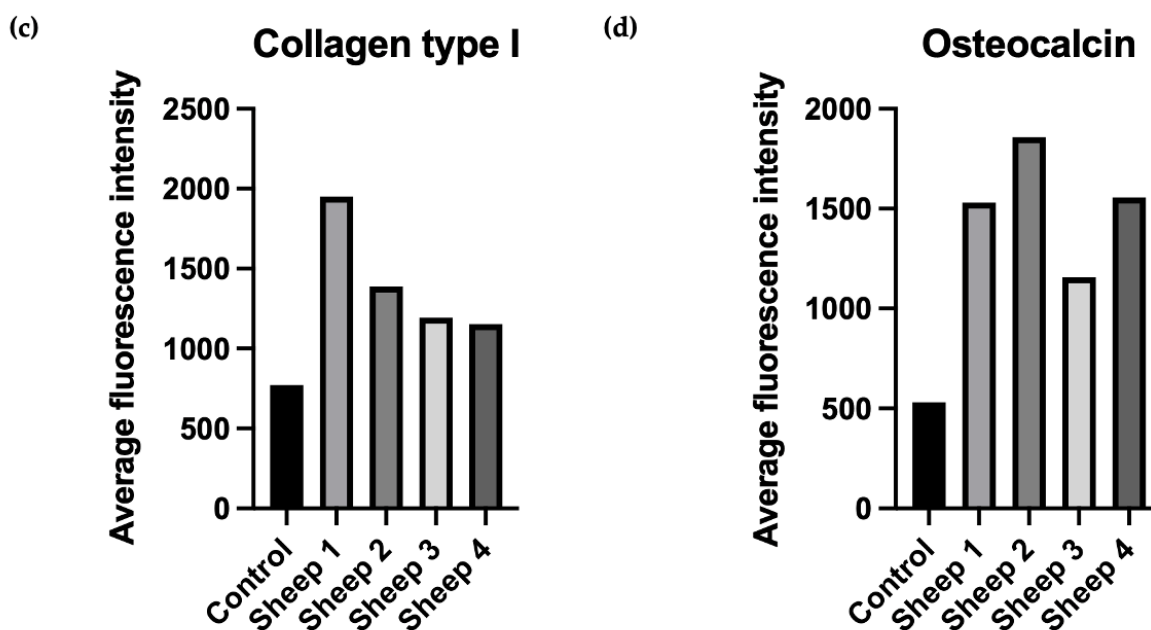


Figure 10. Immunofluorescence analysis of the early osteogenic marker collagen type I (a) and late osteogenic marker osteocalcin (b) for scaffold sections retrieved from sheep 6 months after the implantation of a scaffold and BM-MSCs treated with FGF-2 or FGF-2 and BMP-2. Merged: DAPI staining of the nucleus (blue) and antibody staining (green fluorescence). Intensity of fluorescence of collagen type I (c) and osteocalcin (d) compared to negative controls.

3.11. Cytokine Profile of the Sheep Serum after BM-MSC-Scaffold Grafting

Serum samples were collected from the sheep one week before the BM-MSCs and the nHAP-coated PCL/HAP/ β -TCP scaffold grafting and at three time-points post-surgery: one, two, and four weeks, and were assessed for the presence of 18 cytokines using a semi-quantitative cytokine array (Figure 11). Cytokine expression was assessed relative to baseline one week prior to surgery in order to determine the activity of trophic factors promoting osteogenesis and the immune response in sheep after surgery. Two sheep underwent transplantation with the scaffold and FGF-2-treated BM-MSCs (Figure 11a,b) and another two with the scaffold and FGF-2- and BMP-2-treated BM-MSCs (Figure 11c,d). The secreted frizzled-related protein-3 (sFRP-3), which regulates osteoblast differentiation, showed the highest relative expression level, over 100% of the positive control, in all sheep independently from sampling time. However, a slight reduction in sFRP-3 level was observed in sheep 3 (receiving BM-MSC treated with FGF-2 and BMP-2) four weeks after surgery, but still maintaining a high expression of around 100%. Similarly, decorin, which controls fibrillogenesis, also showed a high relative expression in all sheep. It is worth mentioning that the expression of decorin, which is involved in bone formation, decreased in sheep 1 and 2 from over 100% before the implantation to 60–70% at the time-point of four weeks after surgery. A decrease in decorin expression was also observed in the serum from sheep 3 after the implantation. However, in the serum from sheep 4, decorin level increased from about 60% before surgery to about 80% four weeks after the implantation. The apoptosis-inducing factor (AIF), in addition to controlling programmed cell death, also regulates cell proliferation and differentiation. Its level decreased four weeks after surgery, compared to the baseline before surgery, in sheep 1 and 2, which underwent PCL-HA implantation with FGF-2-treated BM-MSCs. Interestingly, the serum from sheep 3 and 4 treated with the nHAP-coated PCL/HAP/ β -TCP scaffold and BM-MSCs supplemented with both FGF-2 and BMP-2 showed a higher AIF expression after the implantation than before it. An analysis of the level of inflammatory cytokines, such as interleukin 8 (IL-8), interferon gamma (IFN-gamma), interleukin 1 alpha (IL-1 alpha), interleukin 1

beta (IL-1 beta), interleukin 17A (IL-17A), interleukin 21 (IL-21), monokine induced by interferon gamma/CXCL9 (MIG), and the tumor necrosis factor (TNF-alpha) indicated that the serum from sheep 1 and 2 had slightly elevated levels before surgery, whereas four weeks after it, the level of inflammatory cytokines decreased. Conversely, in the serum from sheep 3, which underwent the transplantation of the scaffold and BM-MSCs treated with FGF-2 and BMP-2, the increase in the relative expression of inflammatory cytokines was observed four weeks after surgery, compared to the baseline before surgery. The serum from sheep 4 showed the lowest expression of inflammatory cytokines at the baseline time-point as well as four weeks post-surgery.

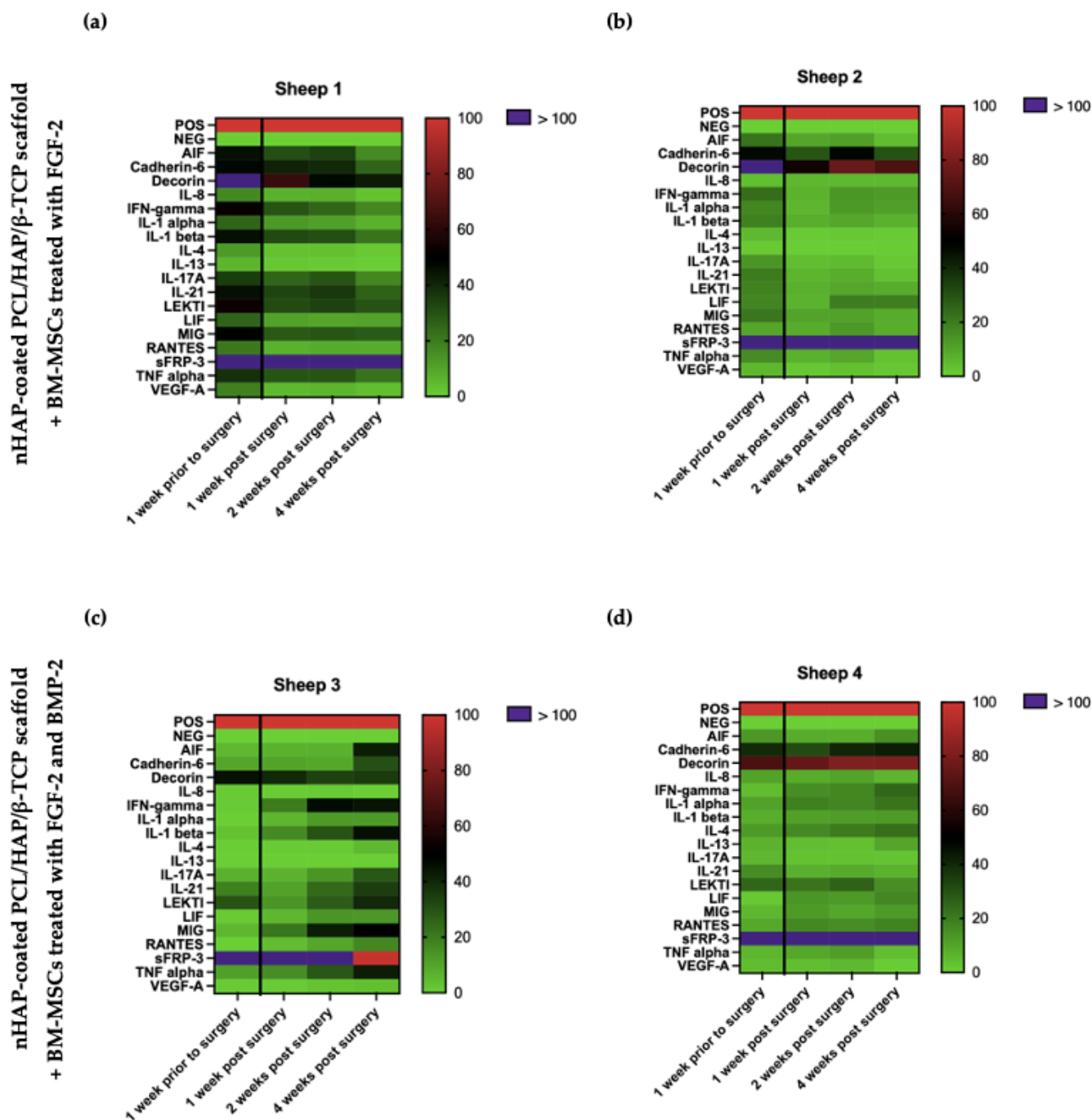


Figure 11. Cytokine profiles of sheep serum 1 week before and 1, 2, and 4 weeks after the transplantation of an nHAP-coated PCL/HAP/ β -TCP scaffold and BM-MSCs treated with FGF-2 (a,b) and FGF-2 combined with BMP-2 (c,d).

4. Discussion

Recently, mesenchymal stem cells have been widely investigated in regenerative medicine for their usefulness in bone defect restoration [35–38]. Although *in vitro* studies have provided many promising results, some problems in *in vivo* studies remain unsolved, such as a limited survival rate of MSCs, maintaining the cells in the injured site, and a low efficacy of differentiation into the specialized cells of the damaged tissue [17]. Consequently, a major challenge for clinical trials involving MSCs is optimizing the cell culture protocol *in vitro* in order to mimic the natural *in vivo* MSC environment [39]. For this purpose, we developed a culture of ovine BM-MSCs on a nHAP-coated PCL/HAP/ β -TCP scaffold and analyzed their osteogenic differentiation ability when treated with FGF-2 alone or using a combination of two cytokines, FGF-2 and BMP-2. The cells were cultured in 3D conditions to mimic a cell environment resembling native tissue and were supplemented with FGF-2 and BMP-2 to confirm our hypothesis that these proteins could improve the osteogenic potential of MSC *in vitro* in 3D culture conditions, as demonstrated in our previous study for a 2D culture [25].

Microscopic observations indicated that the ovine BM-MSCs attached to the scaffold structure well and maintained proliferative activity over 21 days of incubation. Interestingly, FGF-2 and BMP-2 affected the spread of cells on the nHAP-coated PCL/HAP/ β -TCP scaffold. The presence of FGF-2 in the culture medium efficiently supported the cells to grow between the scaffold bars compared to the control medium without supplements. However, the most beneficial effect on cell aggregation was observed when both FGF-2 and BMP-2 were applied, indicating that BMP-2 in combination with FGF-2 enhanced cell distribution and proliferation on the scaffold. Because the arrangement of the cells between the bars of the scaffold cannot be observed under a light microscope, we additionally observed the MSC culture on the scaffold under a fluorescence microscope after DAPI staining. This approach allowed us to obtain a full overview of cell viability on the surface of the scaffold as well as between its bars. Based on DAPI nucleus staining on day 21 of the BM-MSC culture on the nHAP-coated PCL/HAP/ β -TCP scaffold in different culture media, we demonstrated that the ability of the cells to adhere to the scaffold improved when treated with both FGF-2 and BMP-2, compared to the untreated cells. This effect was also confirmed for the standard α MEM and the osteogenic differentiation medium.

To support our microscopic observations of the beneficial effect of FGF-2 and BMP-2 on MSC adhesion and proliferation on the scaffold, we additionally investigated differences in cell attachment to the scaffold according to a culture medium with or without biological factors using the quantitative Picogreen method, as well as cell proliferation and viability using an MTT assay. The number of BM-MSCs on the scaffold was assessed three hours post-seeding. Due to the short incubation time, the adherence capacity of BM-MSCs to the scaffold was analyzed immediately after seeding, which in turn reflected the efficiency of cell deposition on the scaffold before surgery, because the BM-MSCs-scaffold construct was prepared and transplanted into the sheep on the same day. FGF-2-treated ovine BM-MSCs attached to the nHAP-coated PCL/HAP/ β -TCP scaffold over twice as effectively as untreated MSCs. Nonetheless, FGF-2 together with BMP-2 increased cell attachment more than three times. Although the microscopic assessment and the Picogreen test showed the best results for FGF-2- and BMP-2-treated cells, the proliferation rate assessed with the MTT was highest for FGF-2 alone-treated BM-MSCs. However, because microscopic observations of cells are inaccurate due to the imperfection of the human eye, it is difficult to draw conclusions about the number of cells based solely on such observations. On the other hand, the Picogreen assay only tests the number of cells 3 h after seeding, providing an insight into cell attachment rather than proliferation. The MTT assay was conducted at four time points over 7 days. However, on day 7 of observation, the proliferation rate for untreated cells and both FGF-2- and BMP-2-treated cells increased considerably, and there were no significant proliferation differences in all groups. Our previous study indicated that ovine BM-MSCs in standard 2D culture conditions proliferated in the α MEM medium; however, the proliferation was slower compared to a

conditioned medium with the growth factors FGF2 and BMP-2 (observation was performed for up to 4 days) [25]. Similar effects were observed in this study up to day 5. The rapid increase in cell proliferation on day 7 in all culture conditions, with a high likelihood, indicated the start of osteogenic differentiation processes in the BM-MSCs preconditioned with FGF2 and BMP-2, and consequently, a slow-down in the proliferation of the preconditioned cells but not the untreated cells. These results suggest that the nHAP-coated PCL/HAP/ β -TCP scaffold is not toxic for cells in vitro and supports cell proliferation and differentiation. Our previous observations and the present study showed that FGF-2 alone increased cell proliferation of BM-MSCs in both 2D and 3D culture on an nHAP-coated PCL/HAP/ β -TCP scaffold better than FGF-2 together with BMP-2 due to the fact that the cells may have already entered the osteogenic differentiation pathway through the synergistic action of FGF-2 and BMP-2 [25]. Our results are consistent with those obtained in a study by Zhang et al. on the osteogenic differentiation enhancement and slower proliferation of BM-MSCs grown on HA scaffolds carrying microspheres with BMP-2 [40]. Moreover, Xu et al. also reported that BMP-2-coated Poly-L-Lactic Acid (PLLA) fibers improved the osteogenic differentiation of MSCs more than their proliferation [41].

The findings that FGF-2 and BMP-2 increase MSC capacity to adhere and proliferate on an nHAP-coated PCL/HAP/ β -TCP scaffold have not yet been reported elsewhere. However, Hu et al. demonstrated that FGF-2 and BMP-2 support BM-MSC growth and adhesion on another type of scaffold, i.e., a nanohydroxyapatite and collagen nHAP/COL scaffold [42]. Moreover, the loading of FGF-2 and BMP-2 in composite nanofiber scaffolds has been found to promote the adhesion and proliferation of pre-MC3T3-E1 osteoblasts [43].

In addition to the effect of FGF-2 and BMP-2 on ovine BM-MSCs morphology, adhesion, and proliferation on an nHAP-coated PCL/HAP/ β -TCP scaffold, we also investigated their impact on the osteogenic differentiation potential of BM-MSCs in vitro. We focused on matrix mineralization tested with Alizarin Red S staining, ALP activity, and relative expression levels of early osteogenic marker genes: *BMP-2*, *Runx2*, *osterix*, and *collagen type I* and late marker genes: *osteocalcin* and *osteopontin*.

Alizarin Red S staining shows the efficiency of the mineralization stage in the osteogenic differentiation of MSCs and has been considered as a marker for calcium compounds common to bone-like structures [44]. Our study showed that the addition of only FGF-2 to the osteogenic differentiation medium did not significantly impact the matrix mineralization of BM-MSCs grown on the nHAP-coated PCL/HAP/ β -TCP scaffold. However, cells treated with both FGF-2 and BMP-2 showed a higher intensity of Alizarin Red S staining. The increase in calcium nodule deposition was gradual for all medium conditions, whereas ALP activity significantly increased after 21 days of BM-MSCs incubation on the scaffold. Although ALP is a marker of the early osteogenesis of MSCs, its greatest activity was reported at the last time point of observation after 21 days. This result is consistent with that obtained by Davis et al., who also detected an ALP activity increase over 28 days in BMP-2-treated MSCs incubated on apatite-coated scaffolds [45]. As with Alizarin Red S staining, the strongest impact on ALP activity was reported for FGF-2- and BMP-2-treated cells, suggesting the importance of BMP-2 in osteogenic process control. This finding is consistent with a study by Sun et al., which demonstrated that BM-MSCs grown on PCL/decellularized small intestine submucosa (SIS) scaffold showed a significantly improved osteogenic differentiation capacity when the scaffold contained BMP-2 [46]. Furthermore, Ren et al. demonstrated that a combination of bFGF and BMP-2 synergistically enhanced ALP activity and the calcium mineralization capacity of MC3T3-E1 cells on PLGA/HA nanofiber scaffolds [43].

To confirm the synergistic effect of FGF-2 and BMP-2 on the osteogenic differentiation potential of ovine BM-MSCs grown on an nHAP-coated PCL/HAP/ β -TCP scaffold, we also investigated the expression of osteogenesis-related mRNA. As the main osteogenic differentiation characteristics of MSCs are often associated with the upregulation of

specific genes in each stage, we focused on early markers such as *Runx2*, *BMP-2*, *osterix*, and *collagen type I* and late osteogenic marker genes *osteocalcin* and *osteopontin*. Sheep BM-MSCs grown on an nHAP-coated PCL/HAP/ β -TCP scaffold cultured with α MEM supplemented with only FGF-2 or FGF-2 and BMP-2 were compared with those incubated with α MEM medium, which served as a control. At the early time points of 7 and 14 days, no remarkable differences in the relative expression of *Runx2* were detected between the groups. However, after 21 days of incubation, BM-MSCs grown on the nHAP-coated PCL/HAP/ β -TCP scaffold treated with FGF-2 and BMP-2 showed a significantly higher expression of *Runx2* than the untreated cells or cells treated with FGF-2 only. Although *Runx2* is an early marker of osteogenesis, in our study, its upregulation was observed at the last time point of observation. This phenomenon may be explained by the fact that osteoblasts are able to enhance the osteogenic differentiation potential of undifferentiated cells in their surroundings, leading to a higher relative expression of *Runx2* in the late phase [47]. A similar effect was reported by Westhauser et al. for MSCs grown on a β -TCP-based scaffold [48]. The expression of another early marker, *osterix*, increased significantly after 7 and 14 days of incubation in FGF-2- and BMP-2-treated ovine BM-MSCs compared to untreated or only FGF-2-treated cells. However, the highest peak was reported on day 21. Our data suggest that *osterix* expression is BMP-2-dependent at an early as well as late stage of osteogenesis, during which still-undifferentiated BM-MSCs are stimulated towards osteogenic differentiation through the autocrine and paracrine mechanisms regulated by already-differentiated cells. Moreover, our study demonstrates that BMP-2 activates *Runx2* expression, which in turn upregulates *osterix* gene expression. The role of BMP-2 in MSC osteogenic differentiation by means of controlling the expression of *Runx2* and *osterix* has already been extensively investigated by other authors [49–51]. Interestingly, the expression of *BMP-2* increased over time in all culture conditions. On day 14, its highest relative expression level was reported in MSCs treated with both FGF-2 and BMP-2. However, after 21 days, the highest peak was reported in FGF-2-treated cells. This suggests that BMP-2 autoregulates its own expression. Remarkably, *collagen type I* expression decreased after 14 days of MSC incubation regardless of cytokine stimulation to later slightly increased at day 21; however, its level was still lower than at day 7. Although *collagen I* is considered as a significant factor that supports bone tissue, it was downregulated during the osteogenic differentiation of ovine BM-MSCs grown on the nHAP-coated PCL/HAP/ β -TCP scaffold. Nantavisai et al. also reported that *Coll* expression decreased over the course of osteogenic induction in MSC from canine bone marrow and dental pulp [52]. The *Osteocalcin* expression level increased significantly on day 21, as expected; however, its highest peak was reported for FGF-2-treated BM-MSCs, and a lower expression level was observed for both FGF-2- and BMP-2-treated cells. The expression level of the second late osteogenic marker, *osteopontin*, increased slightly over time and was the highest in FGF-2- and BMP-2-treated cells after 21 days of incubation. These results show that FGF-2 plays a crucial role in the osteogenic differentiation of MSCs in 3D culture.

In addition to the impact of FGF-2 and BMP-2 stimulation on the osteogenic potential of ovine BM-MSCs grown on an nHAP-coated PCL/HAP/ β -TCP scaffold in vitro, we assessed scaffold biocompatibility and potential for bone regeneration in vivo in a large animal sheep model. At this stage of research, surgical procedure was performed only in four sheep to assess scaffold biocompatibility and to obtain preliminary data on the osteogenic potential of the BM-MSCs-scaffold construct and post-surgical inflammatory response. Immunofluorescence staining of the tissue sections retrieved 6 months post-grafting for osteoblast-specific proteins collagen type I, as an early marker of osteogenic differentiation, and osteocalcin, as a late marker, showed both proteins were present in the site of scaffold-BM-MSCs implantation in all examined sections. Moreover, there were no significant differences in the immunofluorescence staining intensity of collagen type I and osteocalcin between the sections supplemented with BM-MSCs treated with FGF-2-alone or FGF-2 and BMP-2.

Finally, to assess biocompatibility, we monitored the activity of trophic factors involved in osteogenesis and immune response associated with the healing process of the sheep mandible area after the implantation of the scaffold-BM-MSc construct. The cytokine profile in the serum of the sheep that underwent the surgical procedure analyzed by a semi-quantitative cytokine array measuring 18 cytokines did not show any significant differences between the level before grafting (as the baseline) and over four weeks after surgery. Interestingly, sFRP-3 and decorin levels were significantly high in all analyzed samples regardless of the time-point of collection. sFRP-3 promotes the osteogenic differentiation of MSCs by antagonizing non-canonical Wnt signaling [53], whereas decorin is involved in all phases of bone formation, including cell proliferation, matrix mineralization, remodeling, and mineral deposition [54,55]. The results showed that the osteogenic potential was maintained after the implantation of the nHAP-coated PCL/HAP/ β -TCP scaffold-BM-MSc, as confirmed by the activity of the osteogenic factors in the sheep serum. In the serum samples from sheep 1 and 2 (which underwent nHAP-coated PCL/HAP/ β -TCP scaffold and FGF-2-treated BM-MSc transplantation), inflammatory cytokines, including IL-8, IFN- γ , IL-1 α , IL-1 β , IL-17A, IL-21, MIG, and TNF- α , were found to be at the same or slightly decreased level compared to the pre-operative level. Only the serum from sheep 3 showed an increased level of pro-inflammatory cytokines four weeks after the scaffold-BM-MSc implantation, compared to the baseline. However, there were no clinical signs of inflammation. MSCs are known to not only differentiate into the desired cells but also secrete a variety of bioactive factors with immunomodulatory properties [56]. In this sheep model, MSCs show paracrine activity by affecting immunocompetent cells and modulating the local environment, alleviating the inflammatory response and promoting wound healing.

This preliminary *in vivo* study showed that BM-MSCs preconditioned with FGF-2 and BMP-2 and implanted on an nHAP-coated PCL/HAP/ β -TCP scaffold are biocompatible with sheep tissues and promote bone regeneration. These pilot *in vivo* observations constitute a foundation for further research and will aid the reconstruction of large bone defects in the mandible region of the sheep model. The *in vivo* research will be continued with new surgical procedures and a control group of sheep that will undergo scaffold implantation with untreated BM-MSCs to assess the regeneration potential of a scaffold supported with BM-MSCs preconditioned with FGF-2 and BMP-2.

5. Conclusions

In summary, our results have demonstrated that an nHAP-coated PCL/HAP/ β -TCP scaffold provides a good microenvironment for ovine BM-MSc adhesion and proliferation. Stimulation of the cells with FGF-2 and BMP-2 has a beneficial effect on cell attachment and spread on the scaffold. Our study has shown that simultaneous action of both FGF-2 and BMP-2 increases the osteogenic potential of ovine BM-MSCs grown on the scaffold better than FGF-2 alone. FGF-2 plays a crucial role in MSCs proliferation, whereas BMP-2 influences their osteogenic potential. A tissue engineering construct in the form of an nHAP-coated PCL/HAP/ β -TCP scaffold and ovine BM-MSCs preconditioned with FGF-2 and BMP-2 is biocompatible with the sheep tissue environment. We confirmed the biocompatibility of the implanted scaffold-BM-MSCs through the expression of early (collagen type I) and late (osteocalcin) osteogenic proteins and a lack of an elevated level of proinflammatory cytokines. Overall, these data show a promising strategy for clinical application in the repair of large bone defects.

Author Contributions: Conceptualization, A.K. (Aleksandra Klimczak) and S.S.; methodology, S.S., A.K. (Agnieszka Krawczenko), U.S., \dot{Z} .G., A.A.; formal analysis, A.K. (Aleksandra Klimczak), S.S., Z.K., W. \acute{S} ., W. \acute{L} .; investigation, S.S., Z.G., U.S., A.K. (Agnieszka Krawczenko), A.A.; data curation, S.S., \dot{Z} .G., U.S., A.A.; visualization, S.S., U.S., A.A.; funding acquisition, A.K. (Aleksandra Klimczak), W. \acute{S} ., Z.K.; supervision, A.K. (Aleksandra Klimczak), Z.K., W. \acute{S} ., W. \acute{L} .; writing—original draft

preparation, S.S.; writing—review and editing, A.K. (Aleksandra Klimczak). All authors have read and agreed to the published version of the manuscript.

Funding: This study was funded by The National Center For Research and Development, Strategmed3/306888/3/NCBR/2017.

Institutional Review Board Statement: The animal study protocol was approved by the Animal Ethics Committee at the Institute of Immunology and Experimental Therapy PAS (No. 63/2017).

Informed Consent Statement: Not applicable.

Data Availability Statement: All data generated or analyzed during this study are included in this article.

Conflicts of Interest: The authors declare no conflict of interest. The funders had no role in the design of the study; in the collection, analyses, or interpretation of data; in the writing of the manuscript; or in the decision to publish the results.

References

- Henkel, J.; Woodruff, M.A.; Epari, D.R.; Steck, R.; Glatt, V.; Dickinson, I.C.; Choong, P.F.M.; Schuetz, M.A.; Hutmacher, D.W. Bone Regeneration Based on Tissue Engineering Conceptions—A 21st Century Perspective. *Bone Res.* **2013**, *1*, 216–248. <https://doi.org/10.4248/BR201303002>.
- Marsell, R.; Einhorn, T.A. The biology of fracture healing. *Injury* **2011**, *42*, 551–555. <https://doi.org/10.1016/j.injury.2011.03.031>.
- Figliomeni, A.; Signorini, V.; Mazzantini, M. One year in review 2018: Progress in osteoporosis treatment. *Clin. Exp. Rheumatol.* **2018**, *36*, 948–958.
- Iaquinta, M.R.; Mazzoni, E.; Bononi, I.; Rotondo, J.C.; Mazziotta, C.; Montesi, M.; Sprio, S.; Tampieri, A.; Tognon, M.; Martini, F. Adult Stem Cells for Bone Regeneration and Repair. *Front. Cell Dev. Biol.* **2019**, *7*, 268. <https://doi.org/10.3389/fcell.2019.00268>.
- Ferracini, R.; Martínez Herreros, I.; Russo, A.; Casalini, T.; Rossi, F.; Perale, G. Scaffolds as structural tools for bone-targeted drug delivery. *Pharmaceutics* **2018**, *10*, 122.
- Iaquinta, M.R.; Mazzoni, E.; Manfrini, M.; D’Agostino, A.; Trevisiol, L.; Nocini, R.; Trombelli, L.; Barbanti-Brodano, G.; Martini, F.; Tognon, M. Innovative biomaterials for bone regrowth. *Int. J. Mol. Sci.* **2019**, *20*, 618.
- Trohatou, O.; Roubelakis, M.G. Mesenchymal stem/stromal cells in regenerative medicine: Past, present, and future. *Cell. Reprogramming* **2017**, *19*, 217–224.
- Trávníčková, M.; Bačáková, L. Application of adult mesenchymal stem cells in bone and vascular tissue engineering. *Physiol. Res.* **2018**, *67*, 831–850.
- Amarasekara, D.S.; Kim, S.; Rho, J. Regulation of Osteoblast Differentiation by Cytokine Networks. *Int. J. Mol. Sci.* **2021**, *22*, 2851. <https://doi.org/10.3390/ijms22062851>.
- Charoenlarp, P.; Rajendran, A.K.; Iseki, S. Role of fibroblast growth factors in bone regeneration. *Inflamm. Regen.* **2017**, *37*, 10. <https://doi.org/10.1186/s41232-017-0043-8>.
- Perez, J.R.; Kouroupis, D.; Li, D.J.; Best, T.M.; Kaplan, L.; Correa, D. Tissue Engineering and Cell-Based Therapies for Fractures and Bone Defects. *Front. Bioeng. Biotechnol.* **2018**, *6*, 105. <https://doi.org/10.3389/fbioe.2018.00105>.
- Beederman, M.; Lamplot, J.D.; Nan, G.; Wang, J.; Liu, X.; Yin, L.; Li, R.; Shui, W.; Zhang, H.; Kim, S.H.; et al. BMP signaling in mesenchymal stem cell differentiation and bone formation. *J. Biomed. Sci. Eng.* **2013**, *6*, 32–52. <https://doi.org/10.4236/jbise.2013.68A1004>.
- Gillman, C.E.; Jayasuriya, A.C. FDA-approved bone grafts and bone graft substitute devices in bone regeneration. *Mater. Sci. Eng. C* **2021**, *130*, 112466. <https://doi.org/10.1016/j.msec.2021.112466>.
- Kuhn, L.T.; Ou, G.; Charles, L.; Hurley, M.M.; Rodner, C.M.; Gronowicz, G. Fibroblast growth factor-2 and bone morphogenetic protein-2 have a synergistic stimulatory effect on bone formation in cell cultures from elderly mouse and human bone. *J. Gerontol. A Biol. Sci. Med. Sci.* **2013**, *68*, 1170–1180. <https://doi.org/10.1093/gerona/glt018>.
- Charles, L.F.; Woodman, J.L.; Ueno, D.; Gronowicz, G.; Hurley, M.M.; Kuhn, L.T. Effects of low dose FGF-2 and BMP-2 on healing of calvarial defects in old mice. *Exp. Gerontol.* **2015**, *64*, 62–69. <https://doi.org/10.1016/j.exger.2015.02.006>.
- Gronowicz, G.; Jacobs, E.; Peng, T.; Zhu, L.; Hurley, M.; Kuhn, L.T. Calvarial Bone Regeneration Is Enhanced by Sequential Delivery of FGF-2 and BMP-2 from Layer-by-Layer Coatings with a Biomimetic Calcium Phosphate Barrier Layer. *Tissue Eng. Part A* **2017**, *23*, 1490–1501. <https://doi.org/10.1089/ten.TEA.2017.0111>.
- Stamnitz, S.; Klimczak, A. Mesenchymal Stem Cells, Bioactive Factors, and Scaffolds in Bone Repair: From Research Perspectives to Clinical Practice. *Cells* **2021**, *10*, 1925.
- Caddeo, S.; Boffito, M.; Sartori, S. Tissue Engineering Approaches in the Design of Healthy and Pathological In Vitro Tissue Models. *Front. Bioeng. Biotechnol.* **2017**, *5*, 40. <https://doi.org/10.3389/fbioe.2017.00040>.
- Chen, X.; Fan, H.; Deng, X.; Wu, L.; Yi, T.; Gu, L.; Zhou, C.; Fan, Y.; Zhang, X. Scaffold Structural Microenvironmental Cues to Guide Tissue Regeneration in Bone Tissue Applications. *Nanomaterials* **2018**, *8*, 960. <https://doi.org/10.3390/nano8110960>.
- Rather, H.A.; Jhala, D.; Vasita, R. Dual functional approaches for osteogenesis coupled angiogenesis in bone tissue engineering. *Mater. Sci. Eng. C Mater. Biol. Appl.* **2019**, *103*, 109761. <https://doi.org/10.1016/j.msec.2019.109761>.

21. De Santis, R.; Guarino, V.; Ambrosio, L. Composite biomaterials for bone repair. In *Bone Repair Biomaterials*; Woodhead Publishing: Sawston, UK, 2019; pp. 273–299. <https://doi.org/10.1016/B978-0-08-102451-5.00010-X>.
22. Wong, R.M.Y.; Choy, M.H.V.; Li, M.C.M.; Leung, K.S.; Chow, S.K.; Cheung, W.H.; Cheng, J.C.Y. A systematic review of current osteoporotic metaphyseal fracture animal models. *Bone Joint Res.* **2018**, *7*, 6–11. <https://doi.org/10.1302/2046-3758.71.Bjr-2016-0334.R2>.
23. Muschler, G.F.; Nakamoto, C.; Griffith, L.G. Engineering principles of clinical cell-based tissue engineering. *J. Bone Joint Surg. Am.* **2004**, *86*, 1541–1558. <https://doi.org/10.2106/00004623-200407000-00029>.
24. Ferguson, J.C.; Tangl, S.; Barnewitz, D.; Genzel, A.; Heimes, P.; Hruschka, V.; Redl, H.; Nau, T. A large animal model for standardized testing of bone regeneration strategies. *BMC Vet. Res.* **2018**, *14*, 330. <https://doi.org/10.1186/s12917-018-1648-0>.
25. Gromolak, S.; Krawczyński, A.; Antonczyk, A.; Buczak, K.; Kielbowicz, Z.; Klimczak, A. Biological Characteristics and Osteogenic Differentiation of Ovine Bone Marrow Derived Mesenchymal Stem Cells Stimulated with FGF-2 and BMP-2. *Int. J. Mol. Sci.* **2020**, *21*, 9726. <https://doi.org/10.3390/ijms21249726>.
26. Górecka, Ż.; Teichmann, J.; Nitschke, M.; Chlanda, A.; Choinska, E.; Werner, C.; Swieszkowski, W. Biodegradable fiducial markers for X-ray imaging—Soft tissue integration and biocompatibility. *J. Mater. Chem. B* **2016**, *4*, 5700–5712 <https://doi.org/10.1039/C6TB01001F>.
27. Górecka, Ż.; Idaszek, J.; Kołbuk, D.; Choinska, E.; Chlanda, A.; Świąszkowski, W. The effect of diameter of fibre on formation of hydrogen bonds and mechanical properties of 3D-printed PCL. *Mater. Sci. Eng. C Mater. Biol. Appl.* **2020**, *114*, 111072. <https://doi.org/10.1016/j.msec.2020.111072>.
28. Walejewska, E.; Idaszek, J.; Heljak, M.; Chlanda, A.; Choinska, E.; Hasirci, V.; Swieszkowski, W. The effect of introduction of filament shift on degradation behaviour of PLGA- and PLCL-based scaffolds fabricated via additive manufacturing. *Polym. Degrad. Stab.* **2020**, *171*, 109030. <https://doi.org/10.1016/j.polymdegradstab.2019.109030>.
29. Rogowska-Tylman, J.; Locs, J.; Salma, I.; Woźniak, B.; Pilmane, M.; Zalite, V.; Wojnarowicz, J.; Kędzierska-Sar, A.; Chudoba, T.; Szlęzak, K.; et al. In vivo and in vitro study of a novel nanohydroxyapatite sonocoated scaffolds for enhanced bone regeneration. *Mater. Sci. Eng. C* **2019**, *99*, 669–684. <https://doi.org/10.1016/j.msec.2019.01.084>.
30. Kuśnieruk, S.; Wojnarowicz, J.; Chodara, A.; Chudoba, T.; Gierlotka, S.; Łojkowski, W. Influence of hydrothermal synthesis parameters on the properties of hydroxyapatite nanoparticles. *Beilstein J. Nanotechnol.* **2016**, *7*, 1586–1601. <https://doi.org/10.3762/bjnano.7.153>.
31. Szałaj, U.; Świdowska-Środa, A.; Chodara, A.; Gierlotka, S.; Łojkowski, W. Nanoparticle Size Effect on Water Vapour Adsorption by Hydroxyapatite. *Nanomaterials* **2019**, *9*, 1005. <https://doi.org/10.3390/nano9071005>.
32. Majcher, A.; Wiejak, J.; Przybylski, J.; Chudoba, T.; Wojnarowicz, J. A Novel Reactor for Microwave Hydrothermal Scale-up Nanopowder Synthesis. *Int. J. Chem. React. Eng.* **2013**, *11*, 361–368. <https://doi.org/10.1515/ijcre-2012-0009>.
33. Higuchi, J.; Fortunato, G.; Woźniak, B.; Chodara, A.; Domaschke, S.; Męczyńska-Wielgosz, S.; Kruszewski, M.; Dommann, A.; Łojkowski, W. Polymer Membranes Sonocoated and Electrospayed with Nano-Hydroxyapatite for Periodontal Tissues Regeneration. *Nanomaterials* **2019**, *9*, 1625. <https://doi.org/10.3390/nano9111625>.
34. Woźniak, B.; Szałaj, U.; Chodara, A.; Mizeracki, J.; Łojkowski, M.; Myszka, D.; Łojkowski, W. Mechanism for sonocoating a polymer surface with nano-hydroxyapatite. *Mater. Lett.* **2019**, *249*, 155–159. <https://doi.org/10.1016/j.matlet.2019.04.078>.
35. Pittenger, M.F.; Discher, D.E.; Péault, B.M.; Phinney, D.G.; Hare, J.M.; Caplan, A.I. Mesenchymal stem cell perspective: Cell biology to clinical progress. *npj Regen. Med.* **2019**, *4*, 22. <https://doi.org/10.1038/s41536-019-0083-6>.
36. Wu, X.; Jiang, J.; Gu, Z.; Zhang, J.; Chen, Y.; Liu, X. Mesenchymal stromal cell therapies: Immunomodulatory properties and clinical progress. *Stem Cell Res. Ther.* **2020**, *11*, 345. <https://doi.org/10.1186/s13287-020-01855-9>.
37. Musiał-Wysocka, A.; Kot, M.; Majka, M. The Pros and Cons of Mesenchymal Stem Cell-Based Therapies. *Cell Transpl.* **2019**, *28*, 801–812. <https://doi.org/10.1177/0963689719837897>.
38. Rajabzadeh, N.; Fathi, E.; Farahzadi, R. Stem cell-based regenerative medicine. *Stem. Cell Investig.* **2019**, *6*, 19–19. <https://doi.org/10.21037/sci.2019.06.04>.
39. Noronha, N.d.C.; Mizukami, A.; Caliári-Oliveira, C.; Cominal, J.G.; Rocha, J.L.M.; Covas, D.T.; Swiech, K.; Malmegrim, K.C.R. Priming approaches to improve the efficacy of mesenchymal stromal cell-based therapies. *Stem Cell Res. Ther.* **2019**, *10*, 131. <https://doi.org/10.1186/s13287-019-1224-y>.
40. Zhang, B.J.; Han, Z.W.; Duan, K.; Mu, Y.D.; Weng, J. Multilayered pore-closed PLGA microsphere delivering OGP and BMP-2 in sequential release patterns for the facilitation of BMSC s osteogenic differentiation. *J. Biomed. Mater. Res. Part A* **2018**, *106*, 95–105.
41. Xu, T.; Sheng, L.; He, L.; Weng, J.; Duan, K. Enhanced osteogenesis of hydroxyapatite scaffolds by coating with BMP-2-loaded short polylactide nanofiber: A new drug loading method for porous scaffolds. *Regen. Biomater.* **2019**, *7*, 91–98. <https://doi.org/10.1093/rb/rbz040>.
42. Hu, Y.; Zheng, L.; Zhang, J.; Lin, L.; Shen, Y.; Zhang, X.; Wu, B. Dual delivery of bone morphogenetic protein-2 and basic fibroblast growth factor from nanohydroxyapatite/collagen for bone tissue engineering. *Appl. Biol. Chem.* **2019**, *62*, 49. <https://doi.org/10.1186/s13765-019-0453-1>.
43. Ren, X.; Liu, Q.; Zheng, S.; Zhu, J.; Qi, Z.; Fu, C.; Yang, X.; Zhao, Y. Synergistic delivery of bFGF and BMP-2 from poly(l-lactico-glycolic acid)/graphene oxide/hydroxyapatite nanofibre scaffolds for bone tissue engineering applications. *RSC Adv.* **2018**, *8*, 31911–31923. <https://doi.org/10.1039/C8RA05250F>.

44. Paul, H.; Reginato, A.J.; Schumacher, H.R. Alizarin red S staining as a screening test to detect calcium compounds in synovial fluid. *Arthritis. Rheum.* **1983**, *26*, 191–200. <https://doi.org/10.1002/art.1780260211>.
45. Davis, H.E.; Case, E.M.; Miller, S.L.; Genetos, D.C.; Leach, J.K. Osteogenic response to BMP-2 of hMSCs grown on apatite-coated scaffolds. *Biotechnol. Bioeng.* **2011**, *108*, 2727–2735. <https://doi.org/10.1002/bit.23227>.
46. Sun, T.; Meng, C.; Ding, Q.; Yu, K.; Zhang, X.; Zhang, W.; Tian, W.; Zhang, Q.; Guo, X.; Wu, B.; et al. In situ bone regeneration with sequential delivery of aptamer and BMP2 from an ECM-based scaffold fabricated by cryogenic free-form extrusion. *Bioact. Mater.* **2021**, *6*, 4163–4175. <https://doi.org/10.1016/j.bioactmat.2021.04.013>.
47. Deschaseaux, F.; Sensébé, L.; Heymann, D. Mechanisms of bone repair and regeneration. *Trends Mol. Med.* **2009**, *15*, 417–429. <https://doi.org/10.1016/j.molmed.2009.07.002>.
48. Westhauser, F.; Karadjian, M.; Essers, C.; Senger, A.-S.; Hagmann, S.; Schmidmaier, G.; Moghaddam, A. Osteogenic differentiation of mesenchymal stem cells is enhanced in a 45S5-supplemented β -TCP composite scaffold: An in-vitro comparison of Vitoss and Vitoss BA. *PLoS ONE* **2019**, *14*, e0212799. <https://doi.org/10.1371/journal.pone.0212799>.
49. Xiao, Z.S.; Hjelmeland, A.B.; Quarles, L.D. Selective deficiency of the “bone-related” Runx2-II unexpectedly preserves osteoblast-mediated skeletogenesis. *J. Biol. Chem.* **2004**, *279*, 20307–20313. <https://doi.org/10.1074/jbc.M401109200>.
50. Pérez-Campo, F.M.; Santurtún, A.; García-Ibarbia, C.; Pascual, M.A.; Valero, C.; Garcés, C.; Sañudo, C.; Zarrabeitia, M.T.; Riancho, J.A. Osterix and RUNX2 are Transcriptional Regulators of Sclerostin in Human Bone. *Calcif. Tissue Int.* **2016**, *99*, 302–309. <https://doi.org/10.1007/s00223-016-0144-4>.
51. Takarada, T.; Nakazato, R.; Tsuchikane, A.; Fujikawa, K.; Iezaki, T.; Yoneda, Y.; Hinoi, E. Genetic analysis of Runx2 function during intramembranous ossification. *Development* **2016**, *143*, 211–218. <https://doi.org/10.1242/dev.128793>.
52. Nantavisai, S.; Pisitkun, T.; Osathanon, T.; Pavasant, P.; Kalpravidh, C.; Dhitavat, S.; Makjaroen, J.; Sawangmake, C. Systems biology analysis of osteogenic differentiation behavior by canine mesenchymal stem cells derived from bone marrow and dental pulp. *Sci. Rep.* **2020**, *10*, 20703. <https://doi.org/10.1038/s41598-020-77656-0>.
53. Baksh, D.; Boland, G.M.; Tuan, R.S. Cross-talk between Wnt signaling pathways in human mesenchymal stem cells leads to functional antagonism during osteogenic differentiation. *J. Cell Biochem.* **2007**, *101*, 1109–1124. <https://doi.org/10.1002/jcb.21097>.
54. Waddington, R.J.; Roberts, H.C.; Sugars, R.V.; Schönherr, E. Differential roles for small leucine-rich proteoglycans in bone formation. *Eur Cell Mater.* **2003**, *6*, 12–21. <https://doi.org/10.22203/ecm.v006a02>.
55. Parisuthiman, D.; Mochida, Y.; Duarte, W.R.; Yamauchi, M. Biglycan modulates osteoblast differentiation and matrix mineralization. *J. Bone Miner. Res.* **2005**, *20*, 1878–1886. <https://doi.org/10.1359/jbmr.050612>.
56. Kraskiewicz, H.; Paprocka, M.; Bielawska-Pohl, A.; Krawczenko, A.; Panek, K.; Kaczyńska, J.; Szyposzyńska, A.; Psurski, M.; Kuroпка, P.; Klimczak, A. Can supernatant from immortalized adipose tissue MSC replace cell therapy? An in vitro study in chronic wounds model. *Stem. Cell Res. Ther.* **2020**, *11*, 29. <https://doi.org/10.1186/s13287-020-1558-5>.

Review

Mesenchymal Stem Cells, Bioactive Factors, and Scaffolds in Bone Repair: From Research Perspectives to Clinical Practice

Sandra Stammitz  and Aleksandra Klimczak * 

Laboratory of Biology of Stem and Neoplastic Cells, Hirszfeld Institute of Immunology and Experimental Therapy, Polish Academy of Sciences, 53-114 Wrocław, Poland; sandra.gromolak@hirszfeld.pl

* Correspondence: aleksandra.klimczak@hirszfeld.pl

Abstract: Mesenchymal stem cell-based therapies are promising tools for bone tissue regeneration. However, tracking cells and maintaining them in the site of injury is difficult. A potential solution is to seed the cells onto a biocompatible scaffold. Construct development in bone tissue engineering is a complex step-by-step process with many variables to be optimized, such as stem cell source, osteogenic molecular factors, scaffold design, and an appropriate in vivo animal model. In this review, an MSC-based tissue engineering approach for bone repair is reported. Firstly, MSC role in bone formation and regeneration is detailed. Secondly, MSC-based bone tissue biomaterial design is analyzed from a research perspective. Finally, examples of animal preclinical and human clinical trials involving MSCs and scaffolds in bone repair are presented.

Keywords: stem cell therapy; biomaterials; bone tissue engineering; osteogenic differentiation



Citation: Stammitz, S.; Klimczak, A. Mesenchymal Stem Cells, Bioactive Factors, and Scaffolds in Bone Repair: From Research Perspectives to Clinical Practice. *Cells* **2021**, *10*, 1925. <https://doi.org/10.3390/cells10081925>

Academic Editor: Tong-Chuan He

Received: 30 June 2021

Accepted: 27 July 2021

Published: 29 July 2021

Publisher's Note: MDPI stays neutral with regard to jurisdictional claims in published maps and institutional affiliations.



Copyright: © 2021 by the authors. Licensee MDPI, Basel, Switzerland. This article is an open access article distributed under the terms and conditions of the Creative Commons Attribution (CC BY) license (<https://creativecommons.org/licenses/by/4.0/>).

1. Introduction

Bone tissue disorders affect millions of people worldwide and are one of the major clinical cases in orthopedics. The most common causes of bone defects are accidental injuries, skeletal diseases, osteoporosis-related fractures, tumor resections, congenital bone deformations, and aging [1]. Moreover, due to comorbidities such as diabetes, there is an up to six times greater risk to suffer a fracture and twice as slow healing rate. It is estimated that 10–20% of failed fractured bone treatments end in delayed union or even nonunion despite all modern treatment methods [2]. Additionally, fracture healing disruptions can lead to critical-sized bone defects, over 2 cm long, affecting more than half of the bone diameter [3]. These orthopedic complications remain the most challenging problem in surgery. Patients with complicated bone disorders are disabled and experience a lowered quality of life. Moreover, months of immobility can result in other health issues, including stroke, heart attacks, pressure ulcers, increased risk of infections, muscle and bone loss, and depression. Bone fracture treatment in the United States generates some of the highest costs, resulting in a significant healthcare burden [4].

Currently, the gold standard for the repair of large bone tissue defects is an autograft or allograft. However, while both autografts and allografts are the major substitutes for large bone defects, they have certain drawbacks. An autograft is restricted because of limited bone resource and donor-site morbidity. On the other hand, allografts are readily available, but may cause an immunogenic rejection [1,5]. Therefore, to address these limitations, new approaches are investigated. A promising alternative treatment of clinically challenging bone defects is bone tissue engineering.

Research on the potential beneficial effects of different components used in bone tissue engineering, including mesenchymal stem cells (MSCs), biomaterial scaffolds, and growth factors involved in osteogenesis, may provide a new therapeutic opportunity for critical-sized bone defects and non-union treatment [3]. Thus, this review aims to summarize the newest findings on the role of MSC therapies supporting a scaffold in bone regeneration.

2. The Role of MSCs in Bone Formation and Healing

Knowledge about bone formation and bone healing is necessary to determine effective MSC-based treatment strategies. Only a full understanding of the mechanisms underlying osteogenesis and bone healing enables the potential use of new, innovative, and most importantly, effective and safe alternatives to the traditional treatment methods, which are insufficient. MSCs are important regulators of bone modeling and remodeling as well as bone fracture repair [6].

2.1. Bone Ossification

Osteogenesis is a long process, lasting from the sixth or seventh week of embryonic development to about the age of 25 years. Bone ossification is classified into two types: intramembranous and endochondral. Both begins with MSCs as the precursors for different types of bone cells.

Intramembranous bone formation is responsible for developing most of the cranial bones, flat bones of the skull, and clavicle. This process begins with the differentiation of MSCs into specialized bone-forming osteoblasts, which then group into clusters of ossification centers. Osteoblasts secrete an unmineralized matrix consisting of collagen and proteoglycans, called the osteoid. It can bind calcium, which results in the hardening of the matrix and osteoblast entrapping, followed by osteoblast to osteocyte differentiation. Osteocytes are the most abundant in the bone and regulate bone remodeling. Osteoblasts are surrounded by blood vessels, forming the trabecular/spongy bone, whereas mesenchymal cells form the periosteum, a membrane on the bone surface, and differentiate into osteoblasts, secreting osteoid parallel to the existing one. Thus, new layers are created, called the compact bone, and red marrow is formed by blood vessels [7].

Endochondral ossification forms the axial skeleton and long bones. This process begins in the same manner as the intramembranous process, specifically, with MSCs as the precursors. However, the MSCs do not differentiate directly into bone cells, but intermediately into chondrocytes, secreting the extracellular matrix, and consequently, forming the cartilage model for the bone. Chondrocytes increase rapidly in number, and the matrix is mineralized, resulting in reduced availability of nutrients for the chondrocytes and their apoptosis. Next, the blood vessels start to invade the spaces left by the dead cells and bring stem cells, which differentiate into osteoblasts, responsible for bone deposition, and osteocytes [8].

2.2. Bone Repair

Bone healing is a complex physiological process that engages many different cell types, cytokines, chemokines, growth factors, and cellular responses. As a result, the bone is reconstituted without the scar tissue formation [9]. As with bone ossification, MSCs also play a significant role here. The process of skeletal renewal, also known as bone remodeling, is carried out by key grouping cells. These cells are primarily osteocytes, osteoblasts, osteoclast, and MSCs. The MSCs give rise to osteoblasts through osteogenic differentiation. Furthermore, they migrate to the surface of the bone fracture and modulate the microenvironment for other types of cells [10].

There are two types of bone healing: primary and secondary. The former concerns small fracture gap healing, where no movement occurs at the fracture site. A characteristic feature of primary bone healing is that no callus is formed. Instead, the process resembles normal bone remodeling, i.e., the last stage of secondary bone healing. Nevertheless, primary bone repair is rather rare, with most cases involving secondary healing [9].

Secondary fracture healing consists of four stages: (i) formation of fracture hematoma, (ii) formation of soft callus, (iii) formation of hard callus, and (iv) remodeling.

The first and probably the most important determinant of the bone healing effect is the fracture hematoma. The blood vessels immediately surround the damaged bone site following a fracture in the inflammatory phase. The repair begins with the subsequent infiltration of the inflammatory cells, which prevent infection and secrete pro-inflammatory

cytokines. These chemoattractants recruit other immune cells, MSCs, and endothelial cells [11,12]. The cytokines occurring in the injured site include the bone morphogenetic proteins (BMPs), tumor necrosis factor alpha (TNF- α), vascular endothelial growth factor (VEGF), and interleukin 17 (IL-17), which has a dual role of stimulating bone resorption through osteoclasts and enhancing osteogenic efficiency through osteoblasts [9]. BMPs enhance the differentiation of MSCs into osteogenic cells, whereas VEGF stimulates vascular cells. The final step of hematoma before the next stage of fracture healing, is the generation of the extracellular matrix, which develops into the granulation tissue. This tissue consists primarily of MSCs and endothelial and immune cells [11].

Formation of the soft callus is the second stage of fracture healing, which takes place when the MSCs in the granulation tissue start to differentiate into chondroblasts, fibroblasts, and osteoblasts. The fibrocartilaginous callus is formed during endochondral ossification and connects the ends of the bone in the fracture gap [13].

Hard callus, called the woven bone, forms in the next stage following the formation of the soft callus. However, depending on stability of the fracture site, it may develop directly from the granulation tissue through intramembranous ossification. Osteoblasts produce vesicles with calcium phosphate complexes into the matrix, which in turn causes the formation of a hard, calcified callus [9].

Bone remodeling, the final stage of bone healing, can last from months to many years. The process involves joining the soft callus formed during endochondral ossification with the hard callus of intramembranous ossification, resulting in the regeneration of the weight bearing bone [12]. Osteoclasts and osteoblasts are particularly involved in this stage of repair. They create a balance between resorption and new bone formation. Vasculature also undergoes a substantial remodeling [13]. Bone resorption by the osteoclasts leads to MSC recruitment. These, in turn, create a specific microenvironment to enable bone formation [10].

3. MSC-Based Tissue Engineering Therapies in Bone Repair from a Research Perspective

MSCs were described in 1966 by Friedenstein et al. as cells with fibroblast-like morphology residing in the bone marrow and able to form the ectopic bone. Following the suggestion that MSCs are osteogenic precursors [14], researchers in the field of regenerative medicine began taking interest in them. However, the term “mesenchymal stem cells” was proposed by Caplan in 1991 to describe a type of adult stem cells characterized by a multipotential differentiation ability into the osteogenic, chondrogenic, and adipogenic lineage [15]. Currently, the term MSCs is used to describe a heterogeneous population of multipotential stem/progenitor cells commonly referred to as mesenchymal stem cells, multipotential stromal cells, mesenchymal stromal cells, and mesenchymal progenitor cells [16]. MSCs are in the spotlight as a potential cell-based therapy in orthopedics [17]. Although bone has the ability to self-regenerate, in some circumstances, depending on comorbidities, size of defects, and age, the ability can be reduced or even lost [12]. Moreover, changes in the mechanism of bone remodeling, maintained by a sensitive balance between bone resorption (osteoclasts activity) and new bone formation (osteoblasts activity), may cause certain diseases, such as osteopetrosis due to excessive bone formation or osteoporosis due to excessive bone resorption [10].

Currently, tissue engineering seems to be a promising subject of research related to cases of bone diseases in which the standard surgical procedures and pharmacological treatment have failed [18]. Nevertheless, the development of these bioengineering methods requires a complex, step-by-step approach, in which numerous variables have to be optimized. In particular, the main three components of bone engineering are (1) cells, (2) osteogenic factors, and (3) a scaffold. In the first step, it is necessary to conduct a preliminary but essential, *in vitro* optimization study in order to assess the source of the stem cells, choice of bioactive factors, and scaffold design. Next, before a clinical application in humans is viable, the *in vitro* optimized tissue engineering approach should be tested in

an *in vivo* environment. Therefore, another issue to be considered is the most appropriate experimental animal model [19].

3.1. Sources and Biological Properties of MSCs for Bone Regeneration

A promising skeletal repair strategy in pathological bone disorders is to increase the number of osteogenic progenitor cells [20]. As described above, MSCs fulfil a key function in the processes of bone modeling, remodeling, and repair. They differentiate into the cartilage growth plate forming chondrocytes, which then gradually transdifferentiate into new bone-forming osteogenic cells during endochondral ossification. Alternatively, in the case of intramembranous osteogenesis, MSCs can directly differentiate into osteoblasts [6].

Cells with MSC characteristics can be isolated from adult and perinatal tissue sources [21–23]. Adherent cells, isolated from different tissue sources, should meet the minimal criteria of the MSC phenotype, such as the expression of the non-hematopoietic common markers CD73, CD90, and CD105 in over 95% of the cells, and the lack of expression of the hematopoietic and endothelial surface markers CD34, CD45, CD14 or CD11b, CD19 or CD79a, HLA-DR, and CD31, as defined by the International Society for Cellular Therapy (ISCT) [24]. These markers represent the accepted standards of MSC characteristics. However, controversies still exist regarding the ideal marker or set of markers, depending on the tissue sources of MSCs, culture conditions, and number of passages [22]. To date, bone marrow-derived MSCs (BM-MSCs) have been the most extensively characterized in terms of their phenotype and biological properties. Many studies on the biological characteristics of MSCs derived from other tissues are based on a comparative analysis with BM-MSCs [22,23,25]. In general, BM-MSCs meet the phenotypic criteria defined by the ISCT in terms of the classical positive (CD90, CD105, and CD73) and negative (CD34, CD45, CD14, CD79a, HLA-DR, and CD31) markers. In addition, BM-MSCs express other markers, including CD13, CD29, CD44, CD49, CD54, CD140b, CD146, CD276, and stage-specific embryonic antigen-1 (SSEA-1), but the expression of these markers is uncommon for MSCs derived from other tissue sources [21,26]. Studies showed that the presence of CD146 on BM-MSCs affects osteogenesis and angiogenesis [27]. Moreover, BM-MSCs are the most stable for CD146 expression during the subsequent passages compared to other sources of MSCs, including adipose tissue-derived MSCs (AT-MSCs) [22]. Although AT-MSCs meet the common criteria of the MSCs phenotype, they differ in CD34 expression during the early period of culture when the CD34 antigen displays a different level of expression [23,28]. Moreover, to distinguish AT-MSCs from BM-MSCs, two other markers, such as CD36 (GPIIb) and CD106 (VCAM-1), are employed, because it was reported that AT-MSCs, in contrast to BM-MSCs, do not express CD106, but are positive for CD36 [28]. Comprehensive comparative studies performed on BM-MSCs and the cord blood-derived MSC (CB-MSC) phenotype revealed that among the 246 analyzed surface markers, both types of MSCs showed a high expression of 18 markers, including the classical ones (CD90, CD105, and CD73), as well as the alpha-smooth muscle antigen (SMA), CD13, CD140b, CD276, CD29, CD44, CD59, CD81, CD98, HLA-ABC, and vimentin. The presence of CD143 exclusively on BM-MSCs is suggested as a discriminating marker between adult and perinatal MSCs [23]. In addition to cord blood, MSCs can be obtained from other perinatal tissue sources, including the umbilical cord (UC-MSCs), placenta (PL-MSCs), amniotic fluid (AF-MSCs), and amniotic membrane (AM-MSCs). Although MSCs isolated from perinatal tissues have the characteristics of MSCs, they differ in the osteogenic potential [29,30]. Specifically, AM-MSCs and UC-MSC demonstrated a greater osteogenic differentiation capacity compared to MSCs isolated from other regions of perinatal tissues [30].

Furthermore, in addition to giving rise to the target tissue, MSCs also modulate the bone microenvironment, providing cytokines that support the vascularization of the new bone and facilitate the bone repair process [20]. MSCs exert a paracrine effect on the microenvironment by secreting various bioactive factors with an anti-inflammatory, immunomodulatory, trophic, proangiogenic, and pro-regenerative potential. Immunoregulation constitutes a crucial paracrine activity of MSCs, making them very special cells

that affect not only immune cells, but also the microenvironment during the regeneration process. In response to inflammatory cytokines, such as interleukin-1 (IL-1), IL-2, IL-12, tumor necrosis factor- α (TNF- α), and interferon- γ (IFN- γ), MSCs secrete anti-inflammatory factors, including prostaglandin-2 (PGE-2), transforming growth factor- β 1 (TGF- β 1), IL-4, IL6, IL-10, and IL-1Ra, that stimulate tissue repair and modulate inflammation and immune response. The secretion of anti-inflammatory cytokines results in the downregulation of the function of the different immune cells related to innate and adaptive immunity (macrophages, natural killer cells, dendritic cells, T-lymphocytes, and B-lymphocytes), leading to a decrease in the inflammatory response. The increasing level of IL-4 and IL-10 promotes a shift in T-lymphocytes from the T-helper type 1 (Th1) to the Th2 phenotype and a shift in macrophage balance from the M1 (proinflammatory) to the M2 (anti-inflammatory) phenotype, thus inducing the anti-inflammatory milieu [16,31]. The trophic properties of MSCs are associated with the secretion of bioactive factors involved in cell proliferation and angiogenesis. MSCs produce TGF- α , TGF- β , hepatocyte growth factor (HGF), epithelial growth factor (EGF), insulin-like growth factor 1 (IGF-1), FGF-2, VEGF, angiopoietin-1 (Ang-1), and other growth factors and molecules that regulate cell proliferation and angiogenesis [31–33]. However, a screening of the MSC secretome revealed that BM-MSCs had the highest ability to secrete proangiogenic factors, such as IL-8 or VEGF, compared to AT-MSCs and skin-derived MSCs [22]. An increased production of IL-8 and VEGF by AT-MSCs was also reported in studies on the angiogenic activity of MSCs in a microgravity microenvironment [34]. Thus, the secretion of proangiogenic factors is a very desirable feature of MSCs, especially in the context of creating a living tissue using bone tissue engineering.

Interestingly, the differentiation potential and proliferation rate of MSCs may vary, depending on the tissue source [22,35]. In all likelihood, the specific niche in which they reside modulates the microenvironment and influences MSC properties [36]. Nevertheless, from numerous sources of MSCs, the most popular are bone marrow and adipose tissue, as the best known and well characterized [37]. Adipose tissue-derived MSCs can be isolated at relatively high density, in contrast to BM-MSCs. However, BM-MSCs and MSCs isolated from the human amnion show stronger osteogenic potential compared to AT-MSCs [29,38]. The procedures for obtaining MSCs from both bone marrow and adipose tissue are invasive, whereas MSCs originating from perinatal tissues, including the umbilical cord, placenta, amniotic fluid, and amniotic membrane, are available as medical waste. Among these, Wharton's jelly seems to be a very good source of MSCs because of its ease of isolation and having no ethical concerns. It is worth mentioning that new sources of MSCs are currently considered for tissue regeneration, including muscles, skin, dental pulp, tendons, and the periodontal ligament [21,39]. Interestingly, in addition to the type of MSC source, the patient's age and health are other important factors affecting the properties of the isolated MSCs [40].

Collectively, different sources of MSCs affect their biological properties and regenerative potential. Furthermore, *in vitro* cell culture can also change their ability to proliferate and differentiate. However, manipulating the culture conditions, such as introducing specific media supplements or hypoxia, may result in a more efficient MSC expansion and osteogenic differentiation [41,42].

Safety and Limitation of MSC Therapy

With over 25 years of history, MSC-based therapy has shown a very good safety profile. However, it is still employed as an experimental clinical procedure [16]. The reason lies in the biological diversity of MSCs, depending on their original tissue location, age of the donor, isolation method and expansion, and culture environment. All these factors affect the biological behavior of MSCs, making their *in vivo* activity difficult to predict.

The efficacy of MSCs-based therapy also depends on the delivery route. Intravenous infusion is the most common method of MSC administration. However, the limitation of this method is that a proportion of the transplanted cells are trapped within organs

with a large capillary bed, especially in the lungs and liver, thus impairing the homing of infused MSCs to the target tissue; nevertheless, they are able to home to the injury site [39]. Moreover, the accumulation of MSCs in small capillaries carries a risk of thromboembolic complications [43]. Experimental studies on the pig model have shown that intraarterial BM-MSCs infusion is more effective in avoiding pulmonary BM-MSCs entrapment compared to intravenous infusion [44]. Delivery of MSCs to the site of tissue injury has a beneficial effect on the local anti-inflammatory response and directly affect damaged tissue repair. On the other hand, MSCs delivered locally have a restricted migratory potential, and their pro-regenerative activity may be limited to a small area of the damaged tissue.

It is also difficult to obtain sufficient numbers of MSCs for clinical application during *in vitro* manufacturing, especially in the early passages (up to the fifth passage). Long-term culture affects the biological potential of MSCs [22] and results in a decrease of proliferation and differentiation activity. Moreover, long-term culture of MSCs can increase the potential genetic instability of the cells and lead to a malignant transformation [39]. Therapeutic effectiveness is also related to the number of doses of MSCs when transplanted in allogeneic conditions. The administration of single dose of MSCs is safe and does not trigger the immune response; however, repeated doses of MSCs may induce the alloantibody production [45].

Standardization of the isolation methods and culture conditions and understanding the factors that underlie MSC biology should constitute important points for consideration before the use of MSCs in clinical practice. To date, MSC therapy has undoubtedly shown a favorable safety profile. On the other hand, long-term observations are necessary to assess the therapeutic effects of applied MSCs, including the adverse effects, in terms of cell sources, doses, and route of delivery.

3.2. Cytokines, Growth Factors and Signaling Pathways Enhancing Osteogenesis

It is well known that bone fracture healing involves overlapping processes, *i.e.*, inflammation, angiogenesis, and osteogenesis. Inflammation causes the secretion of various growth factors and cytokines, which in turn affect MSC recruitment and differentiation (Figure 1). Furthermore, these cytokines regulate the formation of vasculature, enabling bone remodeling [46]. In other words, osteogenesis requires not only cellular differentiation and tissue remodeling, but also appropriate molecular signaling. Therefore, it is crucial to understand how cytokines and growth factors enhance the effectiveness of bone repair and thus can promote particular approaches in bone tissue engineering [47]. The main molecular regulators of the bone healing cascade are bone morphogenetic proteins (BMPs), the fibroblast growth factor (FGF), transforming growth factor- β 1, and vascular endothelial growth factor [3]. In addition, multiple signaling pathways regulate osteogenesis, including Wnt, Notch, parathyroid hormone (PTH), and hedgehog (Hh) [48,49].

BMPs, which were originally found in the extracts of demineralized bone, are a group of proteins belonging to the TGF- β superfamily [50]. Currently, these proteins are considered to be the most beneficial in the healing of large bone defects [3]. They are involved in embryogenesis, organogenesis, and cell proliferation and differentiation [51]. Their osteoinductive functions were discovered when they were found to induce *de novo* bone formation in demineralized bone [52]. They are responsible for MSC osteogenic differentiation, bone formation, and skeletal development. In particular, the BMP signaling pathway plays a crucial role in the differentiation of MSCs into the osteochondroprogenitor cells [53], after which they allow the differentiated osteoblasts to secrete the bone formatting matrix [54]. Moreover, BMPs have been shown to increase the expression of osteogenic markers in MSCs, including the early osteogenic markers alkaline phosphatase (Alp), Runt-related transcription factor 2 (Runx2), osterix (Osx), and type I collagen (CollI) and the late markers osteopontin (Opn) and osteocalcin (Ocl) [53,55–57]. Currently, BMP-2 (Medtronic) and BMP-7 (Stryker Biotech) are approved by the Food and Drug Administration (FDA) and available for clinical use in a recombinant form for bone fracture treatment and intervertebral disk regeneration enhancement [57].

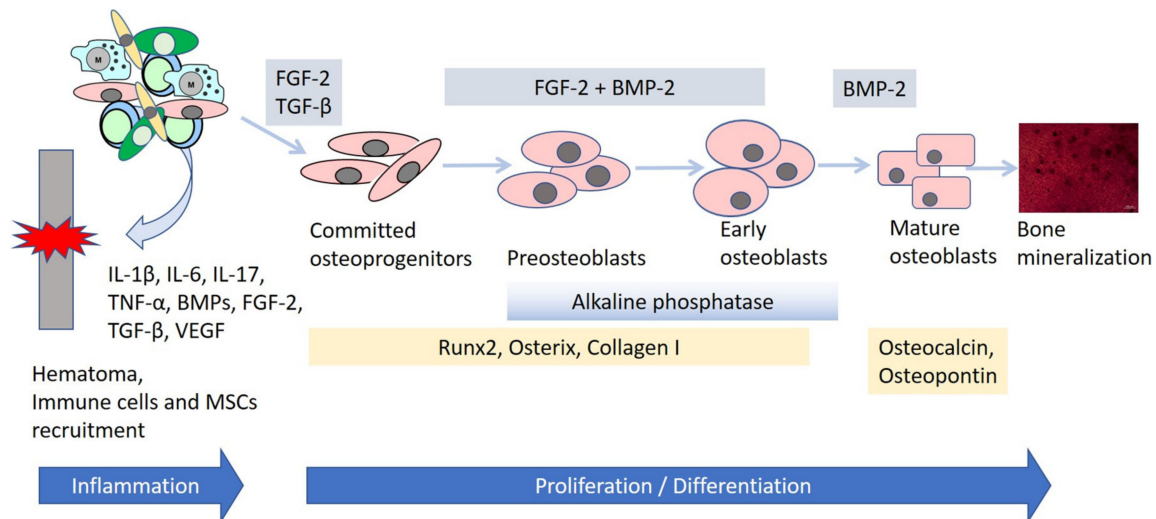


Figure 1. Schematic representation of the osteogenic differentiation of mesenchymal stem cells (MSCs) during bone regeneration. The first step of bone healing is the formation of fracture hematoma. The local hematoma attracts immune cells, creating an inflammatory microenvironment (IL-1 β , IL-6, IL-17, TNF- α) and MSCs with an osteogenic and proangiogenic potential (TGF- β , BMPs, VEGF). Proliferation and osteogenic differentiation of MSCs is warranted by the simultaneous activity of FGF-2, TGF- β , and BMPs. BMPs increase the expression of osteogenic markers in MSCs, including the early osteogenic markers alkaline phosphatase, Runt-related transcription factor 2 (Runx2), osterix, and type I collagen, and the late markers osteopontin and osteocalcin. The bone mineralization image is taken from the authors' own collection of the osteogenic differentiation of MSCs (Alizarin Red staining).

FGFs regulate multiple processes of homeostasis and tissue development, including skeletal formation [58]. However, they do not directly influence osteogenic differentiation; rather, they modulate it, playing the role of an osteogenesis accelerator. They can stimulate osteoblast proliferation, promote differentiation into the osteogenic cell lineage, as well as induce angiogenesis [59]. Studies showed that FGF-2 and BMP-2 could act synergistically in bone regeneration, enhancing the effectiveness of bone formation [56,60,61].

TGF- β s are found in large amounts in the bone and cartilage. TGF- β 1 stimulates bone growth and mineralization through the maintenance and expansion of MSCs, which then give rise to the osteoblastic lineage [62]. TGF- β signaling also enhances the proliferation of osteoprogenitor cells and their early osteogenic differentiation stages. Interestingly, interplay was found between the signaling of TGF- β and FGFs or BMPs in the bone [57]. For instance, TGF- β and FGF-2 stimulate osteoblasts proliferation, but on the other hand, inhibit alkaline phosphatase activity and mineralization. Consequently, it has been suggested that both of these cytokines can be potentially applied in tissue engineering for the induction of bone growth in vitro [63]. Furthermore, TGF- β 1 strongly promotes BMP-2-induced osteogenic functions in bone formation in vitro [57].

VEGF is the most extensively explored angiogenic factor [46]. As bone is a strongly vascularized tissue, it requires re-vascularization after the fracture has occurred. Among others, osteoprogenitor cells, minerals, and signaling factors are thereby brought to the damaged area to promote the formation of new bone [3]. Some authors suggest that VEGF stimulates bone formation not only indirectly by promoting vascularization, but also directly by affecting osteogenesis through osteoblast and osteoclast attraction [47]. Studies have shown that a co-delivery of VEGF and BMPs may increase the efficiency of bone formation [64,65].

The Wnt signaling pathway is known to play a pivotal role in skeletal development and homeostasis, among others, through the promotion of osteoblast proliferation, differentiation, and maturation [66,67]. Wnt proteins bind to their receptors, the Frizzled and low-density lipoprotein receptor-related proteins (Lrp), which activates the main player of the pathway [68,69]. There are two categories of Wnt signaling pathways: canonical and

non-canonical. In the canonical Wnt signaling pathway, the central activated protein is β -catenin. In the absence of Wnt ligand binding, β -catenin is destroyed by the protein complex through phosphorylation, ubiquitination, and degradation by the ubiquitin-dependent proteasomal system [70]. The canonical way inhibits the destructive proteasome complex, resulting in the translocation of β -catenin into the nucleus and the regulation of the Runx2 and Sp7/Osterix gene expression, which are involved in bone formation and differentiation. In turn, Runx2 and Sp7/Osterix positively regulate the gene expression of other osteogenic transcription factors, such as Alp, Opn, and Ocl [68]. It was reported that mice with an activated form of β -catenin in the osteoblasts and knockout of Axin2, one of the β -catenin destruction complex proteins, showed significantly increased bone healing and high bone mass [71]. The non-canonical Wnt signaling pathway, also called β -catenin-independent, uses Wnt5a or Wnt11 binding to a receptor complex and calcium signaling as the central mediator [72]. Studies also showed that Wnt5a-deficient mice had a reduced number of osteoblasts and low bone mass, suggesting that this non-canonical Wnt signaling pathway plays an important role in MSC differentiation into osteoblasts [73].

Another signaling pathway that directly affects osteoblasts and thus plays a significant role in bone tissue development is the Notch signaling pathway [74]. It is activated through the interaction between the Notch receptors and its ligands, resulting in the release of the Notch Intracellular Domain (NICD) and its translocation into the nucleus to activate the target genes [75]. It was demonstrated that the inhibition of the Notch signaling pathway in progenitor bone cells led to the reduction of bone marrow-derived MSCs and bone loss [76]. Moreover, the treatment of MSCs with Jag-1, one of the Notch signaling ligands, increased the expression of osteoblast-related genes: Alp and Bone Sialoprotein [77]. Another study showed that the Notch signaling pathway enhanced the osteogenic differentiation of MSCs in vitro and in vivo through the induction of BMP-9 signaling [78]. Interestingly, Lee et al. suggest that there is a crosstalk between the Notch and Wnt signaling pathways. Their study demonstrated that the regulation of osteoprogenitor cell proliferation during the formation of intramembranous bone was controlled by the Notch pathway, whereas the canonical Wnt pathway initiated the differentiation of osteoprogenitor cells [49].

The signaling pathway of the parathyroid hormone (PTH) is another example of a positive osteoblastogenesis regulator. The secretion of PTH occurs when there is a low level of calcium or calcitriol in the serum [79]. The PTH signaling pathway is activated through the binding between PTH and its receptor, which leads to the downstream signaling induction and activation of the cAMP-responsive element binding (CREB) [48]. In turn, the activated CREB positively affects the expression of osteogenic markers, such as Bmp-2, Ocn, and Bone Sialoprotein (Bsp), enhancing bone formation [80]. Xiao et al. presented results indicating that the crosstalk between FGF2 and Wnt signaling was required to mediate the maximal bone anabolic effects of PTH [81].

The last example of the signaling pathway enhancing osteogenesis concerns the Hedgehog (Hh). It is involved in BM-MSc differentiation into osteoblasts by affecting the expression of Runx2 and Osx [82]. Hh signaling also promotes the receptor activator of the NF κ B ligand (Rankl) expression in osteoblasts by upregulating the expression of the parathyroid hormone related protein (PTHrP). As a result, RANKL regulates osteoclast differentiation and thus maintains homeostasis between bone formation and bone resorption [83]. Osteoblastogenesis in the endochondral skeleton is induced by the synergistic interactions between Hh and BMP [84]. Furthermore, studies found that crosstalk between the Hh and Wnt pathways regulated endochondral bone formation, cartilage development, and synovial joint formation [85].

3.3. Bone Scaffolds in Tissue Engineering

As previously mentioned, tissue engineering is a multidisciplinary field based on cell biology, molecular science, and biomaterial engineering. The third basic element in bone tissue engineering is the scaffold. Cells in the body grow in a three-dimensional environment, which enables them to interact with the extracellular matrix and other cells.

Scaffolds in tissue engineering act as the extracellular matrix, supporting cell proliferation, adherence, differentiation, spreading, and communication [86].

3.3.1. Scaffold Properties

For a safe and successful use in clinical settings, biomaterials for bone tissue engineering should exhibit several properties, such as biocompatibility, biodegradability, osteoinduction and osteoconduction, scaffold pore structure and grain size, and surface topography [1,87]. The scaffold should not stimulate the immunological response while being incorporated into the host tissue and should degrade into simpler substances that can be used by the body. Importantly, the level of degradation must be monitored and precisely matched to the level of bone regeneration [46]. The scaffold should be able to recruit osteoprogenitor cells to the fracture site, as well as induce the osteogenic differentiation of cells [87]. Another significant aspect are the well-defined structural properties of the scaffold, because they directly affect the cellular response. Scaffold porosity enables cell settlement and migration and the transport of nutrients and metabolites. Furthermore, it supports vascularization and production of the extracellular matrix [18]. Highly porous scaffolds are often used in bone regeneration to mimic the porosity of the trabecular bone [46]. Proper grain size provides adsorption sites for proteins and improves cell adhesion, proliferation, and differentiation [88]. In turn, surface topography ensures interactions between biomaterial and tissue [1]. Furthermore, a rough surface stimulates osteoblast-like cell spreading and proliferation [89]. Thus, the properties of the scaffold play a crucial role in regulation of biological responses [90].

3.3.2. Scaffold Types

There are three main types of biomaterials: (1) bioceramics, (2) biodegradable polymers, and (3) composite biomaterials.

1. Bioceramics

Ceramic biomaterials are known for their high biocompatibility. The most commonly used bioceramic material is calcium phosphate (Ca-P) [3]. Among Ca-P ceramics, hydroxyapatite (HA) and tricalcium phosphate (TCP) are particularly interesting due to their similar compositions as natural bone [91]. Apart from effective biocompatibility, they also show high osteoconductivity and an ability to osseointegrate within the fracture site [92]. Furthermore, their biodegradation products are used in human metabolic pathways, enhancing cell activity and bone repair through the creation of an alkaline environment [93]. While HA is very advantageous in bone engineering because of its origin—it is the main mineral in natural bone and is thus highly osteoinductive—it is also very stable and hard to degrade in vivo. On the other hand, TCP is more degradable, and at the same time, it is also an effective bone biomaterial [94].

Currently, ceramics based on Ca-Si and bioactive glasses are studied extensively. This is due to the fact that Ca-Si ceramics have higher mechanical stability than Ca-P ceramics [91]. Ca participates in bone and blood vessel growth [95], whereas Si enhances bone calcification and density and prevents osteoporosis [96]. Bioactive glasses also have a great potential for bone repair through a rapid strong chemical binding with the bone tissue [97]. Furthermore, they are the only bioceramic material to date able to bond with both soft and hard tissues [91].

In general, ceramics are a good candidate for scaffolds used in bone tissue engineering because of their high bioactivity and biocompatibility. However, there are some limitations related to their low toughness and insufficient strength. For this reason, they are limited to load-free or low-load applications. To enhance the mechanical properties of bioceramics, studies are conducted on surface coatings, nanoscale second phase, and self-toughening methods [3,91].

2. Biodegradable polymers

Polymeric biomaterials can be categorized into natural and synthetic [98]. Biopolymers are known to support tissue growth and remodeling prior to their biodegradation [3]. Biodegradable polymers derived from plant and animal tissue, such as cellulose, collagen, and chitosan, are natural and characterized by good bioactivity, availability, cell affinity, non-toxicity, and a low risk of inducing an immune response [99].

An advantage of synthetic polymers is the possibility to modulate their surface properties and degradation degree through molecular design and synthesis [100]. Consequently, their mechanical properties and plasticity can be improved, in contrast to natural polymers [101]. The best known synthetic polymer is the poly(lactic acid) (PLA). It has been shown that PLA can be used as an effective biomaterial in bone repair due to its good biocompatibility, plasticity, and biodegradability and an ability to support osteoprogenitor cell adhesion and growth [102]. The poly(glycolic acid) (PGA) and poly(lactic-co-glycolic acid) (PLGA) are other synthetic biomaterials with good biocompatibility and biodegradability. The development of synthetic biomaterials combining good biological and mechanical properties allowed for PLA, PGA, and PLGA to be approved by FDA for clinical applications, such as bone scaffolds, surgical sutures, and injection capsules [91]. However, the most favorable biomaterial for bone tissue engineering is polycaprolactone (PCL), which is also FDA-approved. Compared with other synthetic biodegradable polymers, PCL shows better mechanical properties [3].

Although polymer scaffolds are widely used in bone tissue engineering, there are some disadvantages, such as weak mechanical properties, risk of deformation, and problems with a strong integration with the bone. In general, synthetic polymers have poor bioactivity and thus poor cell adhesion, whereas natural polymers are difficult to process and control in terms of their degradation and show poor thermal stability [103]. However, these limitations can be addressed through the use of the nanoscale second phase method, as previously mentioned for ceramic biomaterials [104].

3. Composite biomaterials

The mechanical properties of biodegradable scaffolds can be improved through the use of composites, consisting of ceramics combined with polymers. Consequently, biodegradable scaffolds possess the advantages of both types at once, such as improved biocompatibility and bioactivity, mechanical toughness, host-implant interactions, and load-bearing capabilities [105]. Examples of effective composite biomaterials include PLGA and PCL combined with TCP or HA. They have the high bioactive potential of ceramics, promoting the formation of mineralization sites while allowing for the controlled degradation kinetics of the polymers. Moreover, they maintain an appropriate balance between strength and toughness [106].

3.3.3. 3D Printing of Bone Scaffolds

The success of bone tissue engineering-based treatment depends, to a large extent, on scaffolds with appropriate features, such as structure, shape, and chemical, physical, and biological properties [107]. Manufacture of traditional scaffolds relies on the following techniques: lyophilization, solvent casting, electro- and wet spinning, porogen leaching, and gas foaming. Although these methods are widely used in tissue engineering, they have certain limitations, such as a long manufacturing time, use of toxic organic solvents, and low reproducibility [108]. Many studies have shown that one of the most important aspects of tissue engineering are the interactions between the cells and the material. For instance, the size of pores should be optimized to help the cells migrate, proliferate, and differentiate [109–111]. A customized scaffold with the anatomical shape of the bone defect and highly desirable characteristics for bone regeneration can be produced via three-dimensional (3D) printing. The method can create novel scaffolds with favorable architecture, mechanical strength, wettability, and cellular response [107]. Moreover, 3D

modelling and printing are very simple, fast, and accurate, allowing for many tests to be conducted on biomaterials [108].

Three-dimensional printing, also called the additive manufacturing method, is based on piece-by-piece building. The designed object can be manufactured without any loss of material [112], which is the opposite of subtractive methods, in which superfluous material is removed until the appropriate shape is achieved [108]. Before a 3D printer can start creating a solid, complex object layer-by-layer, a computer-aided design (CAD) file must be prepared first [113]. Computer modeling of a patient-specific bone scaffold is divided into two steps: data acquisition and model generation. It is important that these steps be completed with appropriate care due to variations in bone anatomy between the patients. These steps directly affect the quality of the final medical part to be replaced [114]. The anatomical data about the shape and size of a bone defect can be acquired via computed tomography (CT) or magnetic resonance imaging (MRI) [115]. Next, a customized scaffold geometry is obtained using CAD software [114].

The most commonly used type of material in 3D printing are polymers. This is due to their mechanical properties, surface chemistry, and topography. However, other materials are also widely used, such as ceramics and metals [107,116]. In recent years, there has been a rapid rise in the popularity of biocompatible materials, as well as complex 3D products with living cells. These are created with bioprinting and are able to mimic the biological functions of their native tissue analogues [117]. Over the last two years (2019–2020), the number of publications on 3D printing in bone regeneration has skyrocketed, with about 1400 published papers and the number continuing to grow (www.pubmed.ncbi.nlm.nih.gov accessed on 24 July 2021).

Although 3D printing has gained great attention and is widely used in bone tissue engineering, it has some limitations. For example, it is crucial to provide the scaffold with vascularization-enabling oxygen and enough nutrient transportation to support bone regeneration. However, very few scaffolds are designed to regenerate the defected bone with the required vascularization [107]. Three-dimensional printing only considers the initial structure of the designed object and assumes it to be static and inanimate. Interestingly, a new method has been developed to overcome this problem, namely, 4D printing. It is a relatively new technique based on smart biomaterial integration, allowing the shape and functionality transformation of the scaffold to change when exposed to external stimuli [118].

3.4. Animal Models for In Vivo Studies

To predict the clinical efficacy of novel bone treatment techniques based on tissue engineering, it is necessary to provide proof of concept in an animal model. Although in vitro experiments bring an extensive insight into cellular processes and molecular mechanisms, in vivo studies can mimic the many integrated pathways in certain pathological conditions at the level of the entire body [119]. The most commonly used animal models are rodents, for instance mice or rats. This is due to low costs and ease of handling and breeding to assess the reproducibility of an experiment. Furthermore, the mouse is a well-characterized animal, and there are many molecular tools, antibodies, and other materials available for the evaluation of research performed on this animal model. With experimental manipulation, they are also easily adaptable to pathological conditions [120,121]. However, there are many restrictions associated with the use of rodent models, such as a lack of cortical remodeling and limited trabecular bone content [122]. Naturally, the size of the bone defect also plays an important role, as it influences the mechanism of bone regeneration. The biomechanical conditions of human large defects cannot be adequately simulated in small animal models [123]. Therefore, use of large animal models, such as sheep or dog, provides a more advantageous ratio between their body weight and bone size and structure and the same parameters in humans [121]. Moreover, the immune system of large animals is more similar to the human one than that of small animals. This is especially significant in research on the impact of immunogenic factors and cells on bone healing [124]. The

animal's size and anatomy should be as similar to human as possible for the purposes of investigating bone healing processes [125]. Translational proof of concept needs to be provided in a large animal model; however, initial tests on a small animal model are acceptable [119]. Nevertheless, the FDA often finds it necessary to test a new bone therapy in both a small and large animal model before approving it for clinical trials. For instance, this applies to research on osteoporosis [126]. In general, when selecting an animal model for research on bone tissue engineering, first and foremost, it is important to clearly identify the issue to be resolved. Some of the criteria that should be considered are functionality, mechanical testing, histology, and biochemical and molecular assays. They will affect the complexity of the experiment design. As there are many problems to be solved in the bone engineering field, the solutions can be achieved using different animal models [127].

3.5. Preclinical Studies

When developing MSC-based therapies, the extracellular environment has been indicated as the crucial factor that affects MSC survival, proliferation, biologically active growth factor and cytokine secretion, and differentiation [128]. Biomaterials can be used to culture conditions resembling the natural cell microenvironment in the native tissue. However, only in vivo studies using an appropriate animal model mimicking the clinical setting can help to assess the efficacy of the engineered tissue. The regeneration of a functional bone tissue requires an in vivo environment with a complex of biological and biomechanical properties. After this necessary in vivo phase, it may be possible to perform human clinical trials [19]. This section presents examples of successful in vivo studies on bone regeneration performed over the last decade (2010–2020) using MSCs and various types of scaffolds (Table 1).

Table 1. In vivo studies using MSC-based therapies with scaffolds for bone regeneration.

Animal	Cells (Suspension)	Scaffold	Treated Side	Results	References
Rat	Human BM-MSCs (2×10^6 cells/mL)	PLLA	Cranial bone defect	Pre-seeding an MSCs-scaffold construct leads to a higher osteogenic capacity than for MSCs injected into a scaffold during surgery.	[129]
Rat	BM-MSCs	PEG/PLA	Thigh muscle pouches	An MSCs-scaffold construct had an excellent osteogenic potential in vitro and a good biocompatibility in vivo.	[130]
Rabbit	BM-MSCs	PGA	Defect of infraspinatus tendons	16 weeks after implantation, mechanical analysis and the tendon maturing score showed higher values in the MSC-scaffold treated group than in the PGA-only treated rabbits.	[131]
Rat	AT-MSCs (10^4 cells per scaffold)	PLGA	Vertebral body of the spine defect	Between 2 and 4 weeks after MSC-scaffold construct implantation, bone formation occurred. However, in the group treated with osteogenic-induced AT-MSCs and a scaffold, a second bone formation occurred, contrary to the non-induced group.	[132]

Table 1. Cont.

Animal	Cells (Suspension)	Scaffold	Treated Side	Results	References
Rat	Human BM-MSCs (2×10^4 cells/cm ² or 2×10^5 cells/cm ² of scaffold)	nano-fiber PLGA	Collagen-induced arthritis	An MSCs-scaffold construct suppressed bone destruction and arthritis in rats.	[133]
Sheep	BM-MSCs (100×10^6 cells)	PCL-HA + CaP	Segmental tibial bone defect	For a delayed injection of BM-MSCs into a scaffold, 4 weeks after biomaterial implantation biomechanical testing and micro-CT analysis showed improved bone regeneration compared to previously-seeded PCL-HA-cell construct or scaffold-only group.	[134]
Canine	AT-MSCs (1×10^6 cells/50 μ L PBS)	(1) autologous serum-derived albumin (ASA) scaffold, (2) ASA + β -TCP	Segmental ulna bone defect	16 weeks post-implantation, radiograph and histomorphometric analysis showed the most extensive new bone formation in ASA with AT-MSCs compared to untreated, ASA-only, and ASA+ β -TCP with or without AT-MSCs.	[135]
Monkey	BM-MSCs (1.3 – 4.1×10^6 /mL)	β -TCP	Segmental femoral bone defect	12 weeks after transplantation, β -TCP + AT-MSCs treatment led to a higher success rate of bone regeneration compared to β -TCP treatment alone.	[136]
Sheep	BM-MSCs (10^7 cells)	coral scaffold	Long metatarsal bone defect	4 months post implantation, micro-CT and histological analysis showed better bone formation in the group treated with the construct scaffold + BMP-2 + BM-MSCs compared to scaffold + BMP-2 or scaffold + BM-MSCs.	[137]
Sheep	BM-MSCs (10^7 cells)	PLLA-PCL	Segmental tibial bone defect	12 weeks after implantation, significant bone regeneration was confirmed with micro-CT, mechanical testing and histological analysis in the group treated with PLLA-PCL + BM-MSCs compared to PLLA-PCL-only and untreated group.	[138]
Rat	BM-MSCs, osteogenic and endothelial differentiated BM-MSCs (5×10^4 cells/cm ² BM-MSCs sheet)—biomimetic periosteum (BP)	β -TCP	Calvarial defect	8 weeks post-surgery, micro-CT and histological analysis showed better new bone formation in β -TCP + BP and β -TCP + autologous periosteum groups than in the control groups.	[139]

Table 1. Cont.

Animal	Cells (Suspension)	Scaffold	Treated Side	Results	References
Goat	BM-MSCs	β -TCP	Critical size bone defects in tibia	6 months after operation X-ray, micro-CT and histological analysis showed that the defect treatment using β -TCP + BM-MSCs was significantly superior to that using β -TCP alone.	[140]
Pig	Human AT-MSCs	TCP	Segmental long bone defect	8 and 12 weeks after reconstruction, radiographic images and pathological sections analysis showed that TCP + human AT-MSCs promoted bone healing.	[141]
Rabbit	BM-MSCs	PLA-HA	Radius long bone defect	8, 12, and 16 weeks post transplantation, micro-CT, X-ray and histological analysis showed enhanced bone reconstruction in PLA-HA + BM-MSCs combined with induced membrane group compared to the other groups.	[142]
Rat	Human UC-MSCs (2×10^5 cells)	HA-G	Tendon-to-bone interface	After 8 weeks, histological and biomechanical evaluation showed that the total regeneration score was significantly higher in the HA-G + UC MSC group compared to the other groups.	[143]

Abbreviations: ASA—autologous serum-derived albumin, AT-MSC—adipose tissue-derived mesenchymal stem cell, BM-MSC—bone marrow-derived mesenchymal stem cell, BP—biomimetic periosteum, CaP—calcium phosphate, HA—hydroxyapatite, HA-G—hydroxyapatite-gradient scaffold, PCL—polycaprolactone, PEG—poly(ethylene glycol), PGA—polyglycolic acid, PLA—polylactide, PLGA—poly(lactide-co-glycolide) acid, PLLA—poly (l-lactic acid), UC-MSC—umbilical cord-derived mesenchymal stem cell, β -TCP— β -tricalcium phosphate.

In the *in vivo* studies on scaffolds and MSCs in bone regeneration presented above, the most commonly applied scaffolds were bioceramics (especially β -TCP) and biodegradable polymers. Masaoka et al. prepared composites of β -TCP and monkey bone marrow-derived MSCs for large bone defect treatment in a non-human primate model. They succeeded in the reconstruction of 5-cm-long bone defects using β -TCP scaffolds with or without BM-MSCs in a monkey model. However, only three of the nine cases treated with the scaffold alone exhibited bone regeneration. In contrast, scaffolds with cell treatment led to successful bone reconstruction in five out of the seven monkeys [136]. Another study based on β -TCP was conducted for calvarial bone defect repair in rats. Mesenchymal stem cells from rat bone marrow were differentiated into osteogenic cell sheets and induced endothelial-like cells. Then, a vascularized cell sheet was formed by means of induced endothelial-like cell cultivation on an undifferentiated MSC sheet. Together, the osteogenic cell sheet and the vascularized cell sheet formed a biomimetic periosteum (BP), which was then wrapped onto a β -TCP scaffold. As control groups, a β -TCP scaffold with autologous periosteum and a β -TCP scaffold alone were used. The results showed promoted formation of blood vessels and new bone tissue formation in the BP/ β -TCP scaffold treatment as well as the β -TCP scaffold with autologous periosteum treatment [139]. Furthermore, Lin et al. conducted a study on the reconstruction of bone damage involving a loss of periosteum using a TCP scaffold with human MSCs in the pig. The results showed that MSCs and TCP

synergistically enhanced the bone healing effect and increased lamination and vessels [141]. In turn, Chu et al. treated critical size bone defects in goat tibia of 30 mm with MSCs and a β -TCP scaffold. Six months after transplantation, the repair effect was significantly higher in the MSCs/ β -TCP group compared to the β -TCP-only group [140].

Another example of a bioceramic scaffold is hydroxyapatite. Yea et al. investigated a hydroxyapatite-gradient scaffold (HA-G) isolated from adipose tissue with MSCs derived from the umbilical cord (UC) on the gradient structure of the rotator cuff tendon-to-bone interface (TBI) regeneration in a rat model. The study demonstrated the formation of tendon, cartilage, and bone matrices in rats treated with UC-MSCs and an HA-G scaffold. Moreover, the regeneration of the rotator cuff TBI in the rat model was similar to the normal TBI when comparing histological and biomechanical properties [143].

The PLLA scaffold belongs to the second category of scaffolds—biodegradable polymers. It was successfully used to treat cranial bone defects in rats. When MSCs were pre-seeded onto a scaffold and cultured in an osteo-lineage induction medium prior to the transplantation, the highest osteogenic ability of the 3D construct was observed, compared to an injection of MSCs into a scaffold during surgery [129]. In another study, a PEG/PLA scaffold with MSCs was transplanted into the thigh muscle pouches of rats, and the physiological characteristics of the surrounding tissues were evaluated. The results showed a very good osteogenic potential of the MSCs-scaffold construct in vitro and good biocompatibility in vivo. This makes the construct a very promising tool for bone tissue engineering [130]. Another study compared the use of PGA alone and PGA with autologous BM-MSCs in the rabbit model of the infraspinatus tendons defect. Sixteen weeks following implantation, the tendon maturing score and a mechanical analysis results showed higher values in the PGA-MSC-treated group than in the PGA-only treated rabbits [131]. Liang et al. used a PLGA scaffold with osteogenic-induced AT-MSCs to treat a spine defect. Bone formation occurred between two and four weeks after the MSCs-scaffold construct implantation. However, a second bone formation occurred in the group treated with the osteogenic-induced AT-MSCs and the scaffold and not in the group without the osteogenic induction [132]. Zhang et al. efficiently treated arthritis rats with nanofiber PLGA and BM-MSCs. The results revealed that the MSCs-scaffold construct suppressed bone destruction and arthritis. Moreover, in vivo MSC tracing demonstrated that they remained within the scaffold and did not migrate to other organs [133]. A segmental tibial bone defect of 3.5 cm in sheep was treated with PLLA-PCL. Twelve weeks post implantation, the scaffold alone and scaffold combined with skeletal stem cells (SSCs) enhanced bone regeneration. However, significant enhancement was observed only for the scaffold-SSCs group. Therefore, cell therapy combined with a scaffold can promote bone regeneration in a critical-sized bone defect compared to a scaffold alone [138].

A group of scaffolds that is widely used in pre-clinical studies are composite biomaterials. A PCL-HA with CaP scaffold was used to treat critical-sized segmental tibial bone defects in sheep. Interestingly, cell therapy was not applied together with the scaffold immediately after the defect creation. Instead, allogenic bone marrow stem cells were injected four weeks after the scaffold implantation in a post-inflammatory stage. This delayed cell injection significantly improved bone regeneration compared to scaffold-preseeded cell construct and scaffold-only groups [134]. In another study, a PLA-HA scaffold loaded with bone marrow-derived MSCs and induced membrane (IM), which provided growth factors, was used to regenerate large radial defects in rabbits. The results showed the best bone repair and reconstruction effect in the group treated with PLA-HA combined with IM and MSCs compared to PLA-HA alone or PLA-HA with IM [142].

The last two examples are based on the use of biological composites with progenitor cells. Yoon et al. investigated the osteogenetic effect of albumin scaffold derived from canine serum (ASA) and MSCs isolated from canine adipose tissue in segmental bone defects. The animals were treated with the ASA scaffold alone or with MSCs and the ASA scaffold including β -TCP with or without MSCs. Sixteen weeks after transplantation, the ASA scaffold with MSCs accelerated new bone formation significantly higher than the

other groups [135]. In another in vivo study, a coral scaffold with bone marrow-derived MSCs and a low dose of BMP-2 was injected into 25-mm-long metatarsal bone defects in the sheep model. The most successful results were observed for the group treated with the coral scaffold-MSCs and BMP-2 compared to scaffold-BMP-2 or scaffold-MSCs alone [137].

4. Clinical Trials

Preclinical animal studies have shown a beneficial effect of MSCs-scaffold treatment in orthopedic disorders [144]. However, when creating experimental preclinical models, researchers need to remember that various species differ biologically between one another, and the results of animal experiments often depend on the choice of the proper animal model [145]. Nevertheless, animal models are essential for the bench-to-bedside translation of new treatment methods. Preclinical data are reproducible and translatable into clinical use only if animal experiments are properly designed [146]. There are only few publications from the last ten years (from 2010 to 2020) reporting the results of clinical trials based on scaffolds and MSCs used to repair damaged bone tissue (data from www.clinicaltrials.gov and www.pubmed.ncbi.nlm.nih.gov). This is likely due to flawed preclinical research validation, which is crucial to bridge the translational gap to the clinic [146]. In this section, selected examples of human trials using scaffold/MSC constructs for bone regeneration are introduced (Table 2).

Table 2. MSC-based therapies with scaffolds for the repair of bone defects in clinical trials.

Study Number	Disease	Cells (Suspension)	Scaffold	Patients (Groups)	Results	References
Not reported	Osteonecrosis of the femoral head	BMMNCs (1×10^9 cells in 40 mL)	IP-CHA	30 patients: 8 patients treated with cell-free IP-CHA (control group) and 22 patients with IP-CHA + BMMNCs	29 weeks after surgery in the IP-CHA- and BMMNC-treated group, the osteonecrotic lesion decreased in size. In the control group, a severe collapse of the femoral head occurred in 6 patients.	[147]
Study #3096 Ethics Committee of the Heinrich Heine University Duesseldorf	Local bone defects larger than $1 \text{ cm} \times 1 \text{ cm}$	BMAC (8 mL)	Col or HA	39 patients: 12 patients treated with Col + BMAC and 27 patients with HA + BMAC	New bone formation was observed in all treated patients; however, it appeared earlier in the HA group (6.8 weeks) compared to Col (13.6 weeks).	[148]
Not reported	Critical size bone defects	IM as a complex cellular scaffold (rich source of MSCs)		8 patients	Cellular composition and molecular profile of IM-promoted large defect repair.	[149]
3766/2012 Comitato Etico Sperimentazione Farmaco CESF, Azienda Ospedaliero-Universitaria Pisana, Pisa, Italy	Upper limb atrophic pseudarthrosis	BM-MSCs (0.5×10^6 – 2.0×10^6 cells in 2 mL of autologous plasma)	Autologous fibrin clots	8 patients	In all patients, recovery of limb functions was observed.	[144]

Table 2. Cont.

Study Number	Disease	Cells (Suspension)	Scaffold	Patients (Groups)	Results	References
EudraCT number 2012-005599-33 EU Clinical Trials Register	Femoral defects	BM-MSCs ($15 \pm 4.5 \times 10^6$ cells in 1.5 mL)	β -TCP	18 patients: 9 patients treated with β -TCP alone (control group) and 9 patients with β -TCP + BM-MSCs	12 months after surgery, in all 9 patients treated with β -TCP and BM-MSCs, trabecular remodeling was detected, and in the control group, only in one patient.	[150]
ChiCTR-ONC-17011448 Chinese Clinical Trial Registry	Non-unions and others	BM-MSCs	β -TCP	42 patients	In all patients, radiography showed full bone healing after 9 months.	[151]
2017-385-T282 Shanghai Jiao Tong University Affiliated Ninth People's Hospital Medical Ethics Committee	Depressed tibial plateaus fractures	BM-MSCs	β -TCP	39 patients: 23 patients treated only with β -TCP (control group) and 16 patients with β -TCP + BM-MSCs	Excellent or good recovery was observed 2 years post transplantation in 15 of 16 patients treated with MSCs/ β -TCP and in 14 of 23 treated with β -TCP alone.	[152]
EC2012/047 Royal Perth Hospital Ethics Committee	Cranial defects	BM-MSCs (min. 0.5×10^6 cells per mL of scaffold granules)	β -TCP	3 patients	Between 3 and 6 months post transplantation, good cranial contour restoration was maintained in all three patients. However, between 6 and 12 months, there was evidence of construct resorption.	[153]
EudraCT, 2012-003139-50 EU Clinical Trials Register	Severely atrophied mandibular bone	BM-MSCs (20×10^6 cells/ 1 cm^3 of scaffold)	BCP	11 patients	In all patients, successful ridge augmentation and new bone formation of a dental implant were observed.	[154]
EudraCT, 2011-005441-13 EU Clinical Trials Register	Long bone delayed and non-unions	BM-MSCs	BCP	28 patients	3 months after surgery, radiological consolidation amounted to 25.0% (7/28 cases), after 6 months, 67.8% (19/28 cases), and after 12 months, 92.8% (26/28 cases).	[155]

Abbreviations: BCP—biphasic calcium phosphate, BMAC—bone marrow aspiration concentrate, BMMNCs—bone-marrow-derived mononuclear cells, BM-MSCs—bone marrow derived mesenchymal stem cells, Col—collagen sponge, HA—hydroxyapatite, IM—induced membrane, IP-CHA—interconnected porous calcium hydroxyapatite, β -TCP— β -tricalcium phosphate.

The first example of a clinical study was conducted by Yamasaki et al. They have examined the transplantation effectiveness of interconnected porous calcium hydroxyapatite (IP-CHA) and bone marrow-derived mononuclear cells (BMMNCs) on early bone repair

in femoral head osteonecrosis. Twenty-two patients (30 hips) with a mean age of 41 years (18 to 64) were studied. The control group consisted of eight patients (nine hips), who received a cell-free IP-CHA implantation. After a mean follow-up of 29 months (19 to 48), the size of the osteonecrotic lesion decreased in the IP-CHA- and BMMNCs-treated group, whereas subtle bone hypertrophy and a severe collapse of the femoral head was observed in the control group [147].

Jäger et al. investigated the augment bone grafting potency of a commercially available collagen sponge (Col) (Orthoss[®], Fa Geistlich, Wolhusen, Switzerland) or bovine hydroxyapatite (HA) (Gelaspon[®], Fa. Chauvin Ankerpharm GmbH, Berlin, Germany) with 8 mL of bone marrow aspiration concentrate (BMAC). All 39 patients between the ages of 4 and 87 years with local bone defects larger than 1 cm × 1 cm (length × width) showed new bone formation during follow-up. However, bone formation appeared earlier in the HA group (6.8 weeks), and complete bone healing was achieved after 17.3 weeks, in contrast to the Col group (13.6 weeks) with bone healing completed after 22.4 weeks [148].

Cuthbert et al. used induced membrane, which was a rich source of MSCs, to treat eight patients with critical-sized bone defects (mean size 36.25 mm) and a mean age of 60 years (between 18 and 80). They compared 1-cm² biopsy samples after membrane formation and healthy diaphyseal periosteum. The IM had a cellular composition and molecular profile resembling periosteum, which facilitated the repair of the large bone defects [149].

Another study investigated the long-term efficacy and safety of BM-MSCs expanded ex vivo with autologous fibrin clots for the treatment of upper limb atrophic pseudarthrosis. Eight patients with a mean age of 44 years (between 18 and 73), who had undergone at least one unsatisfactory surgical intervention, were selected for the implantation of an autologous MSC/fibrin scaffold construct. The study relied on: use of cells, serum for ex vivo cell culture and scaffold components (an entirely autologous context); reduced cell expansion ex vivo; and short-term osteoinduction of MSCs before implantation. On the day of the surgery, 0.5×10^6 – 2.0×10^6 MSCs were resuspended in 2 mL of autologous plasma and implanted with a fibrin clot at the site of the lesion. After short- and long-term follow-ups (mean: 6.7 and 76.0 months, respectively), healing was evaluated radiographically. In all cases, positive clinical outcomes were shown with recovered limb function. The study demonstrated that the minimal MSC expansion ex vivo and short-term osteoinduction reduced the risk of an uncontrolled proliferation of the transplanted cells and, consequently, the implant overgrowth [144].

Sponer et al. compared the healing efficacy of femoral defects following the implantation of ultraporous β -tricalcium phosphate alone (nine patients, control group) or β -tricalcium phosphate with expanded $15 \pm 4.5 \times 10^6$ autologous bone marrow-derived MSCs (9 patients, trial group). Radiography and DEXA (bone density) scanning were performed 6 weeks and 3, 6, and 12 months post operation. In all nine patients of the trial group, trabecular remodeling was found, whereas in the control group, only in one patient [150].

The another example of a clinical study is registered in the Chinese Clinical Trial Registry and was executed from June 2013 to October 2016. Forty-two patients requiring bone graft received SECCS-based treatment. SECCS is a stem cell screen–enrich–combine (-biomaterials) circulating system, designed by Zhuang and his colleagues. This innovative system can process patients' bone marrow cells and beta-tricalcium phosphate (β -TCP) granules to produce MSC/ β -TCP composites in 10–15 min. patients with a bone defect aged between 15 and 65 years were treated surgically with MSC/ β -TCP composites. The full bone healing, including bone union observed in lateral and anterior–posterior radiography within nine months, was successful in all patients. The mean healing time for nonunion, fresh fracture, and other patients was 6.29, 3.12, and 4.72 months, respectively. The results showed that SECCS, which peri-operatively produces a bioactive composite of MSCs and β -TCP without in vitro culture, may represent a low cost and safe method for bone repair [151].

The same team evaluated the clinical efficacy of MSC/ β -TCP prepared with the SECCS in 39 patients suffering from depressed tibial plateau fractures. Sixteen patients were treated with MSC/ β -TCP composites, whereas another 23 patients only with β -TCP. Eighteen months post MSC/ β -TCP transplantation, new bone formation rate was significantly higher than in the patients treated only with β -TCP. The average new bone ratio in the first group was $91.9 \pm 4.8\%$, and in the β -TCP-treated group, it was $21.9 \pm 12.2\%$ ($W = 231.0$; $p < 0.01$). Two years post implantation, MRI analysis revealed that the grafted composite had been replaced by new well-integrated autologous bone. The Lysholm score assessed the functional recovery of the patients. After two years post implantation, 15 of 16 patients treated with MSC/ β -TCP (93.8%) and 14 of 23 patients treated with β -TCP alone (60.9%, $p = 0.028$) achieved excellent or good recovery. The MSC/ β -TCP composite produced using the SECCS method was effective in the treatment of depressed tibial plateau fractures, promoting osteogenesis and improving joint recovery [152].

Another clinical study, conducted in Australia, involved cranial reconstruction using allogeneic mesenchymal stromal cells. MSCs were seeded on a ceramic carrier and a polymer scaffold to design a tissue-engineered construct. Three patients with cranial defects less than 80 mm in diameter underwent a baseline fine-slice CT to virtually reconstruct the bone defect and create a virtual 3D skull model. Then, a 3D printing method was used to produce the reconstructed surfaces of the defect, consisting of two polymer meshes corresponding to the skull interna and externa. The MSCs were isolated from the bone marrow of healthy donors aged between 18 and 40 years. The operation procedure was as follows. Firstly, the inner polymer mesh was placed, then the MSC-loaded granules, and finally, the outer mesh. The patients were followed up on 3, 6, and 12 months after surgery for visual cosmesis inspection. All patients displayed excellent initial cosmesis without any complications. Post-operative CT scans were conducted on day 1 and 3 and after 12 months to assess bone formation. Analysis of CT data showed good cranial contour restoration, which was maintained between 3 and 6 months post transplantation. However, there was evidence of construct resorption in all patients between 6 and 12 months. The continuously pulsating environment likely caused the lack of construct rigidity and therefore prevented solid bone formation. Nevertheless, a customized allogeneic MSC-bone engineering construct for cranial reconstruction can be produced using computer modeling and tissue engineering. It is crucial to investigate constructs with appropriate rigidity to reconstruct bone defects, which can be achieved using 3D printing [153].

There are also studies evaluating bone formation using MSC-scaffold composites in oral and maxillofacial bone defects. Gjerde et al. from the University of Bergen conducted a clinical trial on 11 patients aged between 52 and 79 years with severe mandibular ridge resorption. The patients were treated with bone marrow-derived MSCs loaded on biphasic calcium phosphate (BCP) granules, implanted in the area of the resorbed alveolar ridge. New bone formation was assessed 4–6 months after healing. X-ray analysis showed a significant total bone volume increase. During implant installation in the newly regenerated area, bone was biopsied for μ -CT and histology to evaluate the formation of mineralized tissues. Successful ridge augmentation and new bone formation adequate for the installation of a dental implant were observed in all patients. During the first 12 months after the dental implant installation, Osstell values (measuring implant stability) increased for all study participants. This clinical trial showed that MSC- and BPC-based treatment of the alveolar ridge is safe, feasible, predictable, and could be considered as a less invasive approach to the reconstruction of maxillofacial bone defects than the current gold standard, which is autologous bone grafting [154].

The last example presents an early efficacy of the long bone delayed and non-union treatment with autologous bone marrow-derived MSCs and scaffold composed of 80% β -TCP and 20% HA. Twenty-eight participants, mean age 39 ± 13 years, with tibial (13 patients), femoral (11), and humeral (4) non-unions that occurred at a mean 27.9 ± 31.2 months prior recruitment, underwent surgical implantation. Bone healing efficacy was reported with clinical and radiological consolidation 3, 6, and 12 months after surgery and CT

sections imaging 3 and 6 months after surgery. Moreover, in two cases, bone biopsies were performed during screw removal. Clinical consolidation results using the visual analogue scale (VAS) were as follows: 3 months, 24/28 patients (85.7%); 6 months, 24/27 (88.9%); and 12 months, 25/25, after completed follow-up. Radiological healing rate was 25% (7/28 patients) after 3 months, 67.8% (19/28) after 6 months, and 92.8% (26/28) after 12 months. Bone formation surrounding the bioceramic scaffold was confirmed with bone biopsies after 8 months [155].

5. Conclusions

Bone tissue engineering constructs based on a biomaterial scaffold and MSCs are undoubtedly a promising alternative to standard bone graft. Although MSCs are known to play a crucial role in bone repair process, there are still some factors and pathways to be fully understand and optimized. Mesenchymal stem cells participate in bone regeneration not only through direct differentiation into osteogenic progenitors, but also through paracrine activity by secreting a variety of cytokines and growth factors. Bioactive factors secreted by MSCs exert an anti-inflammatory and immunomodulatory effect on effector immune cells and modulate the microenvironment of the injured tissue.

Clinical use of an MSC-scaffold construct requires standardized MSC sources, osteogenic signaling factors, as well as scaffold design. MSCs isolated from different tissues are not universal, and for the purposes of bone repair, should be selected based on their osteogenic potential (e.g., BM-MSCs or UC-MSCs). MSCs alone are unable to cover large bone defects. However, modern technologies, such as biomaterials and 3D printing scaffolds with a proper structure employed in bone substitute engineering can support the osteoinductive properties of the applied MSCs. Innovative biomaterials used in tissue engineering for bone regeneration should be biocompatible and biodegradable and should fulfil specific biological properties to allow MSC adhesion, proliferation, and osteogenic differentiation in the injured bone area. It is also necessary to develop an appropriate preclinical animal model to assess the best therapeutic approach. Small animal models are useful for investigating the bone-related mechanism of healing. However, only large animal models are absolutely essential to mimic human clinical settings. Successful preclinical results enable the final step of bone tissue engineering development and application in clinical trials.

Author Contributions: Conceptualization, A.K. and S.S.; writing—original draft preparation, S.S.; writing—review and editing, A.K.; visualization, A.K. and S.S.; supervision, A.K. Both authors have read and agreed to the published version of the manuscript.

Funding: This research received no external funding.

Institutional Review Board Statement: Not applicable.

Informed Consent Statement: Not applicable.

Data Availability Statement: Not applicable.

Conflicts of Interest: The authors declare no conflict of interest.

References

1. Chen, X.; Fan, H.; Deng, X.; Wu, L.; Yi, T.; Gu, L.; Zhou, C.; Fan, Y.; Zhang, X. Scaffold Structural Microenvironmental Cues to Guide Tissue Regeneration in Bone Tissue Applications. *Nanomaterial* **2018**, *8*, 960. [[CrossRef](#)] [[PubMed](#)]
2. Winkler, T.; Sass, F.A.; Duda, G.N.; Schmidt-Bleek, K. A review of biomaterials in bone defect healing, remaining shortcomings and future opportunities for bone tissue engineering: The unsolved challenge. *Bone Jt. Res.* **2018**, *7*, 232–243. [[CrossRef](#)] [[PubMed](#)]
3. Perez, J.R.; Kouroupis, D.; Li, D.J.; Best, T.M.; Kaplan, L.; Correa, D. Tissue Engineering and Cell-Based Therapies for Fractures and Bone Defects. *Front. Bioeng. Biotechnol.* **2018**, *6*, 105. [[CrossRef](#)]
4. Nielsen, J.J.; Low, S.A. Bone-Targeting Systems to Systemically Deliver Therapeutics to Bone Fractures for Accelerated Healing. *Curr. Osteoporos. Rep.* **2020**, *18*, 449–459. [[CrossRef](#)]
5. Chen, Y.; Xu, J.; Huang, Z.; Yu, M.; Zhang, Y.; Chen, H.; Ma, Z.; Liao, H.; Hu, J. An Innovative Approach for Enhancing Bone Defect Healing Using PLGA Scaffolds Seeded with Extracorporeal-shock-wave-treated Bone Marrow Mesenchymal Stem Cells (BMSCs). *Sci. Rep.* **2017**, *7*, 44130. [[CrossRef](#)] [[PubMed](#)]

6. Su, P.; Tian, Y.; Yang, C.; Ma, X.; Wang, X.; Pei, J.; Qian, A. Mesenchymal Stem Cell Migration during Bone Formation and Bone Diseases Therapy. *Int. J. Mol. Sci.* **2018**, *19*, 2343. [[CrossRef](#)] [[PubMed](#)]
7. Breeland, G.; Sinkler, M.A.; Menezes, R.G. *Embryology, Bone Ossification*; StatPearls: Treasure Island, FL, USA, 2020.
8. White, A.; Wallis, G. Endochondral ossification: A delicate balance between growth and mineralisation. *Curr. Biol.* **2001**, *11*, R589–R591. [[CrossRef](#)]
9. Pountos, I.; Giannoudis, P.V. Fracture Healing: Back to Basics and Latest Advances. In *Fracture Reduction and Fixation Techniques: Upper Extremities*; Giannoudis, P.V., Ed.; Springer International Publishing: Cham, Switzerland, 2018; pp. 3–17.
10. Iaquina, M.R.; Mazzoni, E.; Bononi, I.; Rotondo, J.C.; Mazziotta, C.; Montesi, M.; Sprio, S.; Tampieri, A.; Tognon, M.; Martini, F. Adult Stem Cells for Bone Regeneration and Repair. *Front. Cell Dev. Biol.* **2019**, *7*, 268. [[CrossRef](#)]
11. Schell, H.; Duda, G.N.; Peters, A.; Tsitsilonis, S.; Johnson, K.A.; Schmidt-Bleek, K. The haematoma and its role in bone healing. *J. Exp. Orthop.* **2017**, *4*, 5. [[CrossRef](#)] [[PubMed](#)]
12. Walmsley, G.G.; Ransom, R.C.; Zielins, E.R.; Leavitt, T.; Flacco, J.S.; Hu, M.S.; Lee, A.S.; Longaker, M.T.; Wan, D.C. Stem Cells in Bone Regeneration. *Stem Cell Rev. Rep.* **2016**, *12*, 524–529. [[CrossRef](#)]
13. Sheen, J.R.; Garla, V.V. *Fracture Healing Overview*; StatPearls: Treasure Island, FL, USA, 2020.
14. Friedenstein, A.J.; Piatetzky, S., II; Petrakova, K.V. Osteogenesis in transplants of bone marrow cells. *J. Embryol. Exp. Morphol.* **1966**, *16*, 381–390. [[PubMed](#)]
15. Caplan, A.I. Mesenchymal stem cells. *J. Orthop. Res.* **1991**, *9*, 641–650. [[CrossRef](#)] [[PubMed](#)]
16. Pittenger, M.F.; Discher, D.E.; Péault, B.M.; Phinney, D.G.; Hare, J.M.; Caplan, A.I. Mesenchymal stem cell perspective: Cell biology to clinical progress. *NPJ Regen. Med.* **2019**, *4*, 22. [[CrossRef](#)]
17. Knight, M.N.; Hankenson, K.D. Mesenchymal Stem Cells in Bone Regeneration. *Adv. Wound Care* **2013**, *2*, 306–316. [[CrossRef](#)]
18. Logeart-Avramoglou, D.; Anagnostou, F.; Bizios, R.; Petite, H. Engineering bone: Challenges and obstacles. *J. Cell. Mol. Med.* **2005**, *9*, 72–84. [[CrossRef](#)] [[PubMed](#)]
19. Viateau, V.; Logeart-Avramoglou, D.; Guillemain, G.; Petite, H. Animal Models for Bone Tissue Engineering Purposes. In *Sourcebook of Models for Biomedical Research*; Conn, P.M., Ed.; Humana Press: Totowa, NJ, USA, 2008; pp. 725–736.
20. Safarova, Y.; Umbayev, B.; Hortelano, G.; Askarova, S. Mesenchymal stem cells modifications for enhanced bone targeting and bone regeneration. *Regen. Med.* **2020**, *15*, 1579–1594. [[CrossRef](#)]
21. Klimczak, A.; Kozłowska, U. Mesenchymal Stromal Cells and Tissue-Specific Progenitor Cells: Their Role in Tissue Homeostasis. *Stem Cells Int.* **2016**, *2016*, 4285215. [[CrossRef](#)]
22. Kozłowska, U.; Krawczenko, A.; Futoma, K.; Jurek, T.; Rorat, M.; Patrzalek, D.; Klimczak, A. Similarities and differences between mesenchymal stem/progenitor cells derived from various human tissues. *World J. Stem Cells* **2019**, *11*, 347–374. [[CrossRef](#)] [[PubMed](#)]
23. Amati, E.; Perbellini, O.; Rotta, G.; Bernardi, M.; Chieragato, K.; Sella, S.; Rodeghiero, F.; Ruggeri, M.; Astori, G. High-throughput immunophenotypic characterization of bone marrow- and cord blood-derived mesenchymal stromal cells reveals common and differentially expressed markers: Identification of angiotensin-converting enzyme (CD143) as a marker differentially expressed between adult and perinatal tissue sources. *Stem Cell Res. Ther.* **2018**, *9*, 10. [[PubMed](#)]
24. Dominici, M.; Le Blanc, K.; Mueller, I.; Slaper-Cortenbach, I.; Marini, F.; Krause, D.; Deans, R.; Keating, A.; Prockop, D.; Horwitz, E. Minimal criteria for defining multipotent mesenchymal stromal cells. The International Society for Cellular Therapy position statement. *Cytotherapy* **2006**, *8*, 315–317. [[CrossRef](#)] [[PubMed](#)]
25. Jin, H.J.; Bae, Y.K.; Kim, M.; Kwon, S.J.; Jeon, H.B.; Choi, S.J.; Kim, S.W.; Yang, Y.S.; Oh, W.; Chang, J.W. Comparative analysis of human mesenchymal stem cells from bone marrow, adipose tissue, and umbilical cord blood as sources of cell therapy. *Int. J. Mol. Sci.* **2013**, *14*, 17986–18001. [[CrossRef](#)]
26. Rasini, V.; Dominici, M.; Kluba, T.; Siegel, G.; Lusenti, G.; Northoff, H.; Horwitz, E.M.; Schäfer, R. Mesenchymal stromal/stem cells markers in the human bone marrow. *Cytotherapy* **2013**, *15*, 292–306. [[CrossRef](#)] [[PubMed](#)]
27. Harkness, L.; Zaher, W.; Ditzel, N.; Isa, A.; Kassem, M. CD146/MCAM defines functionality of human bone marrow stromal stem cell populations. *Stem Cell Res. Ther.* **2016**, *7*, 4. [[CrossRef](#)]
28. Bourin, P.; Bunnell, B.A.; Casteilla, L.; Dominici, M.; Katz, A.J.; March, K.L.; Redl, H.; Rubin, J.P.; Yoshimura, K.; Gimble, J.M. Stromal cells from the adipose tissue-derived stromal vascular fraction and culture expanded adipose tissue-derived stromal/stem cells: A joint statement of the International Federation for Adipose Therapeutics and Science (IFATS) and the International Society for Cellular Therapy (ISCT). *Cytotherapy* **2013**, *15*, 641–648.
29. Topoluk, N.; Hawkins, R.; Tokish, J.; Mercuri, J. Amniotic Mesenchymal Stromal Cells Exhibit Preferential Osteogenic and Chondrogenic Differentiation and Enhanced Matrix Production Compared With Adipose Mesenchymal Stromal Cells. *Am. J. Sports Med.* **2017**, *45*, 2637–2646. [[CrossRef](#)] [[PubMed](#)]
30. Shen, C.; Yang, C.; Xu, S.; Zhao, H. Comparison of osteogenic differentiation capacity in mesenchymal stem cells derived from human amniotic membrane (AM), umbilical cord (UC), chorionic membrane (CM), and decidua (DC). *Cell Biosci.* **2019**, *9*, 17. [[CrossRef](#)] [[PubMed](#)]
31. Murphy, M.B.; Moncivais, K.; Caplan, A.I. Mesenchymal stem cells: Environmentally responsive therapeutics for regenerative medicine. *Exp. Mol. Med.* **2013**, *45*, e54. [[CrossRef](#)]

32. Kraskiewicz, H.; Paprocka, M.; Bielawska-Pohl, A.; Krawczenko, A.; Panek, K.; Kaczyńska, J.; Szyposzyńska, A.; Psurski, M.; Kuroпка, P.; Klimczak, A. Can supernatant from immortalized adipose tissue MSC replace cell therapy? An in vitro study in chronic wounds model. *Stem Cell Res.* **2020**, *11*, 29. [[CrossRef](#)]
33. Krawczenko, A.; Bielawska-Pohl, A.; Paprocka, M.; Kraskiewicz, H.; Szyposzynska, A.; Wojdat, E.; Klimczak, A. Microvesicles from Human Immortalized Cell Lines of Endothelial Progenitor Cells and Mesenchymal Stem/Stromal Cells of Adipose Tissue Origin as Carriers of Bioactive Factors Facilitating Angiogenesis. *Stem Cells Int.* **2020**, *2020*, 1289380. [[CrossRef](#)]
34. Ratushnyy, A.; Ezdakova, M.; Yakubets, D.; Buravkova, L. Angiogenic Activity of Human Adipose-Derived Mesenchymal Stem Cells Under Simulated Microgravity. *Stem Cells Dev.* **2018**, *27*, 831–837. [[CrossRef](#)]
35. Pevsner-Fischer, M.; Levin, S.; Zipori, D. The origins of mesenchymal stromal cell heterogeneity. *Stem Cell Rev. Rep.* **2011**, *7*, 560–568. [[CrossRef](#)] [[PubMed](#)]
36. Kolf, C.M.; Cho, E.; Tuan, R.S. Mesenchymal stromal cells. Biology of adult mesenchymal stem cells: Regulation of niche, self-renewal and differentiation. *Arthritis Res.* **2007**, *9*, 204. [[CrossRef](#)] [[PubMed](#)]
37. Klingemann, H.; Matzilevich, D.; Marchand, J. Mesenchymal Stem Cells—Sources and Clinical Applications. *Transfus. Med. Hemother.* **2008**, *35*, 272–277. [[CrossRef](#)] [[PubMed](#)]
38. Strioga, M.; Viswanathan, S.; Darinskas, A.; Slaby, O.; Michalek, J. Same or not the same? Comparison of adipose tissue-derived versus bone marrow-derived mesenchymal stem and stromal cells. *Stem Cells Dev.* **2012**, *21*, 2724–2752. [[CrossRef](#)] [[PubMed](#)]
39. Musial-Wysocka, A.; Kot, M.; Majka, M. The Pros and Cons of Mesenchymal Stem Cell-Based Therapies. *Cell Transpl.* **2019**, *28*, 801–812. [[CrossRef](#)]
40. Richardson, S.M.; Kalamegam, G.; Pushparaj, P.N.; Matta, C.; Memic, A.; Khademhosseini, A.; Mobasheri, R.; Poletti, F.L.; Hoyland, J.A.; Mobasheri, A. Mesenchymal stem cells in regenerative medicine: Focus on articular cartilage and intervertebral disc regeneration. *Methods* **2016**, *99*, 69–80. [[CrossRef](#)]
41. Marolt Presen, D.; Traweger, A.; Gimona, M.; Redl, H. Mesenchymal Stromal Cell-Based Bone Regeneration Therapies: From Cell Transplantation and Tissue Engineering to Therapeutic Secretomes and Extracellular Vesicles. *Front. Bioeng. Biotechnol.* **2019**, *7*, 352. [[CrossRef](#)]
42. Labeledz-Maslowska, A.; Bryniarska, N.; Kubiak, A.; Kaczmarzyk, T.; Sekula-Stryjewska, M.; Noga, S.; Boruczkowski, D.; Madeja, Z.; Zuba-Surma, E. Multilineage Differentiation Potential of Human Dental Pulp Stem Cells-Impact of 3D and Hypoxic Environment on Osteogenesis In Vitro. *Int. J. Mol. Sci.* **2020**, *21*, 6172. [[CrossRef](#)]
43. Toyserkani, N.M.; Jørgensen, M.G.; Tabatabaeifar, S.; Jensen, C.H.; Sheikh, S.P.; Sørensen, J.A. Concise Review: A Safety Assessment of Adipose-Derived Cell Therapy in Clinical Trials: A Systematic Review of Reported Adverse Events. *Stem Cells Transl. Med.* **2017**, *6*, 1786–1794. [[CrossRef](#)]
44. Mäkelä, T.; Takalo, R.; Arvola, O.; Haapanen, H.; Yannopoulos, F.; Blanco, R.; Ahvenjärvi, L.; Kiviluoma, K.; Kerkelä, E.; Nystedt, J.; et al. Safety and biodistribution study of bone marrow-derived mesenchymal stromal cells and mononuclear cells and the impact of the administration route in an intact porcine model. *Cytotherapy* **2015**, *17*, 392–402. [[CrossRef](#)]
45. Lutton, B.V.; Cho, P.S.; Hirsh, E.L.; Ferguson, K.K.; Teague, A.G.; Hanekamp, J.S.; Chi, N.; Goldman, S.N.; Messina, D.J.; Houser, S.; et al. Approaches to avoid immune responses induced by repeated subcutaneous injections of allogeneic umbilical cord tissue-derived cells. *Transplantation* **2010**, *90*, 494–501. [[CrossRef](#)]
46. Rather, H.A.; Jhala, D.; Vasita, R. Dual functional approaches for osteogenesis coupled angiogenesis in bone tissue engineering. *Mater. Sci. Eng. C* **2019**, *103*, 109761. [[CrossRef](#)] [[PubMed](#)]
47. Gerstenfeld, L.C.; Edgar, C.M.; Kakar, S.; Jacobsen, K.A.; Einhorn, T.A. Osteogenic growth factors and cytokines and their role in bone repair. In *Engineering of Functional Skeletal Tissues*; Springer: Cham, Switzerland, 2007; pp. 17–45.
48. Amarasekara, D.S.; Kim, S.; Rho, J. Regulation of Osteoblast Differentiation by Cytokine Networks. *Int. J. Mol. Sci.* **2021**, *22*, 2851. [[CrossRef](#)] [[PubMed](#)]
49. Lee, S.; Remark, L.H.; Josephson, A.M.; Leclerc, K.; Lopez, E.M.; Kirby, D.J.; Mehta, D.; Litwa, H.P.; Wong, M.Z.; Shin, S.Y.; et al. Notch-Wnt signal crosstalk regulates proliferation and differentiation of osteoprogenitor cells during intramembranous bone healing. *NPJ Regen. Med.* **2021**, *6*, 29. [[CrossRef](#)] [[PubMed](#)]
50. Wozney, J.M. The bone morphogenetic protein family and osteogenesis. *Mol. Reprod. Dev.* **1992**, *32*, 160–167. [[CrossRef](#)]
51. Zhang, J.; Li, L. BMP signaling and stem cell regulation. *Dev. Biol.* **2005**, *284*, 1–11. [[CrossRef](#)]
52. Urist, M.R. Bone: Formation by autoinduction. *Science* **1965**, *150*, 893–899. [[CrossRef](#)]
53. Beederman, M.; Lamplot, J.D.; Nan, G.; Wang, J.; Liu, X.; Yin, L.; Li, R.; Shui, W.; Zhang, H.; Kim, S.H.; et al. BMP signaling in mesenchymal stem cell differentiation and bone formation. *J. Biomed. Sci. Eng.* **2013**, *6*, 32–52. [[CrossRef](#)]
54. Karsenty, G. The genetic transformation of bone biology. *Genes Dev.* **1999**, *13*, 3037–3051. [[CrossRef](#)]
55. Marupanthorn, K.; Tantrawatpan, C.; Kheolamai, P.; Tantikanlayaporn, D.; Manochantr, S. Bone morphogenetic protein-2 enhances the osteogenic differentiation capacity of mesenchymal stromal cells derived from human bone marrow and umbilical cord. *Int. J. Mol. Med.* **2017**, *39*, 654–662. [[CrossRef](#)]
56. Gromolak, S.; Krawczenko, A.; Antonczyk, A.; Buczak, K.; Kielbowicz, Z.; Klimczak, A. Biological Characteristics and Osteogenic Differentiation of Ovine Bone Marrow Derived Mesenchymal Stem Cells Stimulated with FGF-2 and BMP-2. *Int. J. Mol. Sci.* **2020**, *21*, 9726. [[CrossRef](#)]
57. Chen, G.; Deng, C.; Li, Y.P. TGF-beta and BMP signaling in osteoblast differentiation and bone formation. *Int. J. Biol. Sci.* **2012**, *8*, 272–288. [[CrossRef](#)] [[PubMed](#)]

58. Ornitz, D.M.; Marie, P.J. Fibroblast growth factor signaling in skeletal development and disease. *Genes Dev.* **2015**, *29*, 1463–1486. [[CrossRef](#)] [[PubMed](#)]
59. Charoenlarp, P.; Rajendran, A.K.; Iseki, S. Role of fibroblast growth factors in bone regeneration. *Inflamm. Regen.* **2017**, *37*, 10. [[CrossRef](#)] [[PubMed](#)]
60. Kuhn, L.T.; Ou, G.; Charles, L.; Hurley, M.M.; Rodner, C.M.; Gronowicz, G. Fibroblast growth factor-2 and bone morphogenetic protein-2 have a synergistic stimulatory effect on bone formation in cell cultures from elderly mouse and human bone. *J. Gerontol. A Biol. Sci. Med. Sci.* **2013**, *68*, 1170–1180. [[CrossRef](#)]
61. Song, R.; Wang, D.; Zeng, R.; Wang, J. Synergistic effects of fibroblast growth factor-2 and bone morphogenetic protein-2 on bone induction. *Mol. Med. Rep.* **2017**, *16*, 4483–4492. [[CrossRef](#)]
62. Derynck, R.; Akhurst, R.J. Differentiation plasticity regulated by TGF-beta family proteins in development and disease. *Nat. Cell Biol.* **2007**, *9*, 1000–1004. [[CrossRef](#)]
63. Sasaki, T.; Ito, Y.; Bringas, P., Jr.; Chou, S.; Urata, M.M.; Slavkin, H.; Chai, Y. TGFbeta-mediated FGF signaling is crucial for regulating cranial neural crest cell proliferation during frontal bone development. *Development* **2006**, *133*, 371–381. [[CrossRef](#)]
64. Barati, D.; Shariati, S.R.P.; Moeinzadeh, S.; Melero-Martin, J.M.; Khademhosseini, A.; Jabbari, E. Spatiotemporal release of BMP-2 and VEGF enhances osteogenic and vasculogenic differentiation of human mesenchymal stem cells and endothelial colony-forming cells co-encapsulated in a patterned hydrogel. *J. Control. Release* **2016**, *223*, 126–136. [[CrossRef](#)]
65. Bao, X.; Zhu, L.; Huang, X.; Tang, D.; He, D.; Shi, J.; Xu, G. 3D biomimetic artificial bone scaffolds with dual-cytokines spatiotemporal delivery for large weight-bearing bone defect repair. *Sci. Rep.* **2017**, *7*, 7814. [[CrossRef](#)]
66. Regard, J.B.; Zhong, Z.; Williams, B.O.; Yang, Y. Wnt signaling in bone development and disease: Making stronger bone with Wnts. *Cold Spring Harb. Perspect. Biol.* **2012**, *4*, a007997. [[CrossRef](#)]
67. Hojo, H.; Ohba, S.; Chung, U.I. Signaling pathways regulating the specification and differentiation of the osteoblast lineage. *Regen. Ther.* **2015**, *1*, 57–62. [[CrossRef](#)]
68. Gordon, M.D.; Nusse, R. Wnt signaling: Multiple pathways, multiple receptors, and multiple transcription factors. *J. Biol. Chem.* **2006**, *281*, 22429–22433. [[CrossRef](#)] [[PubMed](#)]
69. Schlickewei, C.W.; Kleinertz, H.; Thiesen, D.M.; Mader, K.; Priemel, M.; Frosch, K.-H.; Keller, J. Current and Future Concepts for the Treatment of Impaired Fracture Healing. *Int. J. Mol. Sci.* **2019**, *20*, 5805. [[CrossRef](#)] [[PubMed](#)]
70. Latres, E.; Chiaur, D.S.; Pagano, M. The human F box protein beta-Trcp associates with the Cul1/Skp1 complex and regulates the stability of beta-catenin. *Oncogene* **1999**, *18*, 849–854. [[CrossRef](#)]
71. Yan, Y.; Tang, D.; Chen, M.; Huang, J.; Xie, R.; Jonason, J.H.; Tan, X.; Hou, W.; Reynolds, D.; Hsu, W.; et al. Axin2 controls bone remodeling through the beta-catenin-BMP signaling pathway in adult mice. *J. Cell Sci.* **2009**, *122*(Pt. 19), 3566–3578. [[CrossRef](#)]
72. De, A. Wnt/Ca2+ signaling pathway: A brief overview. *Acta Biochim. Biophys. Sin.* **2011**, *43*, 745–756. [[CrossRef](#)]
73. Baksh, D.; Tuan, R.S. Canonical and non-canonical Wnts differentially affect the development potential of primary isolate of human bone marrow mesenchymal stem cells. *J. Cell. Physiol.* **2007**, *212*, 817–826. [[CrossRef](#)] [[PubMed](#)]
74. Luo, Z.; Shang, X.; Zhang, H.; Wang, G.; Massey, P.A.; Barton, S.R.; Kevil, C.G.; Dong, Y. Notch Signaling in Osteogenesis, Osteoclastogenesis, and Angiogenesis. *Am. J. Pathol.* **2019**, *189*, 1495–1500. [[CrossRef](#)] [[PubMed](#)]
75. Majidinia, M.; Alizadeh, E.; Yousefi, B.; Akbarzadeh, M.; Zarghami, N. Downregulation of Notch Signaling Pathway as an Effective Chemosensitizer for Cancer Treatment. *Drug Res.* **2016**, *66*, 571–579. [[CrossRef](#)] [[PubMed](#)]
76. Tu, X.; Chen, J.; Lim, J.; Karner, C.M.; Lee, S.Y.; Heisig, J.; Wiese, C.; Surendran, K.; Kopan, R.; Gessler, M.; et al. Physiological notch signaling maintains bone homeostasis via RBPjk and Hey upstream of NFATc1. *PLoS Genet.* **2012**, *8*, e1002577. [[CrossRef](#)] [[PubMed](#)]
77. Zhu, F.; Sweetwyne, M.T.; Hankenson, K.D. PKCdelta is required for Jagged-1 induction of human mesenchymal stem cell osteogenic differentiation. *Stem Cells* **2013**, *31*, 1181–1192. [[CrossRef](#)] [[PubMed](#)]
78. Cao, J.; Wei, Y.; Lian, J.; Yang, L.; Zhang, X.; Xie, J.; Liu, Q.; Luo, J.; He, B.; Tang, M. Notch signaling pathway promotes osteogenic differentiation of mesenchymal stem cells by enhancing BMP9/Smad signaling. *Int. J. Mol. Med.* **2017**, *40*, 378–388. [[CrossRef](#)] [[PubMed](#)]
79. Bhattarai, H.K.; Shrestha, S.; Rokka, K.; Shakya, R. Vitamin D, Calcium, Parathyroid Hormone, and Sex Steroids in Bone Health and Effects of Aging. *J. Osteoporos.* **2020**, *2020*, 9324505. [[CrossRef](#)]
80. Zhang, R.; Edwards, J.R.; Ko, S.Y.; Dong, S.; Liu, H.; Oyajobi, B.O.; Papiasian, C.; Deng, H.W.; Zhao, M. Transcriptional regulation of BMP2 expression by the PTH-CREB signaling pathway in osteoblasts. *PLoS ONE* **2011**, *6*, e20780. [[CrossRef](#)]
81. Xiao, L.; Fei, Y.; Hurley, M.M. FGF2 crosstalk with Wnt signaling in mediating the anabolic action of PTH on bone formation. *Bone Rep.* **2018**, *9*, 136–144. [[CrossRef](#)]
82. Luo, M.; Huang, H.X.; Huang, H.; Li, Z.T.; Lai, Y.Y. Hedgehog signaling pathway and osteoporosis. *Zhongguo Gu Shang* **2014**, *27*, 169–172.
83. Lv, W.T.; Du, D.H.; Gao, R.J.; Yu, C.W.; Jia, Y.; Jia, Z.F.; Wang, C.J. Regulation of Hedgehog signaling Offers A Novel Perspective for Bone Homeostasis Disorder Treatment. *Int. J. Mol. Sci.* **2019**, *20*, 3981. [[CrossRef](#)]
84. Long, F.; Chung, U.I.; Ohba, S.; McMahon, J.; Kronenberg, H.M.; McMahon, A.P. Ihh signaling is directly required for the osteoblast lineage in the endochondral skeleton. *Development* **2004**, *131*, 1309–1318. [[CrossRef](#)]
85. Mak, K.K.; Chen, M.H.; Day, T.F.; Chuang, P.T.; Yang, Y. Wnt/beta-catenin signaling interacts differentially with Ihh signaling in controlling endochondral bone and synovial joint formation. *Development* **2006**, *133*, 3695–3707. [[CrossRef](#)]

86. Caddeo, S.; Boffito, M.; Sartori, S. Tissue Engineering Approaches in the Design of Healthy and Pathological In Vitro Tissue Models. *Front. Bioeng. Biotechnol.* **2017**, *5*, 40. [[CrossRef](#)]
87. Liu, Y.; Lim, J.; Teoh, S.H. Review: Development of clinically relevant scaffolds for vascularised bone tissue engineering. *Biotechnol. Adv.* **2013**, *31*, 688–705. [[CrossRef](#)]
88. Skoog, S.A.; Kumar, G.; Narayan, R.J.; Goering, P.L. Biological responses to immobilized microscale and nanoscale surface topographies. *Pharm. Ther.* **2018**, *182*, 33–55. [[CrossRef](#)]
89. Osathanon, T.; Bessinyowong, K.; Arksornnukit, M.; Takahashi, H.; Pavasant, P. Human osteoblast-like cell spreading and proliferation on Ti-6Al-7Nb surfaces of varying roughness. *J. Oral. Sci.* **2011**, *53*, 23–30. [[CrossRef](#)]
90. Nantavisai, S.; Egusa, H.; Osathanon, T.; Sawangmake, C. Mesenchymal stem cell-based bone tissue engineering for veterinary practice. *Heliyon* **2019**, *5*, e02808. [[CrossRef](#)]
91. Gao, C.; Peng, S.; Feng, P.; Shuai, C. Bone biomaterials and interactions with stem cells. *Bone Res.* **2017**, *5*, 17059. [[CrossRef](#)]
92. Eliaz, N.; Metoki, N. Calcium Phosphate Bioceramics: A Review of Their History, Structure, Properties, Coating Technologies and Biomedical Applications. *Materials* **2017**, *10*, 334. [[CrossRef](#)]
93. Pan, Y.K.; Chen, C.Z.; Wang, D.G.; Lin, Z.Q. Preparation and bioactivity of micro-arc oxidized calcium phosphate coatings. *Mater. Chem. Phys.* **2013**, *141*, 842–849. [[CrossRef](#)]
94. Shuai, C.; Li, P.; Liu, J.; Peng, S. Optimization of TCP/HAP ratio for better properties of calcium phosphate scaffold via selective laser sintering. *Mater. Charact.* **2013**, *77*, 23–31. [[CrossRef](#)]
95. Maehira, F.; Miyagi, I.; Eguchi, Y. Effects of calcium sources and soluble silicate on bone metabolism and the related gene expression in mice. *Nutrition* **2009**, *25*, 581–589. [[CrossRef](#)] [[PubMed](#)]
96. Zhou, X.; Zhang, N.; Mankoci, S.; Sahai, N. Silicates in orthopedics and bone tissue engineering materials. *J. Biomed. Mater. Res. Part. A* **2017**, *105*, 2090–2102. [[CrossRef](#)] [[PubMed](#)]
97. Filipowska, J.; Pawlik, J.; Cholewa-Kowalska, K.; Tylko, G.; Pamula, E.; Niedzwiedzki, L.; Szuta, M.; Laczka, M.; Osyczka, A.M. Incorporation of sol-gel bioactive glass into PLGA improves mechanical properties and bioactivity of composite scaffolds and results in their osteoinductive properties. *Biomed. Mater.* **2014**, *9*, 065001. [[CrossRef](#)]
98. Hammouche, S.; Hammouche, D.; McNicholas, M. Biodegradable bone regeneration synthetic scaffolds: In tissue engineering. *Curr. Stem Cell Res.* **2012**, *7*, 134–142. [[CrossRef](#)]
99. Sonia, T.A.; Sharma, C.P. An overview of natural polymers for oral insulin delivery. *Drug Discov. Today* **2012**, *17*, 784–792. [[CrossRef](#)]
100. Tian, H.; Tang, Z.; Zhuang, X.; Chen, X.; Jing, X. Biodegradable synthetic polymers: Preparation, functionalization and biomedical application. *Prog. Polym. Sci.* **2012**, *37*, 237–280. [[CrossRef](#)]
101. Orchel, A.; Jelonek, K.; Kasperczyk, J.; Dobrzynski, P.; Marcinkowski, A.; Pamula, E.; Orchel, J.; Bielecki, I.; Kulczycka, A. The influence of chain microstructure of biodegradable copolyesters obtained with low-toxic zirconium initiator to in vitro biocompatibility. *Biomed. Res. Int.* **2013**, *2013*, 176946. [[CrossRef](#)]
102. Yang, X.B.; Roach, H.I.; Clarke, N.M.; Howdle, S.M.; Quirk, R.; Shakesheff, K.M.; Oreffo, R.O. Human osteoprogenitor growth and differentiation on synthetic biodegradable structures after surface modification. *Bone* **2001**, *29*, 523–531. [[CrossRef](#)]
103. Asti, A.; Gioglio, L. Natural and synthetic biodegradable polymers: Different scaffolds for cell expansion and tissue formation. *Int. J. Artif. Organs* **2014**, *37*, 187–205. [[CrossRef](#)]
104. Guo, Z.; Lee, S.E.; Kim, H.; Park, S.; Hahn, H.T.; Karki, A.B.; Young, D.P. Fabrication, characterization and microwave properties of polyurethane nanocomposites reinforced with iron oxide and barium titanate nanoparticles. *Acta Mater.* **2009**, *57*, 267–277. [[CrossRef](#)]
105. Niemeyer, P.; Krause, U.; Fellenberg, J.; Kasten, P.; Seckinger, A.; Ho, A.D.; Simank, H.G. Evaluation of mineralized collagen and alpha-tricalcium phosphate as scaffolds for tissue engineering of bone using human mesenchymal stem cells. *Cells Tissues Organs* **2004**, *177*, 68–78. [[CrossRef](#)]
106. De Santis, R.; Guarino, V.; Ambrosio, L. *Composite Biomaterials for Bone Repair*; Woodhead Publishing: Sawston, UK, 2019; pp. 273–299.
107. Wang, C.; Huang, W.; Zhou, Y.; He, L.; He, Z.; Chen, Z.; He, X.; Tian, S.; Liao, J.; Lu, B.; et al. 3D printing of bone tissue engineering scaffolds. *Bioact. Mater.* **2020**, *5*, 82–91. [[CrossRef](#)]
108. Mota, R.; Silva, E.O.d.; Lima, F.F.; Menezes, L.; Thiele, A.C.S. 3D Printed Scaffolds as a New Perspective for Bone Tissue Regeneration: Literature Review. *Mater. Sci. Appl.* **2016**, *7*, 430–452.
109. Leong, K.F.; Cheah, C.M.; Chua, C.K. Solid freeform fabrication of three-dimensional scaffolds for engineering replacement tissues and organs. *Biomaterials* **2003**, *24*, 2363–2378. [[CrossRef](#)]
110. Curran, J.M.; Chen, R.; Hunt, J.A. The guidance of human mesenchymal stem cell differentiation in vitro by controlled modifications to the cell substrate. *Biomaterials* **2006**, *27*, 4783–4793. [[CrossRef](#)] [[PubMed](#)]
111. Kommareddy, K.P.; Lange, C.; Rumpler, M.; Dunlop, J.W.; Manjubala, I.; Cui, J.; Kratz, K.; Lendlein, A.; Fratzl, P. Two stages in three-dimensional in vitro growth of tissue generated by osteoblastlike cells. *Biointerphases* **2010**, *5*, 45–52. [[CrossRef](#)]
112. Kietzmann, J.; Pitt, L.; Berthon, P. Disruptions, decisions, and destinations: Enter the age of 3-D printing and additive manufacturing. *Bus. Horiz.* **2015**, *58*, 209–215. [[CrossRef](#)]
113. De Mori, A.; Peña Fernández, M.; Blunn, G.; Tozzi, G.; Roldo, M. 3D Printing and Electrospinning of Composite Hydrogels for Cartilage and Bone Tissue Engineering. *Polymers* **2018**, *10*, 285. [[CrossRef](#)]

114. Bahraminasab, M. Challenges on optimization of 3D-printed bone scaffolds. *BioMed. Eng. OnLine* **2020**, *19*, 69. [[CrossRef](#)]
115. Salmi, M.; Tuomi, J.; Paloheimo, K.S.; Björkstrand, R.; Paloheimo, M.; Salo, J.; Kontio, R.; Mesimäki, K.; Mäkitie, A.A. Patient-specific reconstruction with 3D modeling and DMLS additive manufacturing. *Rapid Prototyp. J.* **2012**, *18*, 209–214. [[CrossRef](#)]
116. Ghilan, A.; Chiriac, A.P.; Nita, L.E.; Rusu, A.G.; Neamtu, I.; Chiriac, V.M. Trends in 3D Printing Processes for Biomedical Field: Opportunities and Challenges. *J. Polym. Environ.* **2020**, *28*, 1345–1367. [[CrossRef](#)]
117. Gopinathan, J.; Noh, I. Recent trends in bioinks for 3D printing. *Biomater. Res.* **2018**, *22*, 11. [[CrossRef](#)] [[PubMed](#)]
118. Wu, J.-J.; Huang, L.-M.; Zhao, Q.; Xie, T. 4D Printing: History and Recent Progress. *Chin. J. Polym. Sci.* **2018**, *36*, 563–575. [[CrossRef](#)]
119. Ferguson, J.C.; Tangl, S.; Barnewitz, D.; Genzel, A.; Heimel, P.; Hruschka, V.; Redl, H.; Nau, T. A large animal model for standardized testing of bone regeneration strategies. *BMC Vet. Res.* **2018**, *14*, 330. [[CrossRef](#)]
120. Houdebine, L.M. Transgenic animal models in biomedical research. *Methods Mol. Biol.* **2007**, *360*, 163–202. [[PubMed](#)]
121. Simpson, A.H.; Murray, I.R. Osteoporotic fracture models. *Curr. Osteoporos. Rep.* **2015**, *13*, 9–15. [[CrossRef](#)] [[PubMed](#)]
122. Muschler, G.F.; Raut, V.P.; Patterson, T.E.; Wenke, J.C.; Hollinger, J.O. The design and use of animal models for translational research in bone tissue engineering and regenerative medicine. *Tissue Eng. Part B Rev.* **2010**, *16*, 123–145. [[CrossRef](#)] [[PubMed](#)]
123. Muschler, G.F.; Nakamoto, C.; Griffith, L.G. Engineering principles of clinical cell-based tissue engineering. *J. Bone Jt. Surg. Am.* **2004**, *86*, 1541–1558. [[CrossRef](#)] [[PubMed](#)]
124. Cibelli, J.; Emborg, M.E.; Prockop, D.J.; Roberts, M.; Schatten, G.; Rao, M.; Harding, J.; Mirochnitchenko, O. Strategies for improving animal models for regenerative medicine. *Cell Stem Cell* **2013**, *12*, 271–274. [[CrossRef](#)] [[PubMed](#)]
125. Grün, N.; Hahn, D.; Okutan, B.; Marek, R.; Weinberg, A.-M. *Animal Models in Orthopedic Research: The Proper Animal Model to Answer Fundamental Questions on Bone Healing Depending on Pathology and Implant Material*; IntechOpen: London, UK, 2019.
126. Thompson, D.D.; Simmons, H.A.; Pirie, C.M.; Ke, H.Z. FDA Guidelines and animal models for osteoporosis. *Bone* **1995**, *17* (Suppl. S4), 125S–133S. [[CrossRef](#)]
127. Einhorn, T.A. Clinically applied models of bone regeneration in tissue engineering research. *Clin. Orthop. Relat. Res.* **1999**, *367*, S59–S67. [[CrossRef](#)] [[PubMed](#)]
128. Assis-Ribas, T.; Forni, M.F.; Winnischofer, S.M.B.; Sogayar, M.C.; Trombetta-Lima, M. Extracellular matrix dynamics during mesenchymal stem cells differentiation. *Dev. Biol.* **2018**, *437*, 63–74. [[CrossRef](#)] [[PubMed](#)]
129. Baba, S.; Inoue, T.; Hashimoto, Y.; Kimura, D.; Ueda, M.; Sakai, K.; Matsumoto, N.; Hiwa, C.; Adachi, T.; Hojo, M. Effectiveness of scaffolds with pre-seeded mesenchymal stem cells in bone regeneration—Assessment of osteogenic ability of scaffolds implanted under the periosteum of the cranial bone of rats. *Dent. Mater. J.* **2010**, *29*, 673–681. [[CrossRef](#)]
130. Ni, P.; Fu, S.; Fan, M.; Guo, G.; Shi, S.; Peng, J.; Luo, F.; Qian, Z. Preparation of poly(ethylene glycol)/polylactide hybrid fibrous scaffolds for bone tissue engineering. *Int. J. Nanomed.* **2011**, *6*, 3065–3075.
131. Yokoya, S.; Mochizuki, Y.; Natsu, K.; Omae, H.; Nagata, Y.; Ochi, M. Rotator cuff regeneration using a bioabsorbable material with bone marrow-derived mesenchymal stem cells in a rabbit model. *Am. J. Sports Med.* **2012**, *40*, 1259–1268. [[CrossRef](#)]
132. Liang, H.; Li, X.; Shimer, A.L.; Balian, G.; Shen, F.H. A novel strategy of spine defect repair with a degradable bioactive scaffold preloaded with adipose-derived stromal cells. *Spine J.* **2014**, *14*, 445–454. [[CrossRef](#)] [[PubMed](#)]
133. Zhang, X.; Yamaoka, K.; Sonomoto, K.; Kaneko, H.; Satake, M.; Yamamoto, Y.; Kondo, M.; Zhao, J.; Miyagawa, I.; Yamagata, K.; et al. Local delivery of mesenchymal stem cells with poly-lactic-co-glycolic acid nano-fiber scaffold suppress arthritis in rats. *PLoS ONE* **2014**, *9*, e114621. [[CrossRef](#)]
134. Berner, A.; Henkel, J.; Woodruff, M.A.; Steck, R.; Nerlich, M.; Schuetz, M.A.; Hutmacher, D.W. Delayed minimally invasive injection of allogenic bone marrow stromal cell sheets regenerates large bone defects in an ovine preclinical animal model. *Stem Cells Transl. Med.* **2015**, *4*, 503–512. [[CrossRef](#)] [[PubMed](#)]
135. Yoon, D.; Kang, B.J.; Kim, Y.; Lee, S.H.; Rhew, D.; Kim, W.H.; Kweon, O.K. Effect of serum-derived albumin scaffold and canine adipose tissue-derived mesenchymal stem cells on osteogenesis in canine segmental bone defect model. *J. Vet. Sci.* **2015**, *16*, 397–404. [[CrossRef](#)]
136. Masaoka, T.; Yoshii, T.; Yuasa, M.; Yamada, T.; Taniyama, T.; Torigoe, I.; Shinomiya, K.; Okawa, A.; Morita, S.; Sotome, S. Bone Defect Regeneration by a Combination of a beta-Tricalcium Phosphate Scaffold and Bone Marrow Stromal Cells in a Non-Human Primate Model. *Open Biomed. Eng. J.* **2016**, *10*, 2–11. [[CrossRef](#)]
137. Decambron, A.; Fournet, A.; Bensidhoum, M.; Manassero, M.; Sailhan, F.; Petite, H.; Logeart-Avramoglou, D.; Viateau, V. Low-dose BMP-2 and MSC dual delivery onto coral scaffold for critical-size bone defect regeneration in sheep. *J. Orthop. Res.* **2017**, *35*, 2637–2645. [[CrossRef](#)]
138. Smith, J.O.; Tayton, E.R.; Khan, F.; Aarvold, A.; Cook, R.B.; Goodship, A.; Bradley, M.; Oreffo, R.O. Large animal in vivo evaluation of a binary blend polymer scaffold for skeletal tissue-engineering strategies; translational issues. *J. Tissue Eng. Regen. Med.* **2017**, *11*, 1065–1076. [[CrossRef](#)]
139. Zhang, D.; Gao, P.; Li, Q.; Li, J.; Li, X.; Liu, X.; Kang, Y.; Ren, L. Engineering biomimetic periosteum with beta-TCP scaffolds to promote bone formation in calvarial defects of rats. *Stem Cell Res.* **2017**, *8*, 134.
140. Chu, W.; Gan, Y.; Zhuang, Y.; Wang, X.; Zhao, J.; Tang, T.; Dai, K. Mesenchymal stem cells and porous beta-tricalcium phosphate composites prepared through stem cell screen-enrich-combine-(biomaterials) circulating system for the repair of critical size bone defects in goat tibia. *Stem Cell Res.* **2018**, *9*, 157.

141. Lin, C.C.; Lin, S.C.; Chiang, C.C.; Chang, M.C.; Lee, O.K. Reconstruction of Bone Defect Combined with Massive Loss of Periosteum Using Injectable Human Mesenchymal Stem Cells in Biocompatible Ceramic Scaffolds in a Porcine Animal Model. *Stem Cells Int.* **2019**, *2019*, 6832952. [[CrossRef](#)] [[PubMed](#)]
142. Liu, Z.; Ge, Y.; Zhang, L.; Wang, Y.; Guo, C.; Feng, K.; Yang, S.; Zhai, Z.; Chi, Y.; Zhao, J.; et al. The effect of induced membranes combined with enhanced bone marrow and 3D PLA-HA on repairing long bone defects in vivo. *J. Tissue Eng. Regen. Med.* **2020**, *14*, 1403–1414. [[CrossRef](#)]
143. Yea, J.H.; Bae, T.S.; Kim, B.J.; Cho, Y.W.; Jo, C.H. Regeneration of the rotator cuff tendon-to-bone interface using umbilical cord-derived mesenchymal stem cells and gradient extracellular matrix scaffolds from adipose tissue in a rat model. *Acta Biomater.* **2020**, *114*, 104–116. [[CrossRef](#)] [[PubMed](#)]
144. Giannotti, S.; Trombi, L.; Bottai, V.; Ghilardi, M.; D'Alessandro, D.; Danti, S.; Dell'Osso, G.; Guido, G.; Petrini, M. Use of autologous human mesenchymal stromal cell/fibrin clot constructs in upper limb non-unions: Long-term assessment. *PLoS ONE* **2013**, *8*, e73893. [[CrossRef](#)]
145. Perel, P.; Roberts, I.; Sena, E.; Wheble, P.; Briscoe, C.; Sandercock, P.; Macleod, M.; Mignini, L.E.; Jayaram, P.; Khan, K.S. Comparison of treatment effects between animal experiments and clinical trials: Systematic review. *BMJ* **2007**, *334*, 197. [[CrossRef](#)]
146. Denayer, T.; Stöhr, T.; Van Roy, M. Animal models in translational medicine: Validation and prediction. *New Horiz. Transl. Med.* **2014**, *2*, 5–11. [[CrossRef](#)]
147. Yamasaki, T.; Yasunaga, Y.; Ishikawa, M.; Hamaki, T.; Ochi, M. Bone-marrow-derived mononuclear cells with a porous hydroxyapatite scaffold for the treatment of osteonecrosis of the femoral head: A preliminary study. *J. Bone Jt. Surg. Br.* **2010**, *92*, 337–341. [[CrossRef](#)]
148. Jager, M.; Herten, M.; Fochtmann, U.; Fischer, J.; Hernigou, P.; Zilkens, C.; Hendrich, C.; Krauspe, R. Bridging the gap: Bone marrow aspiration concentrate reduces autologous bone grafting in osseous defects. *J. Orthop. Res.* **2011**, *29*, 173–180. [[CrossRef](#)] [[PubMed](#)]
149. Cuthbert, R.J.; Churchman, S.M.; Tan, H.B.; McGonagle, D.; Jones, E.; Giannoudis, P.V. Induced periosteum a complex cellular scaffold for the treatment of large bone defects. *Bone* **2013**, *57*, 484–492. [[CrossRef](#)] [[PubMed](#)]
150. Šponer, P.; Filip, S.; Kučera, T.; Brtková, J.; Urban, K.; Palička, V.; Kočí, Z.; Syka, M.; Bezrouk, A.; Syková, E. Utilizing Autologous Multipotent Mesenchymal Stromal Cells and β -Tricalcium Phosphate Scaffold in Human Bone Defects: A Prospective, Controlled Feasibility Trial. *Biomed. Res. Int.* **2016**, *2016*, 2076061. [[CrossRef](#)]
151. Zhuang, Y.; Gan, Y.; Shi, D.; Zhao, J.; Tang, T.; Dai, K. A novel cytotherapy device for rapid screening, enriching and combining mesenchymal stem cells into a biomaterial for promoting bone regeneration. *Sci. Rep.* **2017**, *7*, 15463. [[CrossRef](#)]
152. Chu, W.; Wang, X.; Gan, Y.; Zhuang, Y.; Shi, D.; Liu, F.; Sun, Y.; Zhao, J.; Tang, T.; Dai, K. Screen-enrich-combine circulating system to prepare MSC/beta-TCP for bone repair in fractures with depressed tibial plateau. *Regen. Med.* **2019**, *14*, 555–569. [[CrossRef](#)] [[PubMed](#)]
153. Morrison, D.A.; Kop, A.M.; Nilasaroya, A.; Sturm, M.; Shaw, K.; Honeybul, S. Cranial reconstruction using allogeneic mesenchymal stromal cells: A phase 1 first-in-human trial. *J. Tissue Eng. Regen. Med.* **2018**, *12*, 341–348. [[CrossRef](#)]
154. Gjerde, C.; Mustafa, K.; Hellem, S.; Rojewski, M.; Gjengedal, H.; Yassin, M.A.; Feng, X.; Skaale, S.; Berge, T.; Rosen, A.; et al. Cell therapy induced regeneration of severely atrophied mandibular bone in a clinical trial. *Stem Cell Res.* **2018**, *9*, 213. [[CrossRef](#)]
155. Gomez-Barrena, E.; Padilla-Eguiluz, N.; Rosset, P.; Gebhard, F.; Hernigou, P.; Baldini, N.; Rouard, H.; Sensebe, L.; Gonzalo-Daganzo, R.M.; Giordano, R.; et al. Early efficacy evaluation of mesenchymal stromal cells (MSC) combined to biomaterials to treat long bone non-unions. *Injury* **2020**, *51* (Suppl. S1), S63–S73. [[CrossRef](#)]

Conclusions

- 1) MSCs isolated from sheep bone marrow and supplemented with FGF-2 or FGF-2 and BMP-2 in long-term culture maintained the phenotype of native MSCs and had the ability to differentiate into bone, cartilage and adipose tissue cells.
- 2) FGF-2 and BMP-2 increased the osteogenic potential of sheep BM-MSCs and modulated their secretory profile.
- 3) Sheep BM-MSCs treated with FGF-2 and BMP-2 had significantly higher adhesion and osteogenic potential on PCL/HAP/ β -TCP scaffold coated with nHAP, compared to cells treated with FGF-2 alone or untreated.
- 4) The tissue engineered construct composed of nHAP-coated PCL/HAP/ β -TCP scaffold and autologous BM-MSCs treated with FGF-2 or FGF-2 in combination with BMP-2 was biocompatible with sheep tissues and had a beneficial effect on the bone regeneration in the sheep mandible area, thus constitute a promising strategy for clinical application in the repair of large bone defects.